DESIGN OF A SLED TEST FIXTURE FOR CIVILIAN HELICOPTER SEATS


A THESIS SUBMITTED TO
THE GRADUATE SCHOOL OF NATURAL AND APPLIED SCIENCES
OF
MIDDLE EAST TECHNICAL UNIVERSITY


BY

ALİCAN SEÇGİN


IN PARTIAL FULFILLMENT OF THE REQUIREMENTS
FOR
THE DEGREE OF MASTER OF SCIENCE
IN
MECHANICAL ENGINEERING


JULY 2019

Approval of the thesis:

**DESIGN OF A SLED TEST FIXTURE FOR CIVILIAN HELICOPTER SEATS**

submitted by **ALİCAN SEÇGİN** in partial fulfillment of the requirements for the degree of **Master of Science in Mechanical Engineering Department, Middle East Technical University** by,

Prof. Dr. Halil Kalıpçılar
Dean, Graduate School of **Natural and Applied Sciences**                    _____

Prof. Dr. M. A. Sahir Arıkan
Head of Department, **Mechanical Engineering**                    _____

Prof. Dr. Mustafa İlhan Gökler
Supervisor, **Mechanical Engineering, METU**                    _____


**Examining Committee Members:**

Prof. Dr. Haluk Darendeliler
Mechanical Engineering, METU                    _____

Prof. Dr. Mustafa İlhan Gökler
Mechanical Engineering, METU                    _____

Prof. Dr. R. Orhan Yıldırım
Mechanical Engineering, METU                    _____

Prof. Dr. Ender Ciğeroğlu
Mechanical Engineering, METU                    _____

Prof. Dr. S. Kemal İder
Mechanical Engineering, Çankaya Uni.                    _____


Date: 25.07.2019

**I hereby declare that all information in this document has been obtained and presented in accordance with academic rules and ethical conduct. I also declare that, as required by these rules and conduct, I have fully cited and referenced all material and results that are not original to this work.**


Name, Surname: Alican Seçgin

Signature:

**ABSTRACT**

**DESIGN OF A SLED TEST FIXTURE FOR CIVILIAN HELICOPTER SEATS**

Seçgin, Alican
Master of Science, Mechanical Engineering
Supervisor: Prof. Dr. Mustafa İlhan Gökler

July 2019, 133 pages

Crashworthiness of civilian helicopter seats are important since it affects the survivability of occupants. For this reason, there are some established criteria for the authorization of civilian helicopter seats. In this study, vertical crash criterion and floor deformation criterion, which are stated on CS 29.562 by European Aviation Safety Agency (EASA), regarding to civilian helicopter seats are investigated. The Simplified Helicopter Seat (SHS), the Interchangeable Floor Deformation Unit (IFDU), and Sled Test Fixture (STF) are designed and validated using bolt preload analyses, floor deformation analysis, and crash analyses. IFDU and STF are novel designs aiming to validate the civilian helicopter seats in terms of floor deformation effect and vertical crash criterion, respectively. Mapping technique is utilized for transferring the results of analyses among themselves. The bolt preload analysis and the crash analysis are investigated for SHS. IFDU is utilized for observing the effect of floor deformation when SHS is mounted to IFDU before the crash analysis of IFDU and SHS. The bolt preload analysis, the floor deformation analysis, and the crash analysis are investigated for IFDU. STF is designed to perform an analysis simulating the accelerating type sled tests. The crash loads representing the sled tests are applied to STF and the concluding results are discussed.

# ÖZ

## SİVİL HELİKOPTER KOLTUKLARI İÇİN HASARSIZ ÇARPIŞMA TEST FİKSTÜRÜ TASARIMI

Seçgin, Alican
Yüksek Lisans, Makina Mühendisliği
Tez Danışmanı: Prof. Dr. Mustafa İlhan Gökler

Temmuz 2019, 133 sayfa

Sivil helikopter koltuklarının kaza elverişliliği önemli bir kavramdır çünkü yolcuların hayatta kalması buna bağlıdır. Bu sebeple, sivil helikopter koltuklarının doğrulanmasıyla ilgili bazı kıstaslar bulunmaktadır. Bu çalışmada, Avrupa Havacılık Sertifikasyon Ajansı (EASA) tasarından yayımlanan CS 29.562' deki sivil helikopter koltuklarıyla ilgili dikey çarpma kriteri ve yer deformasyonu kriteri incelenmiştir. Basitleştirilmiş Helikopter Koltuğu (BHK), Ayarlanabilir Yer Deformasyon Ünitesi (AYDÜ) ve Hasarsız Çarpışma Test Fikstürü (HÇTF) tasarlanıp cıvata ön gerilme analizleri, yer deformasyonu analizi ve çarpışma analizleriyle doğrulanmıştır. AYDÜ ve HÇTF sivil helikopter koltuklarını yer deformasyonu etkisi ve dikey çarpışma kriteri açısından doğrulamayı amaçlayan yenilikçi tasarımlardır. Analiz sonuçları arasındaki transfer yapılması için haritalama metodu kullanılmıştır. BHK için cıvata ön gerilme analizi ve çarpma analizi incelenmiştir. AYDÜ, BHK' ya monte edilerek yer deformasyonu etkisini incelemek için tasarlanmıştır. AYDÜ için cıvata ön gerilme analizi, yer deformasyonu analizi ve çarpma analizi yapılmıştır. KTF pozitif ivmelenen hasarsız çarpışma testlerine benzetim kurmak için tasarlanmıştır. Hasarsız çarpışma testlerin çarpışma yükleri HÇTF' e uygulanmış ve sonuçlar tartışılmıştır.

Anahtar Kelimeler: Kaza Elverişlilik, Sivil Helikopter Koltukları, Dikey Çarpma, Haritalama, Cıvata Ön Yükleme Analizi, Yer Deformasyonu Analizi, Çarpışma Analizi.

To My Family

# ACKNOWLEDGEMENTS

# TABLE OF CONTENTS

# LIST OF TABLES

TABLES

# LIST OF FIGURES

FIGURES

# LIST OF ABBREVIATIONS

ABBREVIATIONS

ATD:  Anthropometric Test Device

CAD:  Computer Aided Design

DM:   Dummy mass

EASA: European Aviation Safety Agency

FAA:  Federal Aviation Administration

FEA:  Finite Element Analysis

IE:   Internal energy

IFDU: Interchangeable Floor Deformation Unit

KE:   Kinetic energy

PD:   Plastically deformed

RM:   Representative mass

SHS:  Simplified Helicopter Seat

STF:  Sled Test Fixture

# CHAPTER 1

# INTRODUCTION

## 1.1. Explanation of Crash and Crashworthiness

The word of "crash" has various meanings and uses in many areas. However, all meanings include "sudden" and "negativity". The technical description of the crash is the physical impact of two or more objects in very high speeds. In real life, crash is applicable to the vehicles that have occupants in themselves. Resultantly, the crash may have serious effects on humans such as acute and/or chronic injuries, or fatalities.

Crashworthiness provides a measure of the ability of a vehicle and its components to protect the occupants in survivable crashes via withstanding impact loads, sustaining occupiable volume, and limiting loads on the occupants [1,2]. "Crashworthiness" term arises to balance the crash phenomenon. In other words, crashworthiness focuses on reducing the effects of crash and protecting humans that are involved in crashes. Crashworthiness involves several steps such as defining measurable speed and/or acceleration inputs, Computer Aided Design (CAD), Finite Element Analysis (FEA), crashworthiness tests.

## 1.2. Crashworthiness of Vehicles

As explained in previous section, crash and crashworthiness have effects on vehicles that are land vehicles, marine vehicles, and air vehicles. Any kind of transportation could be affected by crashes. Hence, crashworthiness of vehicles is important for the survivability of their occupants.

For land vehicles, nearly all studies are focused on cars rather than railway vehicles. These studies investigate many aspects of crashworthiness such as design, FEA, protection devices, statistics, tests, biomechanics, Anthropometric Test Devices

1

(ATD) and analytical methods [1,3-10]. The crashworthiness of land vehicles can be mainly divided into the occupant protectiveness and the vehicle protectiveness in terms of protectiveness. The occupant protectiveness means the survivability of occupants after crash and the vehicle protectiveness means the maintenance of the self-structural integrity during post-crash [3]. Another classification is made on the regions of cars that are subjected to collusions. These are frontal collisions (FC), rear-end collisions (ReC), side collisions (SC), angle collusions (AC), and rollover collusions (RC) [1,3]. These locations, except rollover collusions, are visualized in Figure 1.1.
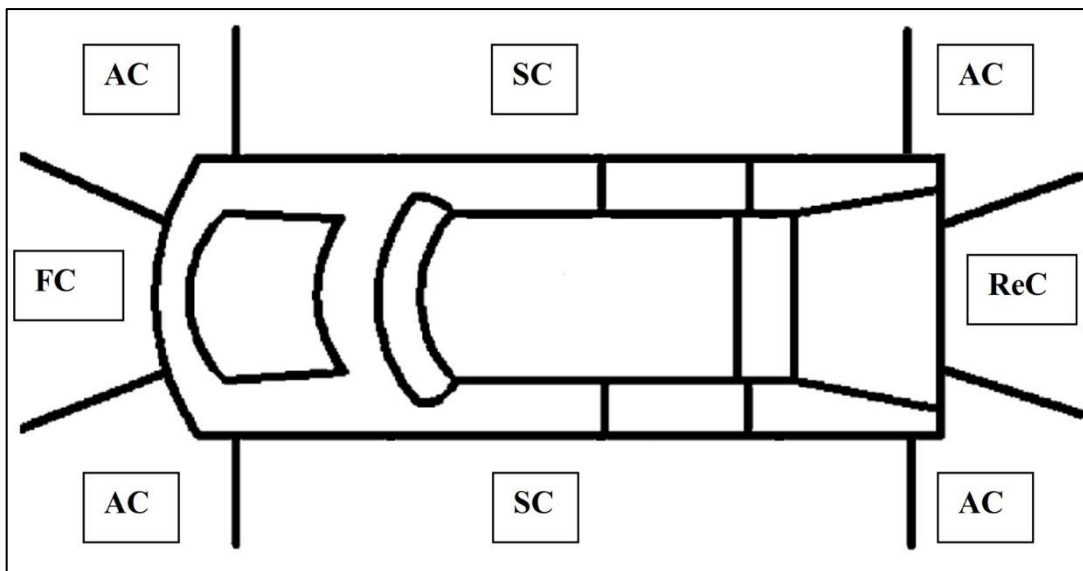


Figure 1.1. Impact locations on a car [3]

For frontal collusions, plastically deformable frontal structural parts must exist to absorb the kinetic energy of the crash. Moreover, frontal parts must prevent the intrusion of items such as trees, traffic barriers, and light poles [1]. Similarly, deformable rear structure is required for the protection of fuel tank and rear passenger compartment. For side and angle collusion, side structures must be properly designed so as not to collapse towards to the occupants. In addition, the doors could still be properly openable after crash. For rollover crashes, roof structures must be strong to protect to occupants during single or multiple rollovers [1]. Properly designed restraint

systems should accommodate the structural parts in a harmony. The car restraint systems could be exemplified as deployable frontal and side airbags, seat belts [1].

The crashworthiness testing is a necessity despite the fact that there are many improvements in FEA, computational mechanics. Although, the analysis reduces the number of tests, final decision depends on tests. This phenomenon is especially true for vehicle certification [1]. The crashworthiness tests of land vehicles consists of component tests, sled tests, and full-scale tests. The complexity of the tests and associated variables increase from component to full-scale tests.

The component test identifies the dynamic or quasi-static response of the loading of isolated components. These tests are related to the determination of crash mode and energy absorption capacity [1]. In sled tests, the engineers use a vehicle with all or some of interior components. Sled tests aims to observe the mechanical behavior of restraints such as structural components, and protection devices. ATDs that are seated in the test bucket are subjected to dynamic loads that simulate the vehicle impact pulses resulting from impacts. The test results are derived via high-speed photography and various sensors located on the dummy occupant [1]. Full-scale tests include a deformable barrier that is instrumented with several monitoring the force – time history. Human injury thresholds for head, chest, and legs are determined [1]. Typically, a full-scale test is done for a vehicle in order to get license from government or authority mandated regulations such as United States Federal Motors Vehicle Safety Standard (FMVSS) or European New Car Assessment Program (Euro NCAP). These authorities investigates crashes, get a basis of crashworthiness and regulate the automotive industry in terms of crashworthiness [5].

Researches about marine vehicle crashes are done using statistical and FEA by many researchers [11-13]. These collusions include ship-to-ship, ship-to-offshore structures and ship collusions with high sea waves. A ship wreck caused by high sea waves is presented in Figure 1.2. Today, there is great interest in saving human lives, preventing oil spillage, and reducing the damage of ships and offshore structures caused by

crashes [11]. In marine collusions, the impact energy is greatly absorbed by surrounding structure of ships without damaging oil tanks and main sections of ships [11]. Therefore, these facts require the serious consideration of the crashworthiness of marine vehicles. The ships have many welded parts unlike air vehicles and they should be carefully analyzed in crashworthy studies [11].



Figure 1.2. Collapse of a tanker [11]

Crashworthiness term was initially used in the aerospace industry in 1950's [1,2]. There are numerous researches are done in aviation history, mostly on helicopters and its components rather than airplanes. Some researches focus on air vehicles or the components of air vehicles generally. These researches aim either being sole academic studies [2,14-26] or constructing aviation crashworthiness standards [27-30]. On the other hand, many researches are specifically concerned with the helicopter seats and their subcomponents. Some of them are pure academic studies [31-39], the others construct helicopter seat standards [40-43]. In this study, the crashworthiness of helicopter seats are investigated. General information about helicopters is outlined in

Section 1.3 to provide background. Besides, the crashworthiness of helicopter components is explained in Section 1.4.

## 1.3. General Information about Helicopters

A helicopter is an air vehicle that is lifted and pushed forward with main rotor, which consist of two or more rotary blades and connecting hub [44,45]. Helicopters have the ability of taking off and landing vertically, moving in any direction, and remaining stationary in the air unlike planes [45].

The word "helicopter" is adapted from the French word "hélicoptère", coined by Gustave de Ponton d'Amecourt in 1861 [44]. It is comprised from the Greek words "helikos" (means spiral or turning) and "pteron" (means wing). The helicopter could also be called as "rotorcraft" due to its unique rotor system. The history of vertical flight began as early as 1100's; there are historical references to a Chinese flying top that used a rotary wing as a source of lift. During 15th century, Leonardo da Vinci made sketches of a helicopter that uses aerial airscrew to obtain lift. There were many helicopter design trials shown in Figure 1.3 between 1100 and 1939 [45].
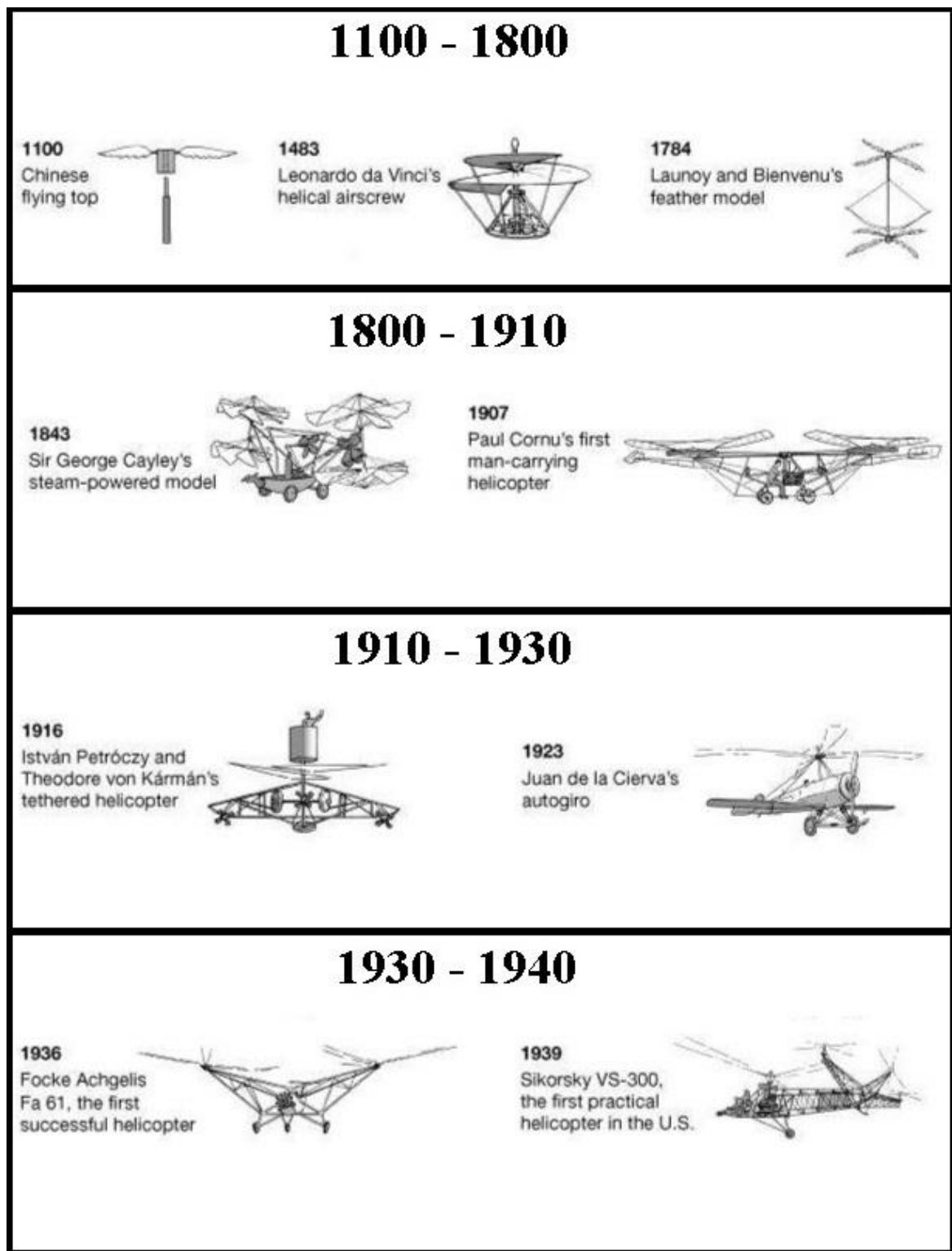
Figure 1.3. History of helicopters [45]

In USA, Igor Sikorsky pioneered his VS-300 helicopters after a long period of development and test periods in 1939. These helicopters possessed most of the modern helicopter features [45]. A sketch of modern helicopter with its coordinate axes is presented in Figure 1.4.
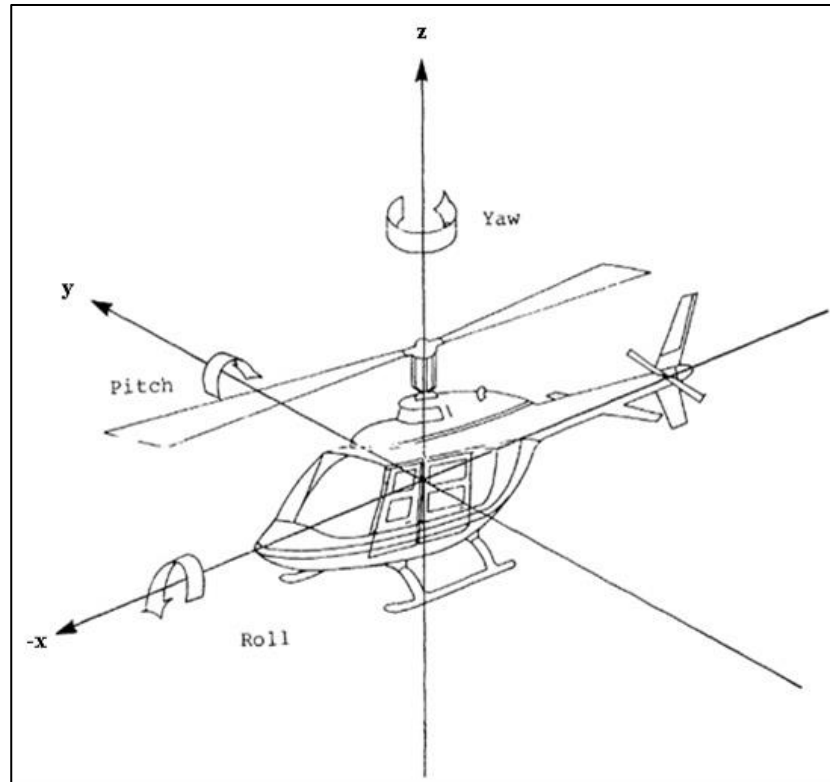


Figure 1.4. Typical helicopter with coordinate axes [19]

Due to its unique operational characteristics, helicopters are used in many tasks. They are mainly grouped as civil and military helicopters. For military purposes, helicopters are operated for gun and rocket firing, and aerial transferring of troops as it can be observed in Figure 1.5. For civilian purposes, helicopters as seen in Figure 1.6 are used for transporting passengers and cargo, search and rescue missions to places where land or sea vehicles cannot reach [44].

(a)  Attack

(b)  Utility

Figure 1.5. Mission types of military helicopters [46,47]

Figure 1.6. Mission types of civilian helicopters [44,48]

Main components of a typical helicopter are presented in Figure 1.7.
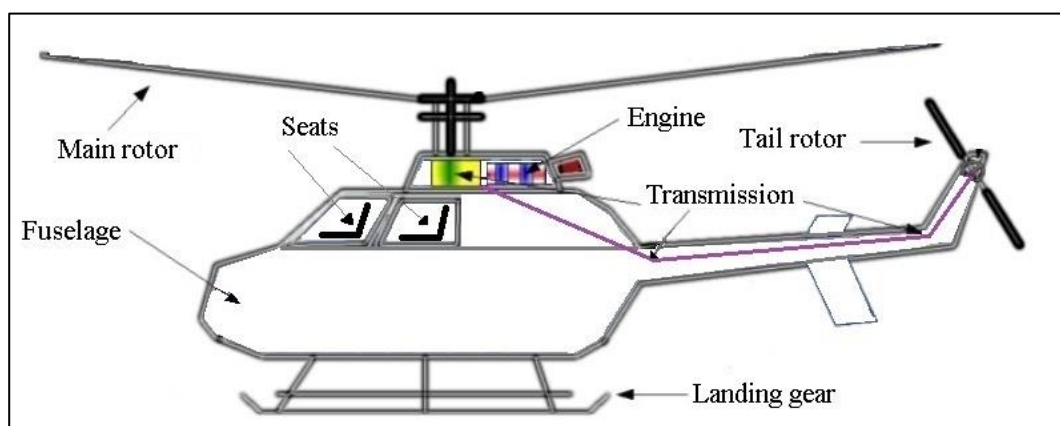


Figure 1.7. Main components of helicopters [49]

The fuselage forms the outer surface of the helicopter. The fuselage is the body section. It houses the cabin for the crew, passengers, and cargo. The fuselage also houses the engine and the transmission [44]. The helicopter seats are used for pilots, passengers or crews. They are fixed to the cabin floor of the fuselage.

The main rotor is the rotating part of a helicopter which generates lift. The main rotor consists of a vertical shaft, rotor blades, and connecting hub [44]. The tail rotor is structurally similar to the main rotor. It provides the anti-torque that is required by the main rotor [44]. The engine provides the flying power to helicopter with fuel ignition. In helicopters, there could be one engine or two engines. The transmission system transfers power from the engine to the main rotor and the tail rotor during flight [44]. The landing gear provides means the stationary position of helicopter. Skids can be used as a landing gear, as shown in Figure 1.7. Skids are fixed ground items without wheels. On the other hand, landing gear may consist of retracting or non-retracting wheels.

## 1.4. Crashworthiness of Helicopters

The objective of designing for crash resistance is to eliminate injuries and fatalities by minimizing the effects of impact in helicopter crashes [50]. Designing for helicopter crash protection aims managing the energy dissipation of impact and thereby limiting the load transmitted to the occupant to a tolerable level, which is called energy absorption [15]. Moreover, the design of the civilian helicopters requires a comprehensive knowledge of the crash environment to achieve crash survivability [19]. Crash survivability aims maintaining a livable volume, restraining the occupant, keeping occupant crash loads in non-injury tolerance, and providing means and time to escape [15]. In addition, it leads to a crash-resistant helicopter, which will also reduce helicopter crash impact damage [50].

In order to provide as much occupant protection as possible, a systems approach must be followed [50]. It means that the landing gear, fuselage, and occupant seats must be designed to work together to absorb the kinetic energy and convert it to inelastic

10

energy by plastic deformation [21,50]. Resultantly, these actions slow the occupants to rest without injurious loadings. These energy absorption parts are shown in Figure 1.8 [50]. Left of the figure shows the situation before crash whereas the right hand side shows the situation after crash.
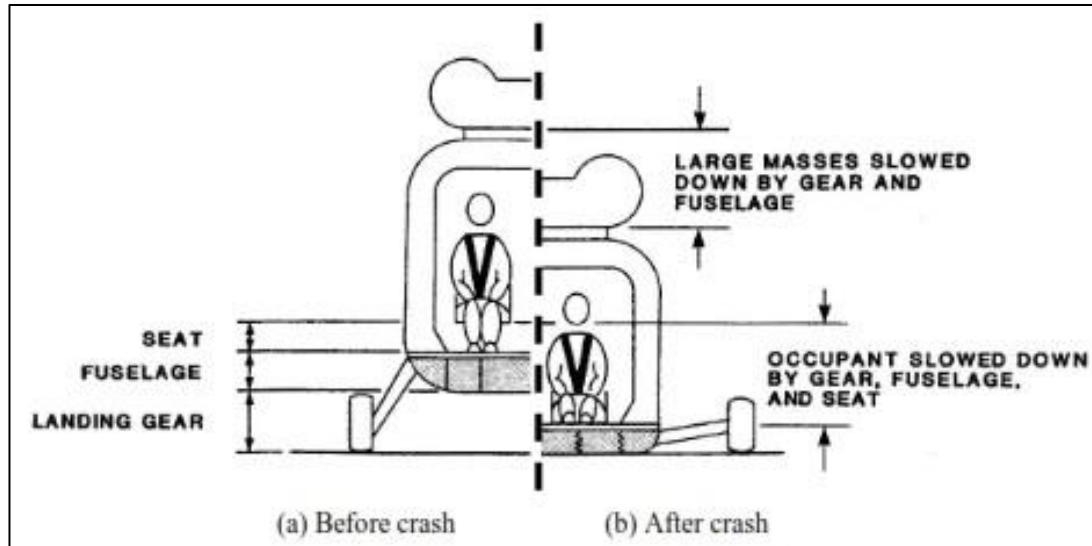


Figure 1.8. Energy absorption systems of a helicopter [50]

Helicopter design concepts shall meet structural and crashworthiness requirements preventing fire, collapse of cabin structure, collusion between occupants and hard objects. That could be done by providing a protective shell for the occupants via energy absorbing elements integrated to the landing gear, subfloor section of fuselage and the seats that are illustrated in Figure 1.8 [20].

The landing gear with high energy absorbing capacity can protect the fuselage from low velocity impact and provide occupant protection for high velocity impact of hard surfaces. Though, during impact with soft surfaces like water or uneven surfaces caused by hills, rocks etc. the force acting on the landing gear may not be great enough to function as energy absorbing unit. Helicopters with skids, instead of wheels, could provide better protection for such impacts due to the greater surface area of skids [50].

The fuselage has more important role in energy absorption since modern civil helicopters mostly employ retracting landing gears [50]. Subfloor of the fuselage has

11

a relatively large space that can be designed for impact energy dissipation. By optimizing the structure, the peak acceleration can be reduced and less acceleration can be transmitted to the occupant [21]. Under crash loads, riveted intersection elements behave like deformable structural columns and play a high role in energy absorption. A typical subfloor structure of helicopter is presented in Figure 1.9.
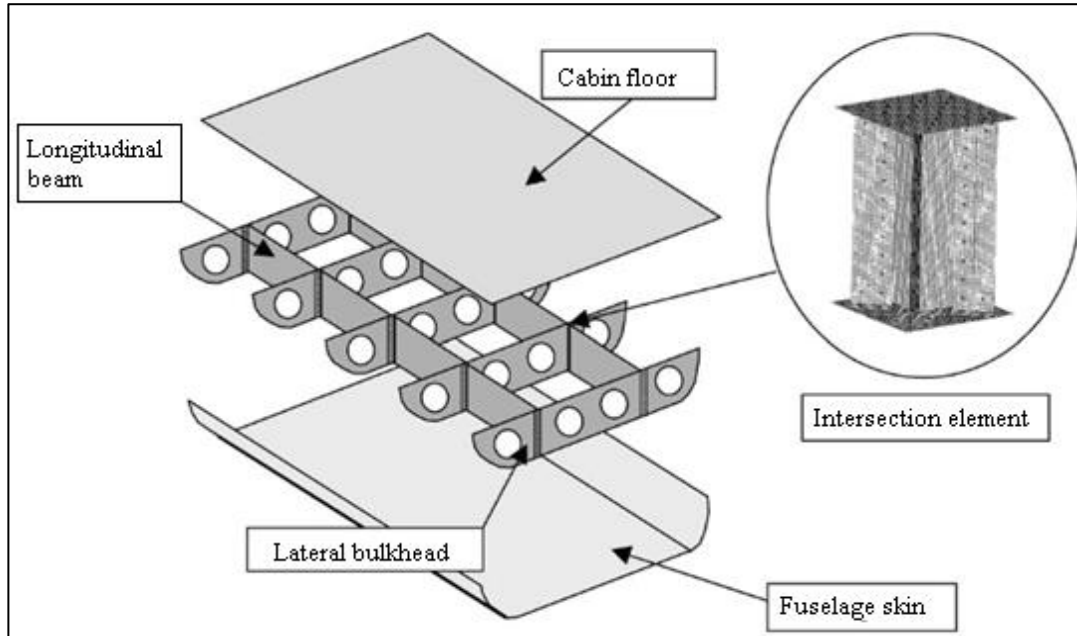


Figure 1.9. The subfloor structure of a helicopter [21]

Helicopter seats are the closest component to the occupant in energy absorption. As a matter of fact, while the subfloor structure in a helicopter is limited in thickness, the seats can give high contribution to the survivability [36]. Modern helicopter seats are equipped with an energy absorbers to reduce lumbar spine load during crash landing. A typical helicopter seat is presented in Figure 1.10.

Figure 1.10. A typical helicopter seat [38]

## 1.5. Classification of Helicopter Seats

As mentioned in the previous section, the helicopter seat is an essential part of the helicopter. In a typical helicopter, besides the pilot seats, there are troop (military) seats presented in Figure 1.11, or passenger (civilian) seats presented in Figure 1.12. Their uses and certification requirements are different. Troop seats are generally designed considering simplicity and compactness. On the contrary, civilian seats are more complex since aesthetics and comfort should also be taken into account. The known helicopter passenger seat vendors are Fischer Seats, Safran Seats, BAE Systems, and Martin Baker.

Figure 1.11. A sample troop (military) seat [51]



Figure 1.12. A sample passenger (civilian) seat [52]

Designing and testing requirements for the helicopter seats exist for both military and civilian helicopters. "The Aircraft Crash Survival Design Guide", which contains

criteria for the design of all crashworthiness features including seats of helicopters, was first published in 1967 as Technical 67-22. Detailed requirements for military troop seats were defined in MIL-S-85510, which was first issued in 1981. For civilian helicopter seats, SAE AS8049 was first issued in 1990 [32,34].

Federal Aviation Administration (FAA) and European Aviation Safety Agency (EASA) govern the rules of crashworthiness standards in civilian helicopters. FAA and EASA are founded in United States and Europe, respectively. The name of the standard regulated by EASA is "CS 29 – Certification Specification for Large Rotorcraft". In particular, CS 29.562 deals with the crashworthiness [27]. In this study, satisfying the obligations of CS 29.562, which is issued by European Aviation Safety Agency, is sufficient for the passenger seat certification.

Significant differences exist in the crash environments of military and civilian helicopters. If the military crash resistance design criteria were applied to the civil fleet, a huge mass and cost penalty would be imposed on civilian helicopters. The vertical impact test requirements, which is the focus of this study, for the civilian passenger seat and the military troop seats are presented in Table 1.1 [32].

G means the gravitational acceleration of the earth. Although the gravitational acceleration slightly changes from poles to equator, a single value is used in engineering calculations when the scope of the engineering problem is on or close to Earth.  1 G is taken as 9.807 m/s$^2$ in this study.

Table 1.1. Vertical impact requirements of the seats [32]

|  | Civilian passenger seat | Military troop seats |
|---|---|---|
| **Requirements of:** | CS 29.562 | MIL-S-85510 |
| **Min. peak acceleration [G]** | 30 | 32 |
| **Max. time to min. peak acceleration [s]** | 0.031 | 0.087 |
| **Min. impact velocity [m/s]** | 9.144 | 15.2 |
| **Pitch angle [deg]** | 60 | 60 |
| **Mass of ATD [kg]** | 77 | 77.5 |
| **Floor deformation** | YES | YES |

## 1.6. Scope of the Thesis

The explanations of crash and crashworthiness are done as an introduction to the study. The crashworthiness studies regarding to air vehicles, which include both airplanes and helicopters, are introduced by many researchers [2, 14-44, 50, 53]. These studies are concentrated only on airplanes [21-23, 31], only on helicopters [2, 14-20, 24, 27-29, 32-39, 42-44, 50, 53], and on both air vehicles [25, 26, 30, 40, 41]. Some crashworthiness studies regarding to helicopters are related to seats [32-43] and some are focused on other aspects [2, 14-20, 24-30, 44, 50, 53].

None of the studies on helicopter seats [32-43] investigates the design of fixtures which are needed for the validation of the vertical crash criterion and the floor deformation effect stated in Table 1.1. In this study, the Interchangeable Floor Deformation Unit (IFDU) and the Sled Test Fixture (STF) are designed to validate the civilian helicopter seats in terms of floor deformation effect and vertical crash criterion, respectively. IFDU is a novel design aiming the FEA simulation of floor deformation of helicopter for the validation of the seats. STF is also a novel design aiming the vertical crash simulation of civilian helicopter seats for the validation of seats.

Helicopter crash scenarios, which are constructed by authorities, are thoroughly explained in Chapter 2. The crash test that are performed for these scenarios are described with the justification of the test facility that is used for this study. All design models used in this study are briefly explained in the final section of this chapter giving general design information. These are named as the Simplified Helicopter Seat (SHS), the Interchangeable Floor Deformation Unit (IFDU), and the Sled Test Fixture (STF).

In Chapter 3, considerations in FEA are outlined since they form a basis to all subsequent analyses. These considerations are named as geometry, material properties, mesh types, assembly module, step module, interaction module, and

boundary conditions. The final part of this chapter gives specific information about the bolt preload analysis utilized in this study.

A Simplified Helicopter Seat (SHS) is designed to perform the FEA regarding to crashworthiness as it is explained Chapter 4. The design of Simplified Helicopter Seat (SHS) is justified with its dimensions, and requirements. Bolt preload analysis and crash analysis are performed for the seat. The results are discussed.

A novelty of this study is the design of the Interchangeable Floor Deformation Unit (IFDU) that are discussed in Chapter 5 since none of the researches about air vehicle seats [32-43] is interested in the design and validation of such design that is a requirement of CS 29.562, which is explained in Chapter 2. In Chapter 5, the rationale behind Interchangeable Floor Deformation (IFDU) is outlined. The functionality of IFDU is explained with showing design data. The bolt preload analysis, floor deformation and pin insertion analyses, and crash analysis performed for IFDU are discussed in the final section of this chapter.

In Chapter 6, another novelty of this study is the design and validation of STF considering CS 29.562, which is explained in Chapter 2, since none of the studies [32-43] is interested in validating such test fixture. The crash analysis is done for STF as if it has the same loads with the sled tests, which is explained in Chapter 2.

The conclusions and future works are presented in Chapter 7.

# CHAPTER 2


# HELICOPTER CRASH SCENARIOS AND CRASH TESTS
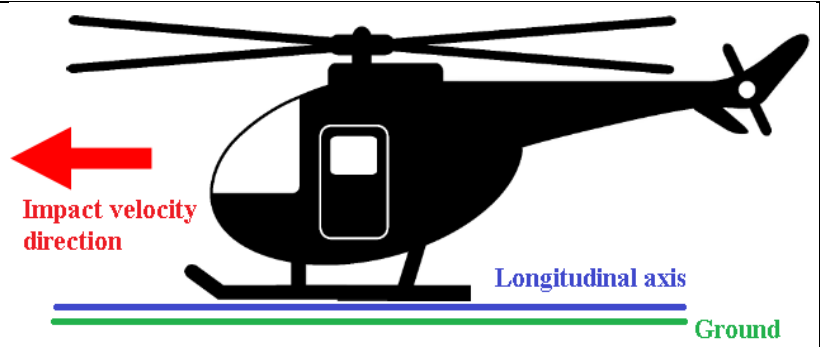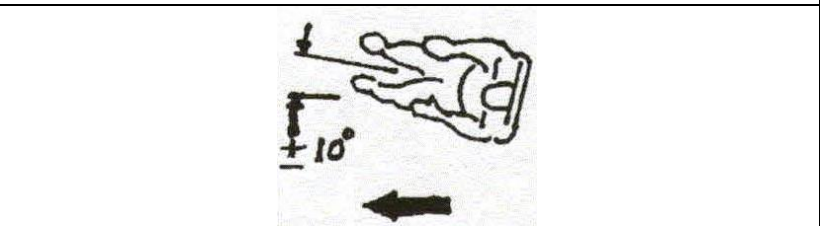

## 2.1. Helicopter Crash Scenarios

The helicopter must be designed to protect all occupants when it is subjected to crash. In other words, each type of seat design is obligated to follow this rule [27]. Since this study concentrates on the civilian passenger seats, the crash scenarios of CS 29.562 are explained in this section.

There are two types of crash for civilian helicopters: downward (ie. vertical) crash and forward (ie. horizontal) crash. Additionally, floor deformation should be considered for both crashes that represents the possible wrap of the floor during the crash. The crash tests are conducted with a 77 kg ATD sitting in normal upright position [27].

The forward impact scenario requires that the impact velocity vector is parallel to the horizontal plane. In addition, the seat is turned $10^0$ in the yaw direction, which is shown in Figure 1.4, with respect to the impact velocity direction. The change in the forward velocity must not be less than 12.802 m/s. The peak floor acceleration must occur in no more than 0.071 s after the impact and must reach a minimum of 18.4 G [27]. All relevant data are presented in Table 2.1. Moreover, the impact pulse of the forward impact and the velocity of impact versus time are presented in Figure 2.1 and Figure 2.2, respectively.

Table 2.1. Forward impact [27,53]

| | |
|---|---|
| Impact direction |  |
| Seat positioning |  |
| Min impact velocity [m/s] | 12.802 |
| Peak acceleration [G] | 18.4 |
| Max duration of peak acceleration [s] | 0.071 |
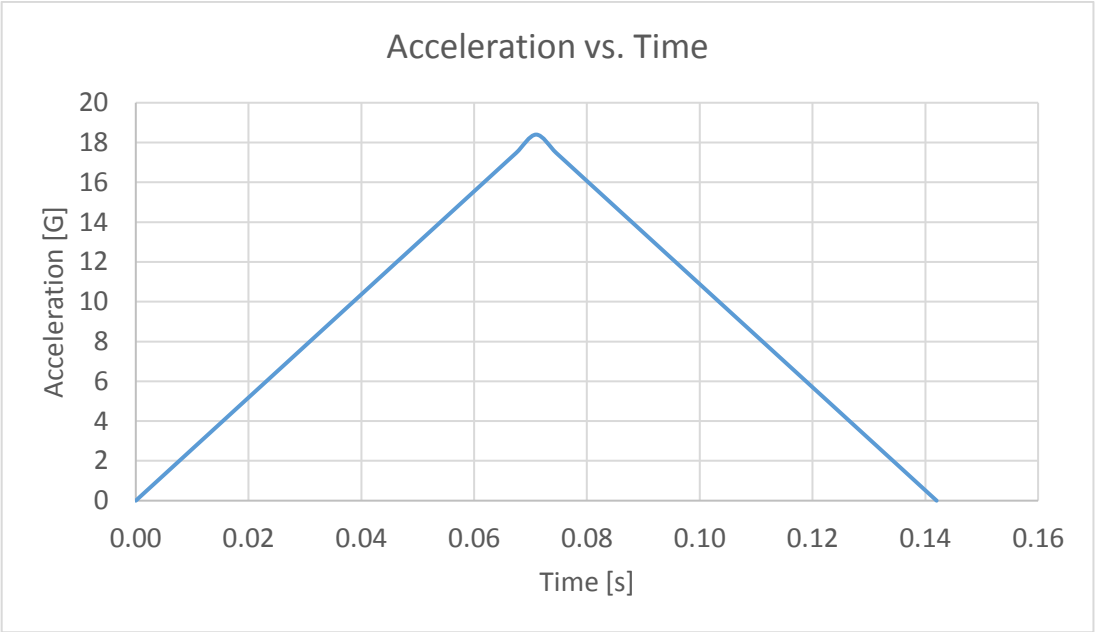


Figure 2.1. Acceleration vs. time (forward crash) [27,53]
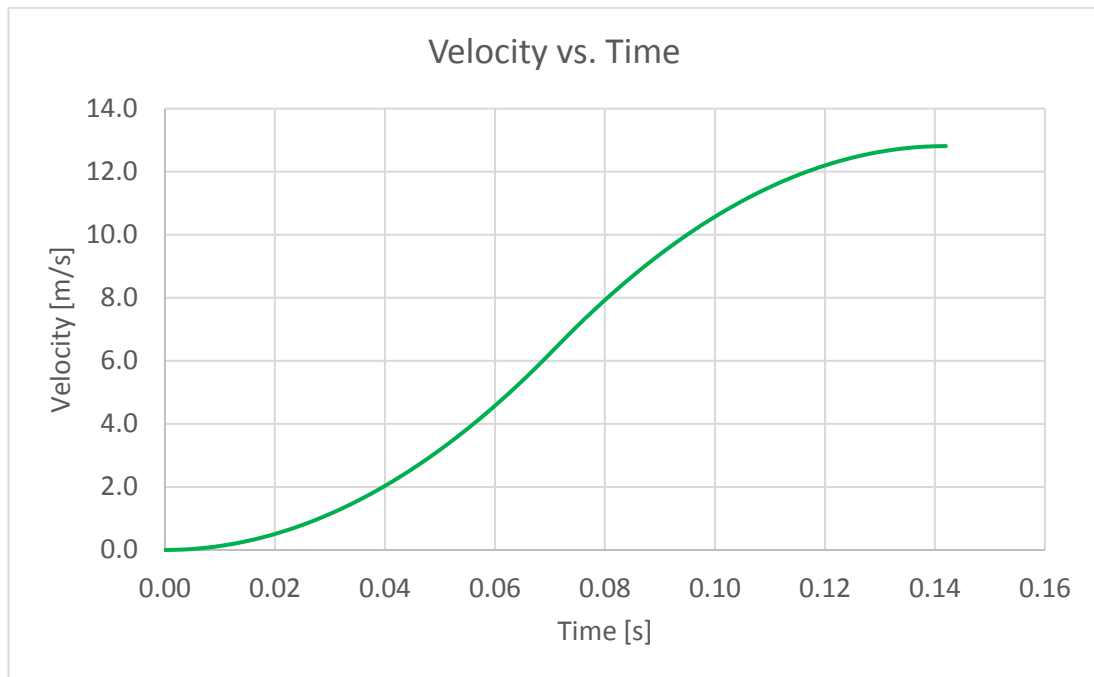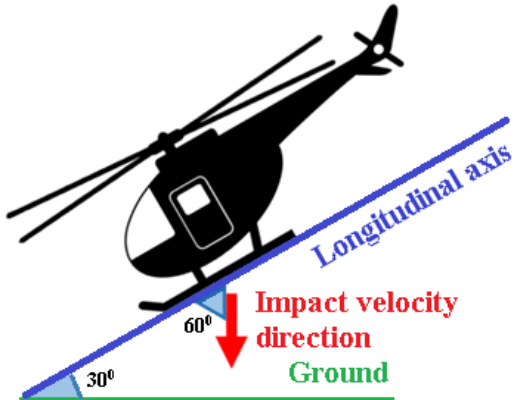
Figure 2.2. Velocity vs. time (forward crash) [27,53]

In the downward crashworthiness scenario, the longitudinal axis of the helicopter is turned to the ground where impact occurs. The angle between the longitudinal axis and the impact velocity vector, which is in z direction, is 60°. The helicopter's lateral axis is perpendicular to the plane containing the impact velocity vector and the longitudinal axis. There is no change in the seat orientation unlike the forward impact. The change in the downward velocity must not be less than 9.144 m/s as displayed in the left column of Table 1.1. The peak floor acceleration must occur in no more than 0.031 s after the impact and must reach a minimum of 30 G [27]. The relevant information regarding to the authority criteria is shown in Table 2.2. In addition, the impact pulse and the related velocity are displayed in Figure 2.3 and Figure 2.4.

Table 2.2. Downward impact [27,53]

| Impact direction |  |
|---|---|
| Seat positioning | Normal position with respect to the helicopter |
| Min impact velocity [m/s] | 9.144 |
| Peak acceleration [G] | 30 |
| Max duration of peak acceleration [s] | 0.031 |
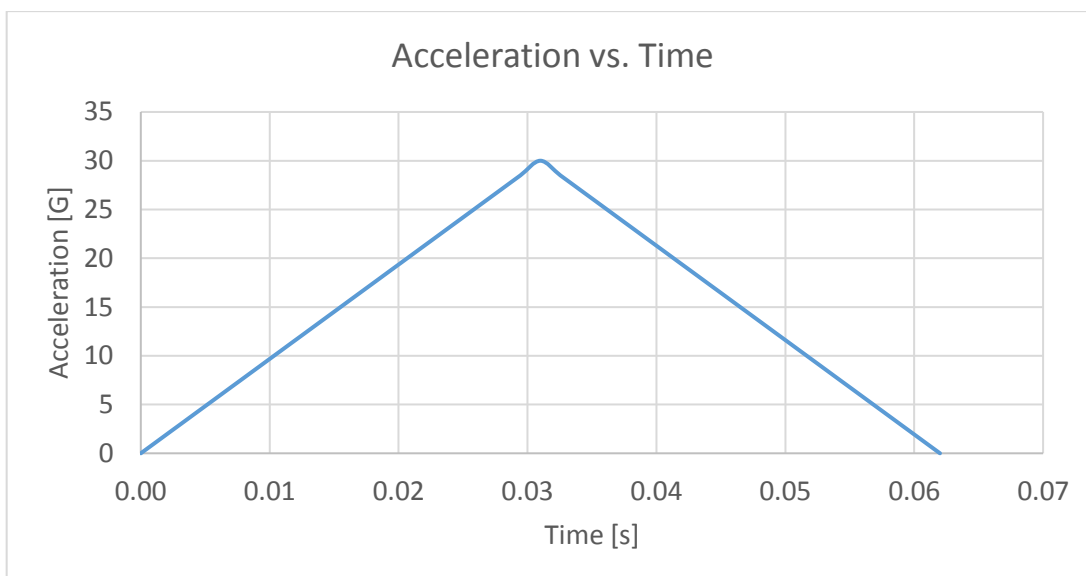


Figure 2.3. Acceleration vs. time (downward crash) [27,53]
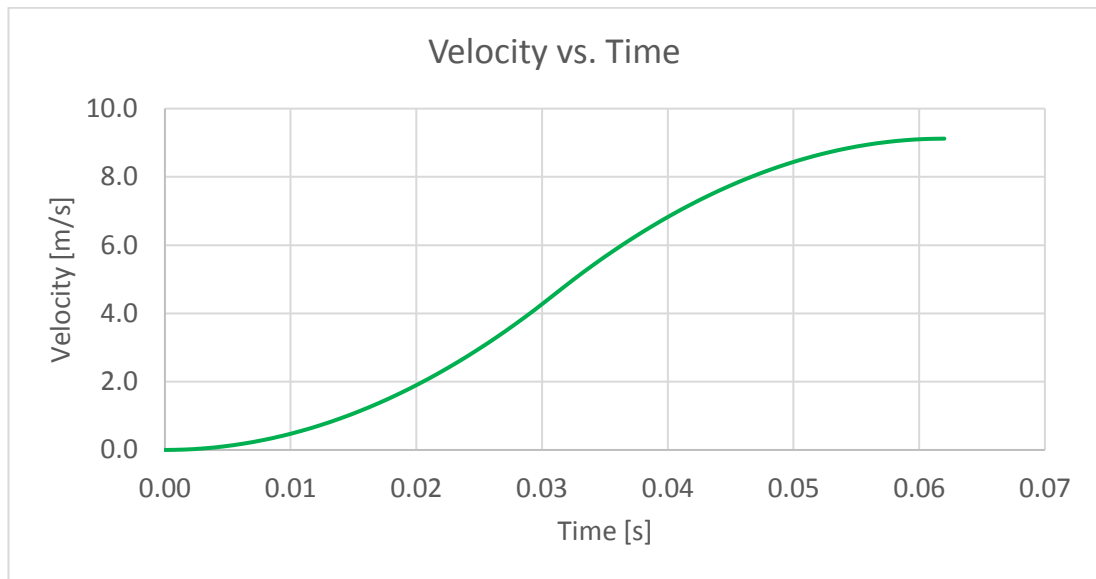
Figure 2.4. Velocity vs. time (downward crash) [27,53]

The floor deformation effect is applied to both of the forward impact and the downward impact before the impact occurs. It is intended to evaluate the seat tracks and the seat leg fitting joints tolerance to angular misalignment prior to the crash [53]. In other words, it accounts possible floor wrap. As shown in Figure 2.5, in the tests the floor deformation fixture is necessary for this purpose. It consists of two parallel beams, called the pitch beam and the roll beam. The roll beam rotates +/- $10^0$ about a longitudinal (x) axis. Then, the pitch beam rotates +/- $10^0$ about a lateral (y) axis.

ORIGINAL
POSITION

NOTE:
FOR CLARITY,
LOAD TRANS-
DUCERS ARE
NOT SHOWN

POSITION
AFTER FLOOR
DEFORMATION

PITCH AXIS
UNDER REAR ₵
LEG ATTACHMENT

ORIGINAL
POSITION

ROLL BEAM

PITCH
BEAM

MINIMUM SEAT TRACK
TO BE TESTED

10° ROLL
LEFT OR RIGHT

DETAIL (A)
EXAMPLE OF AIRCRAFT
TRACK BEAM
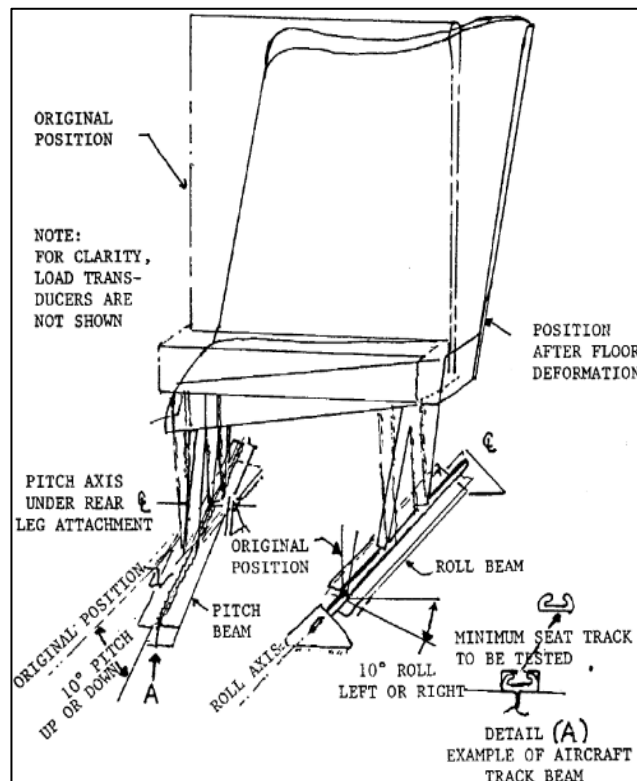
Figure 2.5.  Floor deformation fixture (seat legs attached at floor level) [53]

## 2.2. Crash Test Facilities

The test facilities for crash are used for the certification purposes regarding to the authority approval as described in Section 1.4. They can be grouped based on their impact generation method. They are vertical drop towers, horizontal deceleration and horizontal acceleration type sled facilities.

The drop towers operates on the principle of deceleration. They can be built and operated since they do not require any accelerating or decelerating devices and they use the 1 G gravitational acceleration to have the impact speed prior to impact. These type of test setup works on the principle of destructive tests unlike acceleration and deceleration sled test facilities. This means the replacement of the test specimen before every test. Moreover, they require a lot of vertical space to achieve the impact speed by gravitational acceleration [53]. This vertical space should be carefully designed and reinforced not to have the collapse of the drop tower.

24

The deceleration type sled facilities represent the actual helicopter crash since they occur as deceleration in real life. Hence, the crash loads are applied smoothly as the impact pulse takes place as a deceleration. The test fixture gains the appropriate impact speed first, than it stops in very little time to represent the crash. In other words, the crash takes place at the end of the test by applying the brakes where the face of test specimen and the velocity of sled have the same direction. However, the sled must reach the impact speed with small acceleration in order not to have dynamic behavior prior to the crash. Otherwise, this behavior would affect the test results making confusion with actual crash results. In addition, this could move the test specimen prior to impact [53]. Hence, the length of track of deceleration type sled test facilities is longer compared to acceleration type sled test facilities.

The acceleration type sled facilities provide the impact pulse as a controlled acceleration at the beginning of the test. The face of test specimen and the velocity of sled have opposite directions to observe the crash effects on the test specimen. Being out of position of the test specimen is not an issue in these facilities since the impact takes place at the beginning. Similar with the deceleration sled facilities, after reaching the maximum speed, the sled must stop with small deceleration not to have dynamic behavior of impact [53].

## 2.3. METU-BILTIR Center Vehicle Safety Unit Sled Test Facility

A photo of METU-BILTIR Center Vehicle Safety Unit Sled Test Facility, which is located in Middle East Technical University Campus, Ankara, is shown in Figure 2.6. This sled test facility uses the principle of acceleration type sled. It has a hydraulic piston that starts the impact by applying an initial impact pulse. The hydraulic piston, which behaves as a linear impactor, contacts with the sled until the impact pulse is over. After the impact pulse, the test assembly resumes its action some time (in milliseconds) before it stops. The sled forms a base to the test fixture and it transforms the acceleration of hydraulic pistons. 3D model of the sled in METU-BILTIR Center Vehicle Safety Unit is displayed in Figure 2.7.

Figure 2.6. METU-BILTIR Center Vehicle Safety Unit Sled Test Facility [54]
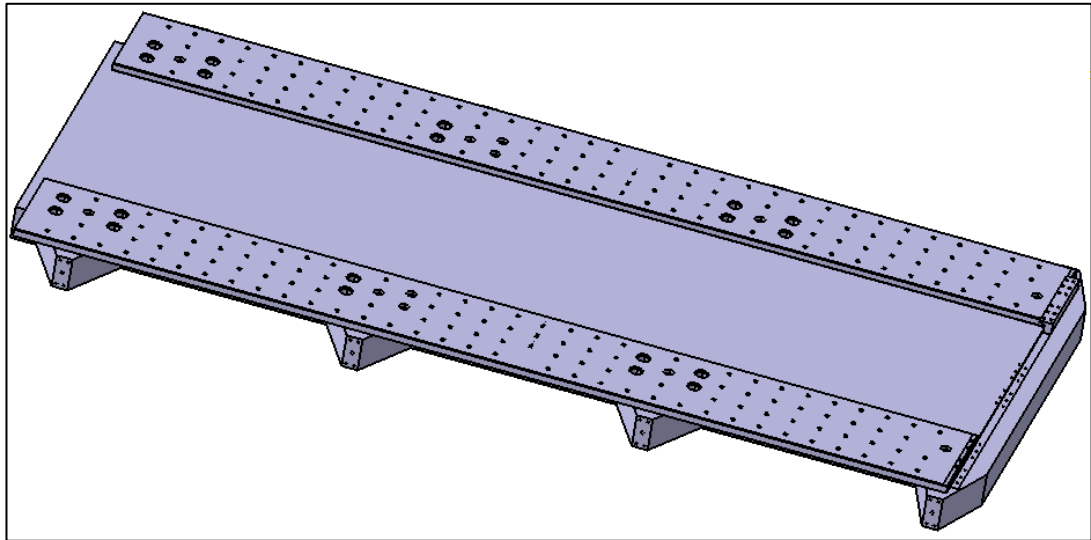
Figure 2.7. 3D model of the sled in METU-BILTIR Center Vehicle Safety Unit

The capabilities of this facility includes carrying out accredited sled tests about the safety belt tests of automobiles, whiplash tests of Euro NCAP, seat tests of land and marine vehicles. Data of tests are acquired with high speed cameras and data acquisition systems. Frontal and rear crash simulation tests, whiplash tests, seatbelt and airbag development systems tests, seat anchorages and head restraint tests, child restraint systems tests, road ambulances and medical devices tests, marine vehicles and air vehicles seat tests are performed on the sled [54].

## 2.4. General Design Information of the Study

As mentioned in Section 2.3, the sled is necessary for performing sled tests of helicopter seats. However, the downward impact and the floor deformation criteria, which are described in Section 2.1, require designing of the Sled Test Fixture (STF), the Interchangeable Floor Deformation Unit (IFDU), and the Simplified Helicopter Seat (SHS). In addition, the 77 kg dummy mass (DM) is designed to simulate the 77 kg ATD stated in Section 2.1. IFDU is mounted to STF. SHS is mounted to IFDU. DM is mounted to SHS. All above items are located on the sled of the test system as shown in Figure 2.8.
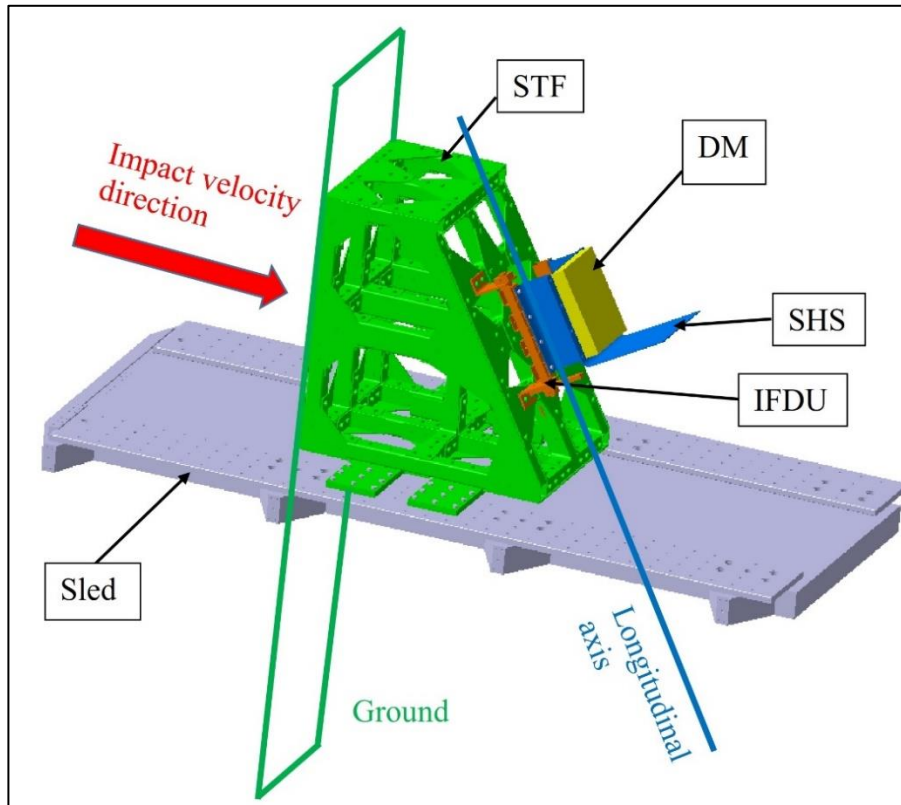
Figure 2.8. General assembly of the specimen on the sled

STF is designed to ensure $60^0$ slope with impact velocity direction, which is explained in Section 2.1, preserving its structural integrity during crash tests. STF is thoroughly explained in Chapter 6.

IFDU is designed to observe the floor deformation effect on SHS. As outlined in Section 2.1, IFDU must allow $10^0$ roll rotation and $10^0$ pitch rotation when it is assembled to SHS with DM. Moreover, it must protect its structural integrity when it is subjected to crash loads. IFDU is investigated in Chapter 5.

SHS is designed to validate IFDU. In this study, a real helicopter passenger seat cannot be used since design data of passenger seat vendors are commercially protected and it is not available. The detailed information about SHS is shared in Chapter 4.

# CHAPTER 3

# GENERAL CONSIDERATIONS IN FINITE ENEMENT ANALYSIS

## 3.1. General Information about Finite Element Analysis

Finite Element Analysis (FEA) of a part or an assembly consists of applying the appropriate load and the boundary conditions, which represent real life applications, material properties, meshing. It is utilized for the validation of design with its computational capabilities. Moreover, FEA is a crucial tool since it may decrease the number of drop or sled tests and therefore testing costs.

Two types of analyses are performed in this study named "quasi-static" and "dynamic" FEA. These terms differ in terms of their loading rate. Quasi-static analysis involves loadings where strain rate is close to zero, generally between $10^{-4}$/s and $10^{-2}$/s. On the other hand, the forces created by collusions are exerted and removed in very short time in dynamic analysis [55]. The strain rate of dynamic loading ranges between $10^{-2}$/s and $10^{2}$/s. The crash analyses in this study are dynamic by their nature.

The implicit method deals with the solution of a system of equations implicitly at each solution increment. A set of nonlinear equations must be solved at each time increment. The implicit solvers have stable results but they require many computational resources to achieve a solution. On the other hand, the explicit method finds a solution forward through time in small time increments. The explicit procedure performs a large number of small time increments. Each increment is inexpensive compared to the implicit methods because there is no solution for a set of simultaneous equations in time unlike the explicit methods. Although the explicit method is faster, the errors may accumulate if correct inputs are not used [56].

In this study, Abaqus 6.14, which is a commercially available FEA, is utilized as the analysis tool since it is proven and widely used in automotive and aerospace industry.

Abaqus is based on the actual time period analysis. Abaqus/Standard (ie. implicit solver) and Abaqus/Explicit sub tools are utilized for analyses [56].

Abaqus/Standard is utilized for performing static or quasi-static analyses. It has the implicit built-in solver to compute and solve the equations in which all contact conditions must be carefully defined one by one for the analysis.

Abaqus/Explicit is ideally suited for the dynamic analyses with performing incremental calculations. It is computationally efficient for the analysis of large models. Moreover, it can solve the problems that have complex contacts by simplifying the treatment of contacts. Abaqus/Explicit can also be applied to the analysis of quasi-static processes, which is explained in detail in Section 3.2.9.

FEA in this study is carried out on the computer that has Intel Core i7-4700MQ CPU @2.40 Ghz, 4 cores, 8 logical processors, 8 GB RAM, NVIDIA GeForce GT 470M. The actual completion durations of all FEA regarding to SHS, IFDU, and STF are expressed in Section 4.3, Section 4.4, Section 5.3, Section 5.4, Section 5.5, and Section 6.3. However, the durations of FEA runs may change if a computer with different configuration is used.

## 3.2. Finite Element Analysis Considerations in the Study

Finite Element Analysis (FEA) requires the correct input data in order to get reasonable results. Geometry, material properties, mesh types, assembly module, step module, interaction module, and boundary conditions play important roles in FEA. These are discussed in the following sub sections to form a basis for all analyses of SHS, as explained in Chapter 4, IFDU, as explained in Chapter 5, and STF, as explained in Chapter 6.

Two specialized techniques: "mapping" and "utilization of Abaqus/Explicit to quasi-static cases", are explained in Section 3.2.9 and Section 3.2.10, respectively. Mapping is used for the analyses of SHS as described in Chapter 4 and IFDU as described in Chapter 5. Whereas, the utilization of Abaqus/Explicit is applied to the floor

deformation and pin insertion analyses of IFDU as seen in Section 5.4. Notation used in this study for parts and fasteners is also briefed in Section 3.2.11.

### 3.2.1. Geometry

The CAD software CATIA V5 has been used to create the geometry of parts. The 3D geometry is the starting point for design, analysis and manufacturing. The part to be manufactured, which is the physical part, and CAD data of the part must be exactly the same with the designed geometry. In FEA, geometry of the part may be modified to reduce time cost of modeling, meshing, and analysis. The modifications of this study are the omissions of fillets and radii. Physical form and analysis form of floor support are shown in Figure 3.1.
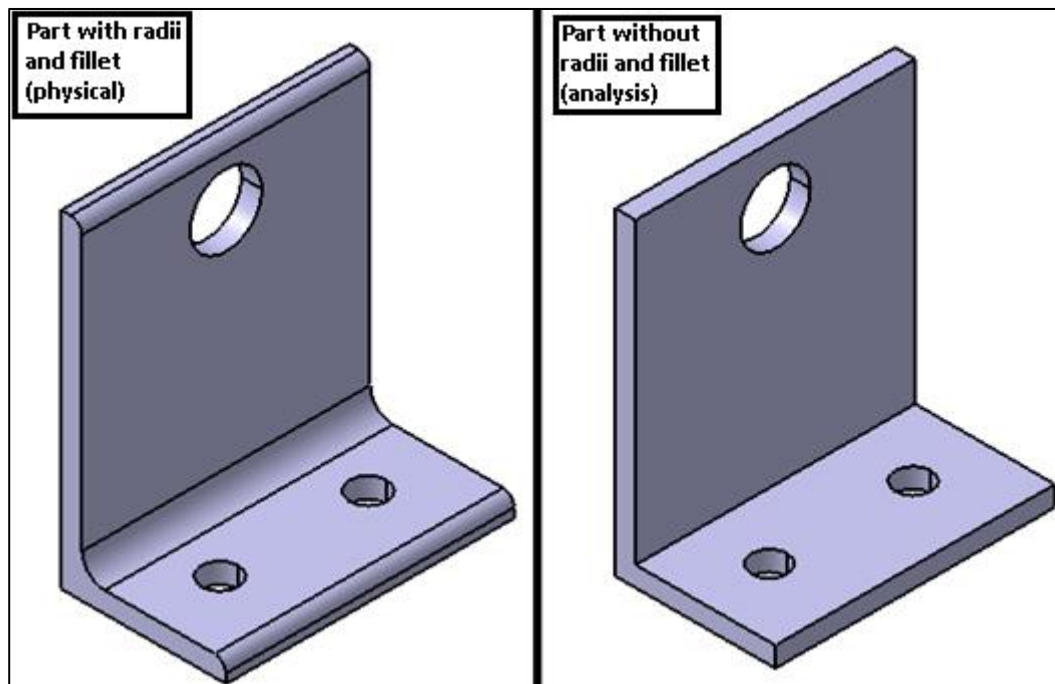


Figure 3.1. Comparison of physical geometry used in Finite Element Analysis

### 3.2.2. Material Properties

All materials used in this study are either aluminum alloys or steel alloys. In this study, the selection of the types of aluminum and steel alloys are based on their availability in the market.

For all steel parts, A284 Steel, Grade D is selected as the basic material since they are highly available in the market. On the other hand, the plasticity data of A284 Steel, Grade D is not available. Therefore, a correlation is done between A284 Steel Grade D, and Steel 4340, which is present in the academic literature [57]. This correlation is explained in Appendix A. The strain rate effect for the material is neglected for both quasi-static analyses and crash analyses. A284 Steel, Grade D are utilized for IFDU and STF, where the design details are given in Section 5.1 and Section 6.1, respectively.

8.8 Grade Steel is selected for all bolts and nuts since this material type of fasteners are highly available in the industry. The same correlation approach of A284 Steel, Grade D is also utilized for 8.8 Grade Steel as it is explained in Appendix A. The strain rate effect for the material is neglected for both quasi-static analyses and crash analyses. This material is utilized for all fasteners of SHS, which is described in Section 4.1, IFDU, which is explained in Section 5.1, and STF, which is described in Section 6.1. In addition, it is used for the pins of IFDU, which is outlined in Section 5.1.

Al 2024-T351 aluminum alloy is preferred for the parts of SHS which is explained in Section 4.1. This material is also available in the industry. Its plasticity data is available in the literature [57] whereas the strain rate effect for the material is neglected for both quasi-static analyses and crash analyses.

Some important properties that are created from existing references [57,58], or from engineering interpolation are tabulated in Table 3.1.

Table 3.1. Mechanical properties of materials

| Material | A284 Steel, Grade D | 8.8 Grade Steel | Al 2024-T351 |
|---|---|---|---|
| Density [kg/m$^3$] | 7850 | 7850 | 2780 |
| Poisson's Ratio [m/m] | 0.29 | 0.29 | 0.33 |
| Modulus of Elasticity [GPa] | 200.0 | 200.0 | 73.1 |
| (True) Yield Strength [MPa] | 230.0 | 543.9 | 265.0 |
| (True) Ultimate Tensile Strength [MPa] | 338.3 | 800.0 | 547.9 |

### 3.2.3. Mesh Types

Meshing plays a key role for the analysis since the results can be highly affected if inappropriate meshing is used. The analysis would have a time burden if the meshing is not satisfactory. The meshing elements, the number of meshes, and the meshing library are important criteria for this purpose.

The selection of meshing element is crucial to solve the problems. Abaqus has an extensive element library to solve different kind of problems such as continuum, shell, rigid, beam elements [56]. In addition, the correct choice of the mesh element could reduce the time cost of analysis. In this study, C3D8R continuum element, which is presented in Figure 3.2, is used. "C", "3D", "8", and "R" correspond to "continuum", "three dimensional element", "eight nodes", and "reduced integration", respectively. This type of element is suitable for all analyses of this study which are investigated in Chapter 4, Chapter 5, and Chapter 6. Moreover, this element is appropriate for the mapping process which is explained in Section 3.2.8.
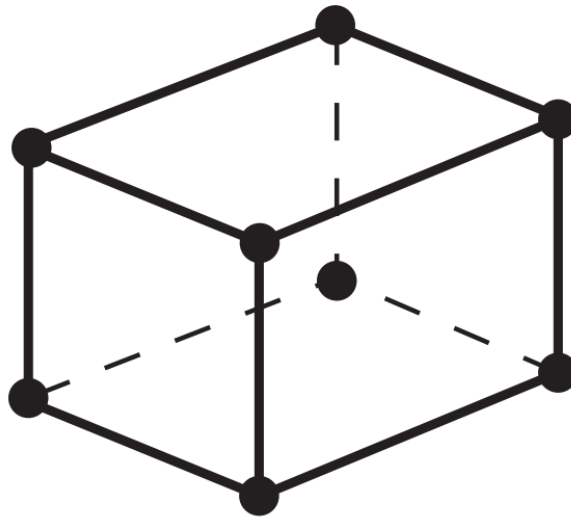


Figure 3.2. C3D8R meshing element

The number of mesh elements in an analysis dramatically effects the run times of FEA. The results of the analyses should be obtained with less elements, not more than $10^5$ elements if possible.

The mesh density should be carefully selected especially for shaft and hole contacts to obtain reasonable outcomes. In this study, at least 4 element rows are generated per thickness, which is exemplified in Figure 3.3. The reason for this approach is to detect the stresses at different locations of the same cross section. If less rows were used, the results would be over simplified.
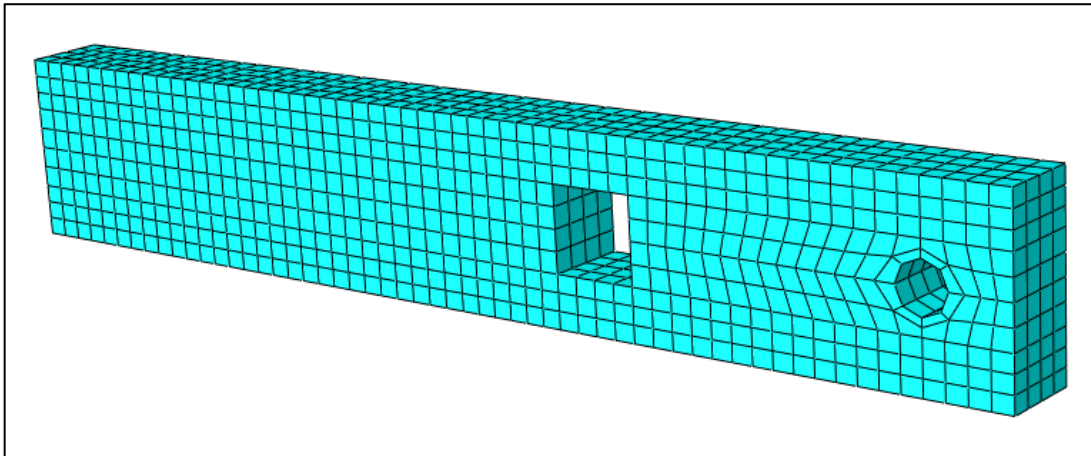


Figure 3.3. The mesh elements of the lever

### 3.2.4. Assembly Module

The assembly module provides the mounting of parts with fasteners. Although, constructing the assembly is a straightforward process, it must be done with great care because the analysis does not give warning or error if a wrong assembly, in which two or more clashing parts exist, is formed.

The parts can be assembled by using position constraints or by directly translating and rotating each part or fastener in the Cartesian coordinate system. Constraining describes the fixation of each part or fastener in three translational motions (x − y − z axes) and three rotational motions about these axes.

### 3.2.5. Step Module

The step module defines each process of which the analysis consists of. It includes the initial step and the analysis steps. Initial steps provides the definition of initial

34

boundary conditions and interactions. The analysis step is the actual step that described whether the analysis is dynamic or quasi-static. The total time of the analysis is determined in this step. It directly affects the mesh selection and boundary conditions because some meshes and boundary conditions are only valid for specific analysis steps [56]. Each of the crash analyses of SHS as seen in Section 4.4, IFDU as seen in Section 5.5, and STF as seen in Section 6.3 is selected as 100 ms. to observe the effects of the impact. This value is sufficient to observe the effects of crash since the downward crash criteria is considered in a 62 ms time period as stated in Table 2.2.

### 3.2.6. Interaction Module

The interaction module integrates the contacting regions of connecting parts and fasteners [56]. If the interaction is not defined in the analysis model, the algorithm cannot understand the mating surfaces contacts or not even if they are connected in the assembly module. General explicit contact, surface-to-surface contacts, tie constraints, coupling constraints are used in interaction models of this study.

General explicit contact does not need any specific contact type for any contacting surfaces. It readily identifies the contacting regions of each coupled parts [56]. It is embedded in Abaqus/Explicit and is used for crash analyses of SHS as seen in Section 4.4, IFDU as seen in Section 5.5, and STF as seen in Section 6.3. Moreover, it is used for the floor deformation and pin insertion analyses of IFDU as seen in Section 5.4.

Surface-to-surface contacts are useful for locating the erroneous contacts easier than general explicit contact. However, this type of contacts needs the selection of contacting surfaces one-by-one, which is a cumbersome task. Tie constraints allows the fusion of two regions of adjoining parts. Tie constraints state that these two regions are moved together as they have the same displacement. Surface-to-surface contacts and tie constraints are used for bolt preload analyses of SHS as observed in Section 4.3 and IFDU as observed in Section 5.3. Moreover, the tie constraints are used to fix the DM to SHS.

Coupling constraints are utilized to constrain the motion of a surface with its connecting surface [56]. They are used to transmit the motion from one part to another. They are utilized for the floor deformation and pin insertion analyses of IFDU as observed in Section 5.4 where motion transmission is needed. Its details are explained in Section 5.1 and Section 5.2.

### 3.2.7. Boundary Conditions

Boundary conditions are the driving tools for the analysis. They can be applied to the assemblies fully or partially. They have a huge influence on the analysis directly affecting the results. The boundary conditions are the initial inputs of analyses, the fixation of parts, the rotation of parts, and the translation of parts.

The initial inputs are applied at time=0 of the analyses. They are mainly derived from the regulations of CS 29.562. The initial impact velocity of 9.144 m/s, as stated in Table 2.2, is used for the crash analysis of SHS as seen in Section 4.4 and the crash analysis of IFDU as seen in Section 5.5.

The fixation of parts is used for the fixation of rigid plane where SHS crashes as seen in Section 4.4 or IFDU crashes to the rigid plane as seen in Section 5.5.

The rotation boundary condition is performed to give the $10^0$ rotation in roll and pitch directions as explained in Section 2.1. The translation boundary condition is used for the movement of pins to lock IFDU mechanism, which is detailed in Section 5.1. Both boundary conditions are used for the floor deformation and pin insertion analyses as seen in Section 5.4. Moreover, impact pulse of Figure 2.3 is also a translational boundary condition utilized for the crash analysis of STF as seen in Section 6.3.

### 3.2.8. Mapping

The mapping is a procedure which is used for the transformation of FEA results as the initial condition to another analysis. This is done because the predecessor analysis has an influence on the successor analysis.

Bolt preload analysis of SHS as seen in Section 4.3 is mapped into the crash analysis of SHS as given in Section 4.4. Bolt preload analysis of IFDU as given in Section 5.3 is mapped into the floor deformation and pin insertion analyses of IFDU as given in Section 5.4. The floor deformation and pin insertion analyses of IFDU as given in Section 5.4 are mapped into the crash analysis of IFDU as given in Section 4.4.

### 3.2.9. Utilization of Abaqus/Explicit for Quasi-Static Cases

Although Abaqus/Standard can be used for quasi-static analyses, it is not suitable for assemblies that have complex contacts. Abaqus/Explicit can handle these kind of analyses better as it is outlined in the interaction module as seen in Section 3.2.6.

It is impractical to simulate the event in its natural time when Abaqus/Explicit is used for a quasi-static case. The aim is to select the shortest time period considering inertial forces remain insignificant. If the time period is shortened too much, the dynamic affects will dominate increasing the kinetic energy which is not desired in quasi-static analyses. The ratio of the kinetic energy to the internal energy must be close to zero for the success of Abaqus/Explicit when it is used for quasi-static processes. On the contrary, if the time period is too long, time cost of the analysis will increase although the result is quasi-static.

The utilization of Abaqus/Explicit for quasi-static cases is carried out for the floor deformation and pin insertion analyses as seen in Section 4.4. The success of these analyses are investigated in Appendix B.

### 3.2.10. Information about Bolt Preload Analysis

A bolt and a nut are designed as a single fastener as it is thoroughly explained in Section 3.2.3. Threads of bolts and nuts are not fully modelled with their threads. They are modelled as if they have cylindrical contacting surfaces. This approach is suitable since the structural behavior of threads is not included in this study.

"Bolt and nut meshing" require special attention since they are not meshed separately. Moreover, their threads are not modelled for simplicity. In other words, bolts and nuts

are modelled and meshed as if they are a single part. M12x10 analysis part is exemplified as shown in Figure 3.4. M12 or Ø 12 mm shows the diameter value. However, 10 mm, which is the height value, shows the initial height of clamped parts. It does not represent the height of the bolt.
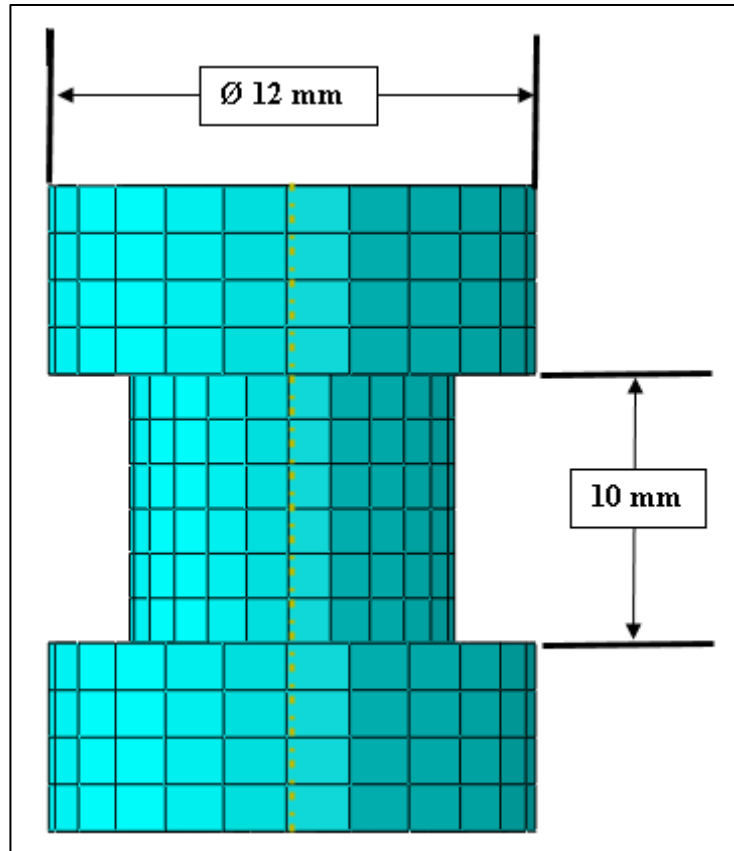


Figure 3.4. Meshing of bolt and nut combination

Bolt preload is created by employment of the fastening of bolts and nuts. Applying torque to the bolts and/or the nuts makes the bolts preloaded. In other words, the bolts will be in tension and the joined parts will be in compression after the torque application. Hence, they offer joining of two or more parts illustrated in Figure 3.5.
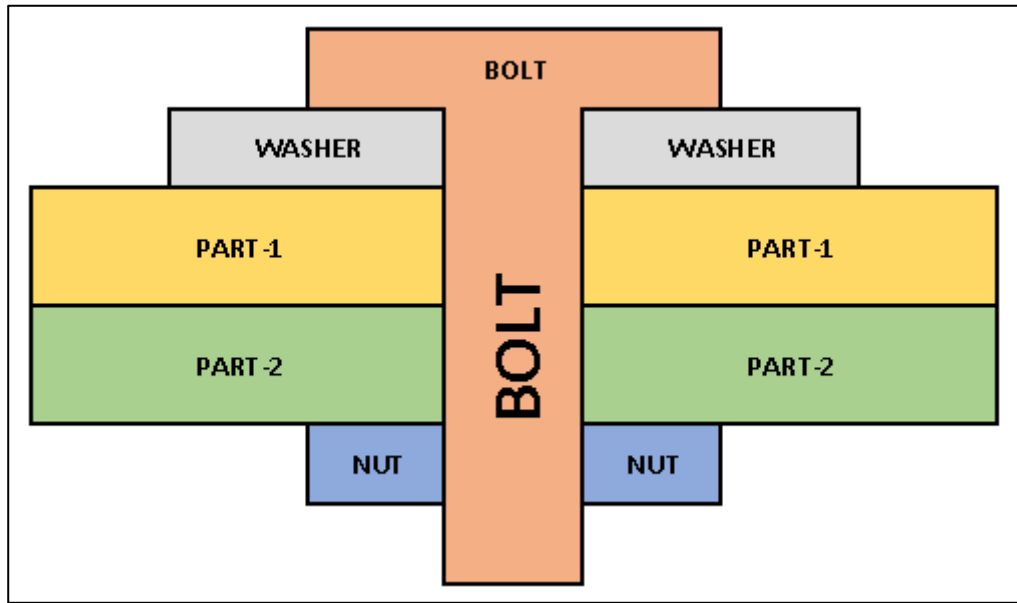
Figure 3.5. Cross-section illustration of bolt and nut combination

If the bolt preload approach is not utilized in the analysis, bolt – nut fastening couples do not make any difference from pins which do not include any preload. The bolt preload approach should be carefully examined. When the bolt preload is lower than the desired preload range, the adjoining parts may dissemble due to the lack of the clamping force. On the contrary, when the bolt preload is higher than the desired preload range, it may harm the adjoining materials, bolt or nut.

Since bolts and nuts are fastened by applying torques, the application of torques should be controlled by torque values, which vary with nominal diameter of bolts and nuts. In this study, the torque values are taken from ordinary industrial catalogues. In addition, these torque values must be converted to bolt preload forces by using mathematical formulae [59].

Bolt preload analysis is performed prior to the subsequent analyses to observe the effects of the stresses caused by bolt preloads. It is investigated in the bolt preload analysis of SHS as seen in Section 4.3 and the bolt preload analysis of IFDU as seen in Section 5.3.

### 3.2.11. Notation Used in the Study for Parts and Fasteners

The study consists of many parts and fasteners so a notation rule is needed to designate them.

The first column of a part is "P" as a shortcut of "part". The second, third, and fourth columns show the unique number of a unique part. The fifth column is period sign. The sixth column is the instance number that means the number of the same part. For instance, P390.2 means that the 2$^{nd}$ unit of P390 parts.

The first column of a fastener is "M" as a shortcut of "metric". After "M" the nominal diameter and the length of the fastener are written with "x" sign between them. Then, period sign and the instance number comes. For instance, M12x10.4 means that the 4$^{th}$ unit of M12x10 fasteners.

# CHAPTER 4

# DESIGN AND ANALYSES OF THE SIMPLIFIED HELICOPTER SEAT

## 4.1. Design Information of the Simplified Helicopter Seat

As explained in Section 1.4, the helicopters use the passenger seats that have energy absorption system. The Simplified Helicopter Seat (SHS) is designed instead of a real helicopter seat since the designs of passengers seats are protected in terms of intellectual property and cannot be used for research purposes. SHS is utilized for the validation of the Interchangeable Floor Deformation Unit (IFDU) and the Sled Test Fixture (STF) as it is expressed in Section 2.8. It does not have any energy absorption system since it is not in the focus of the study.

The seat bucket and the seat legs are mounted to each other with eight M12x10 fasteners. SHS model is displayed in Figure 4.1 with its outer dimensions. The outer dimensions are consistent with a typical helicopter passenger seat. In addition, the thicknesses of the seat bucket and the seat leg are chosen as 5 mm to balance the mass of SHS.
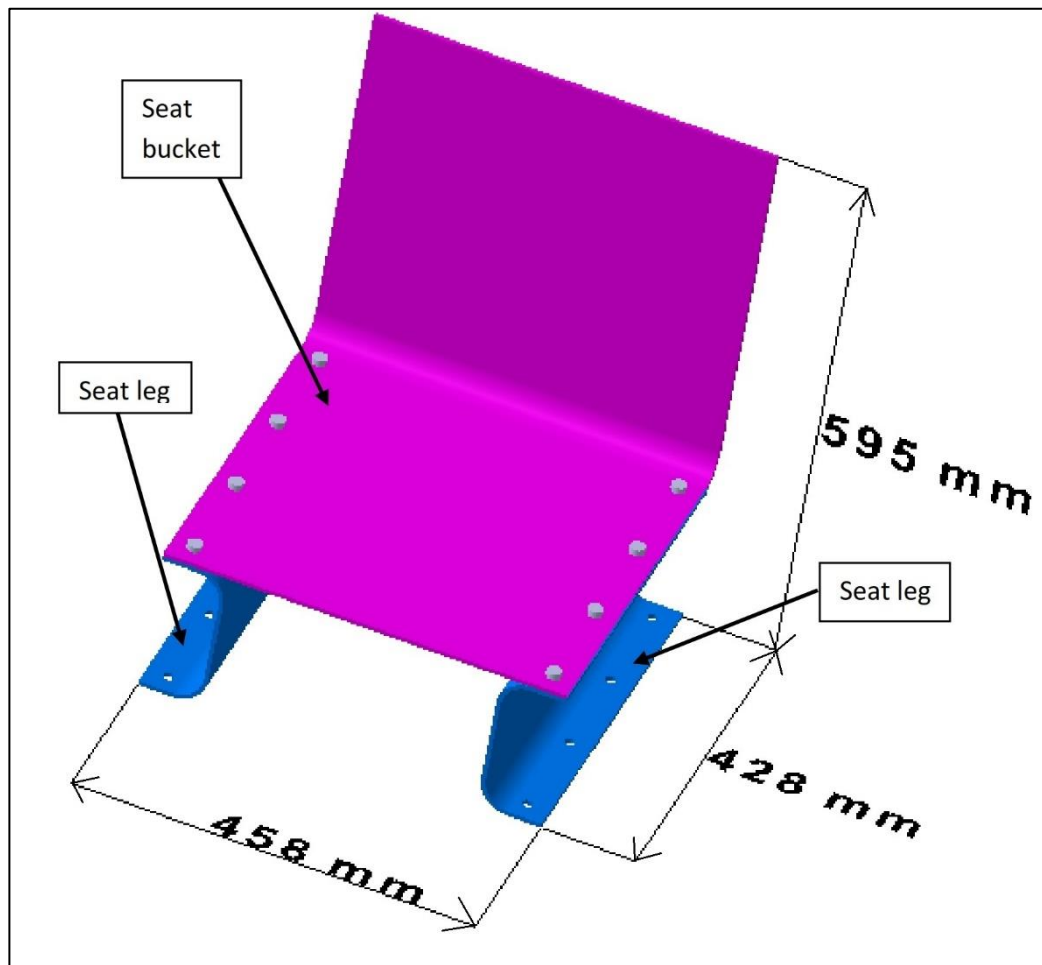
Figure 4.1. The model of the Simplified Helicopter Seat

SHS consists of two seat legs (P390) and one seat bucket (P460) that are made of Al 2024-T351 material. The critical dimensions of the seat legs and the seat bucket are visualized in Figure 4.2 and Figure 4.3, respectively.
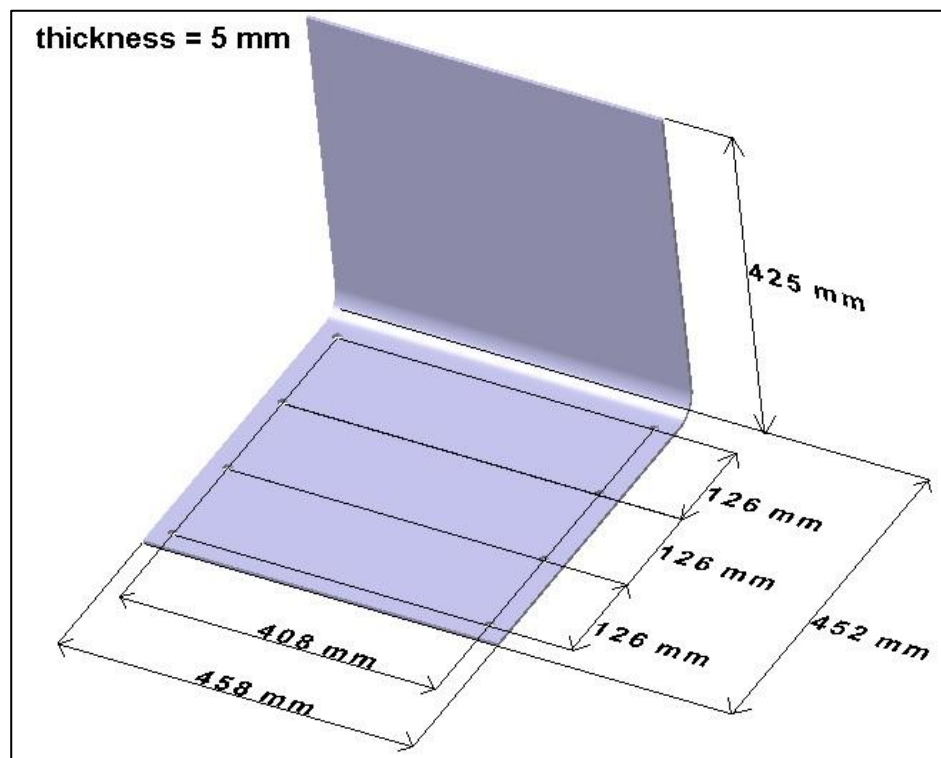
Figure 4.2. Dimensions of the seat bucket (P460)
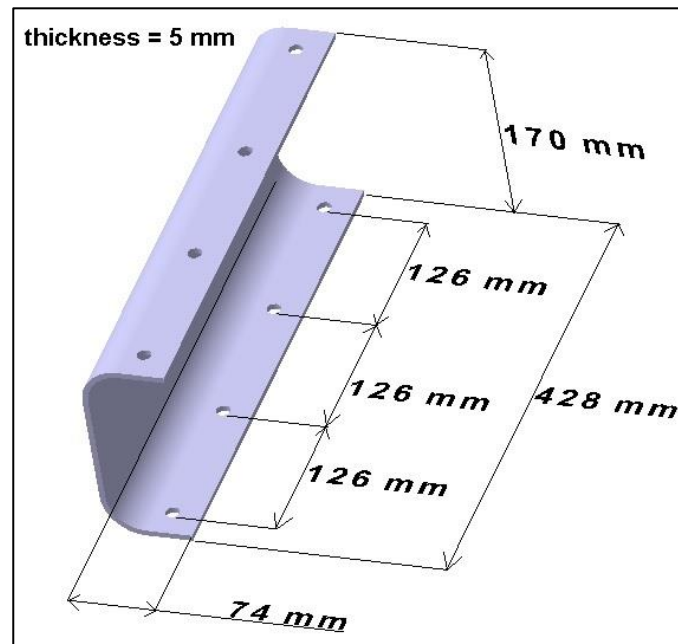


Figure 4.3. Dimensions of the seat leg (P390)

For the design, manufacturability and the low cost are considered. For these purposes, sheet metal part design is preferred for the seat bucket and the seat legs. Besides, primary materials of the parts are selected as aluminum.

The outer dimensions of the seat bucket (P460) and the seat legs (P390) are selected to balance the mass and the outer dimensions of SHS since it must represent the properties of a typical helicopter passenger seat. The mass data of SHS is displayed in Table 4.1 where all fasteners of SHS have a total mass of 0.30 kg. Resultantly, SHS has a mass of 8.83 kg.

Table 4.1. Mass data of the Simplified Helicopter Seat

| Part No | Part Name | Material | Unit Mass (kg) | Qty. | Total Mass (kg) |
|---------|-----------|----------|----------------|------|-----------------|
| P390A | Seat Leg | Al 2024-T351 | 1.61 | 2 | 3.22 |
| P460A | Seat Bucket | Al 2024-T351 | 5.31 | 1 | 5.31 |

**4.2. Finite Element Information of the Simplified Helicopter Seat**

SHS must be designed in a manner that it must withstand the downward impact loads mentioned in Section 2.1. Finite element analysis is performed in order to achieve this goal. In order to have a successful analysis 77 kg mass effect, which is the mass of ATD as seen in Table 1.1, on SHS must be included.

As outlined in Section 2.4, 77 kg dummy mass (DM), which has the part number of P470, is used in the analysis in order to reflect the mass effect on the seat as seen in Figure 4.4. DM is a rectangular block made of steel. It is fixed to SHS without the usage of any fasteners by using tie constraints in FEA as stated in Section 3.2.6.
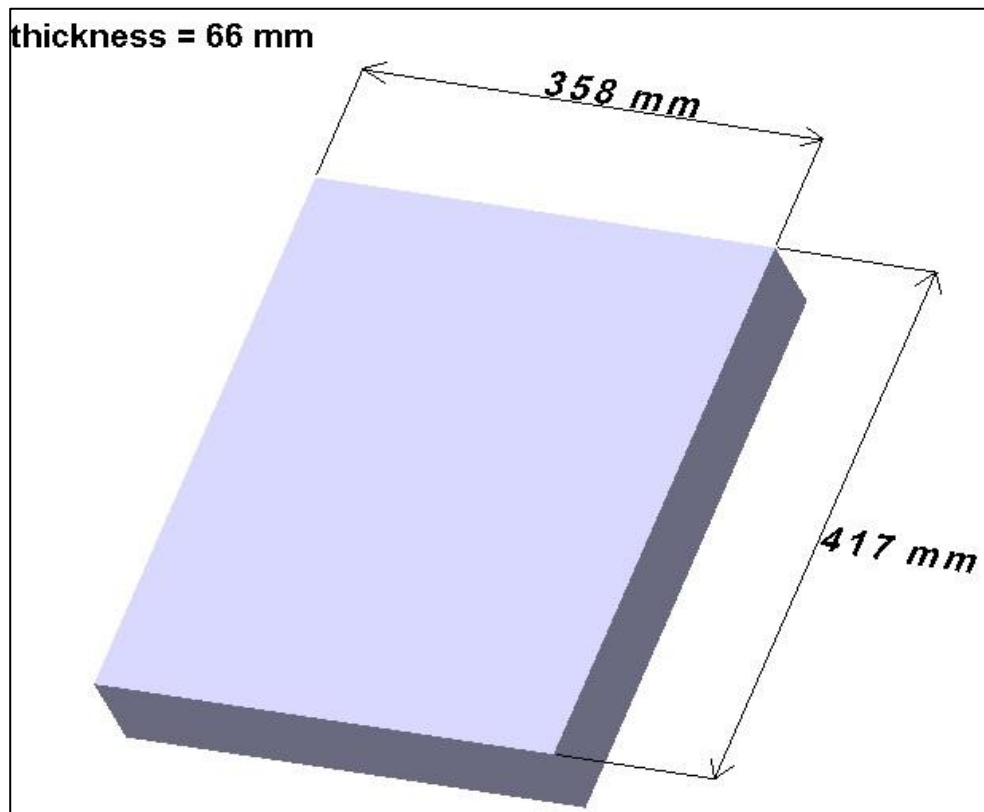
Figure 4.4. The illustration of the 77 kg dummy mass (DM)

Another part that is created for FEA is the rigid plane representing the ground, which is shown in Figure 4.5. It is the 2D crashing plane for SHS as outlined in Section 3.2.7.
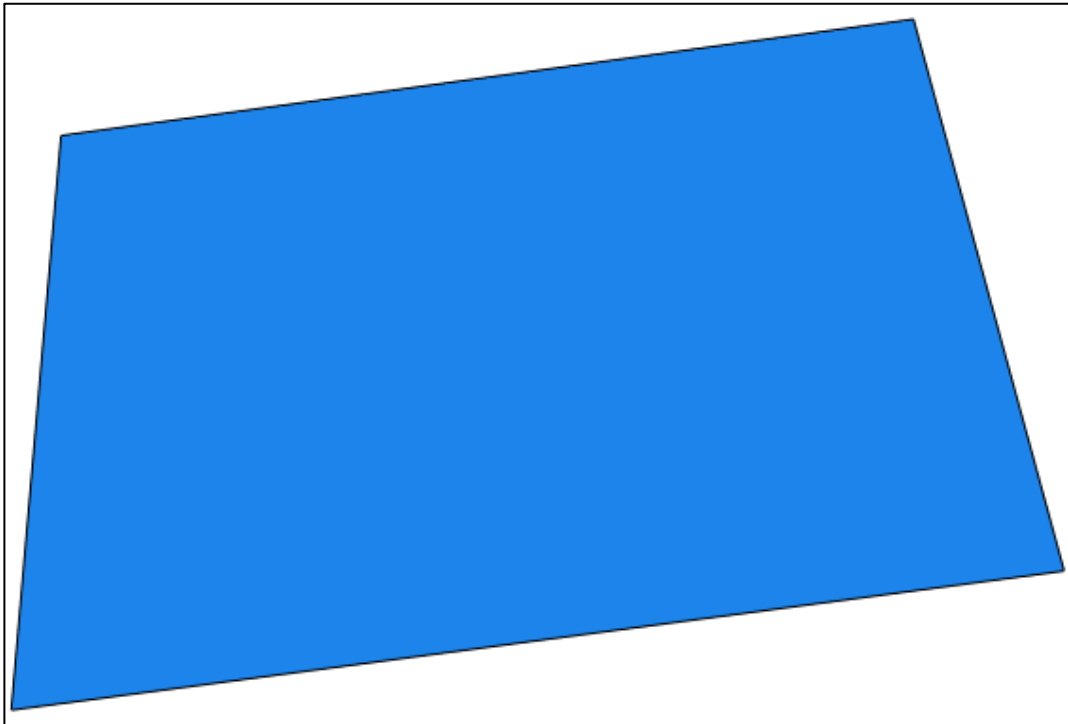
Figure 4.5. The rigid plane

The parts and fasteners of FEA displayed in Figure 4.6 is explained in Section 4.3.
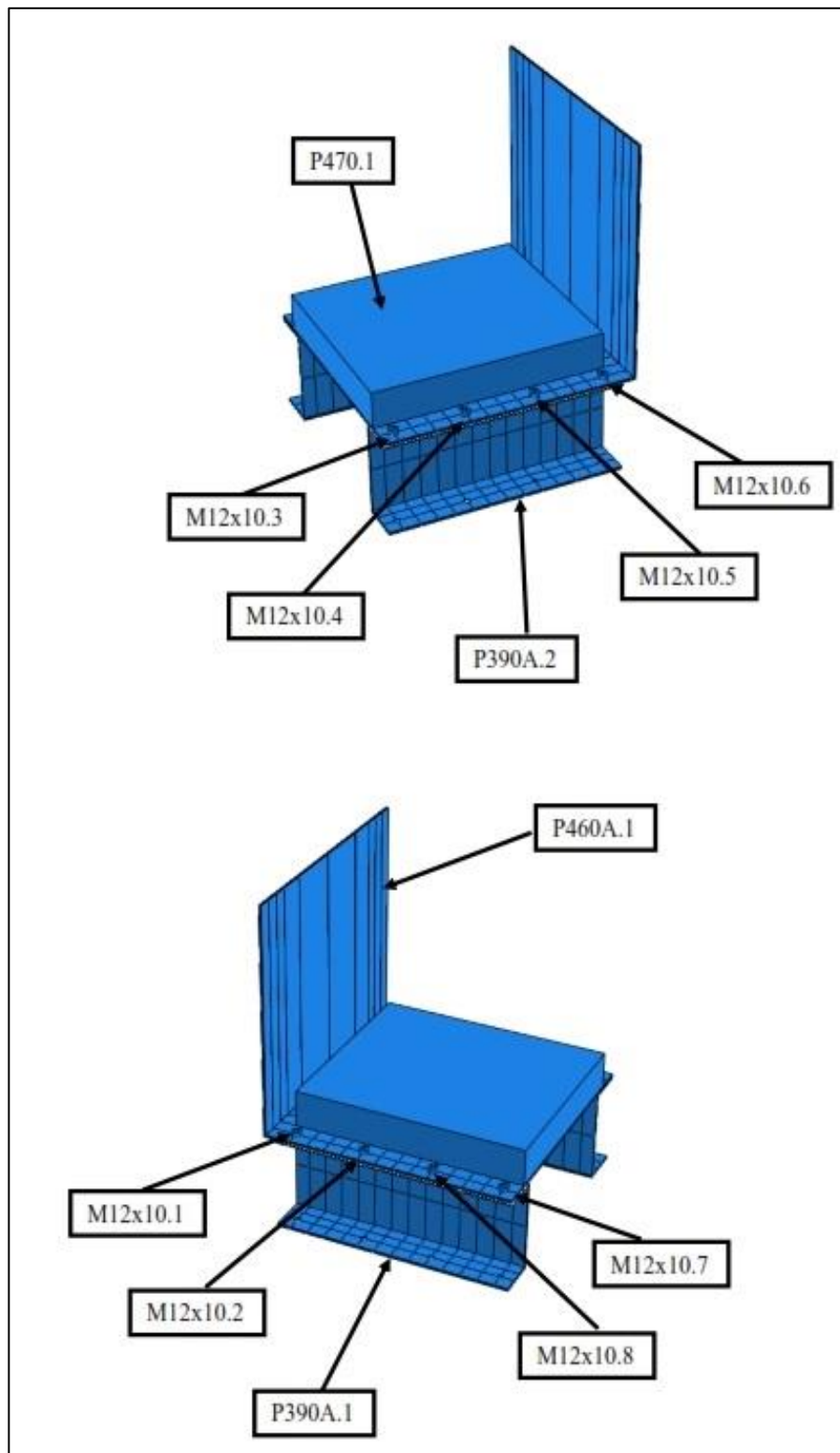
Figure 4.6. The assembly regarding to the Simplified Helicopter Seat

## 4.3. Bolt Preload Analysis of the Simplified Helicopter Seat

The importance of the bolt preload analysis is explained in Section 3.2.10. The fasteners of the seat bucket and the seat legs are joined by applying torque at the assembly stage. However, to observe the mass effect of DM, torque is applied to these fasteners while DM is on SHS.

The assembly prior to bolt preload process is displayed in Figure 4.7. The seat bucket and the seat legs are connected to each other with M12x10 bolts and nuts. By its nature, this analysis simulates a static task and it is done by using Abaqus/Standard with the application of the bolt torque values as explained in Section 3.1 and Section 3.2.10.
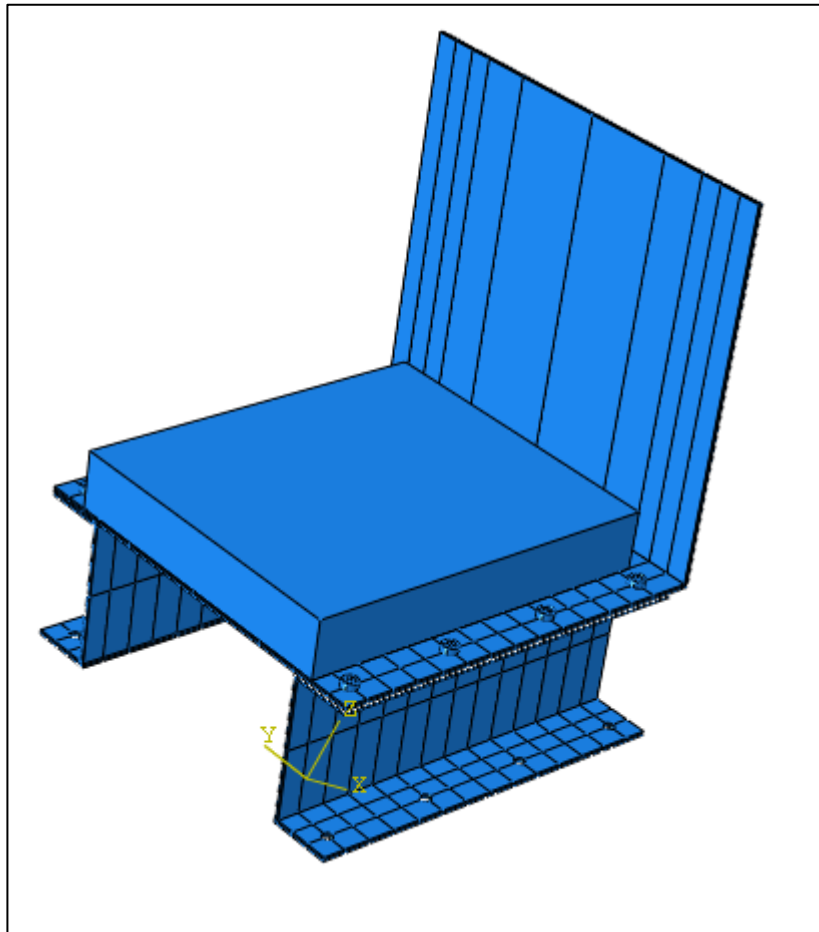


Figure 4.7. Initial condition of the bolt preload analysis of SHS

The core input of this analysis is the torque value as explained in Section 3.2.10. It is selected as 66.5 Nm. This torque value turns into 27,700 N of axial bolt preload tension. This phenomenon is visualized with double arrows in Figure 4.8.
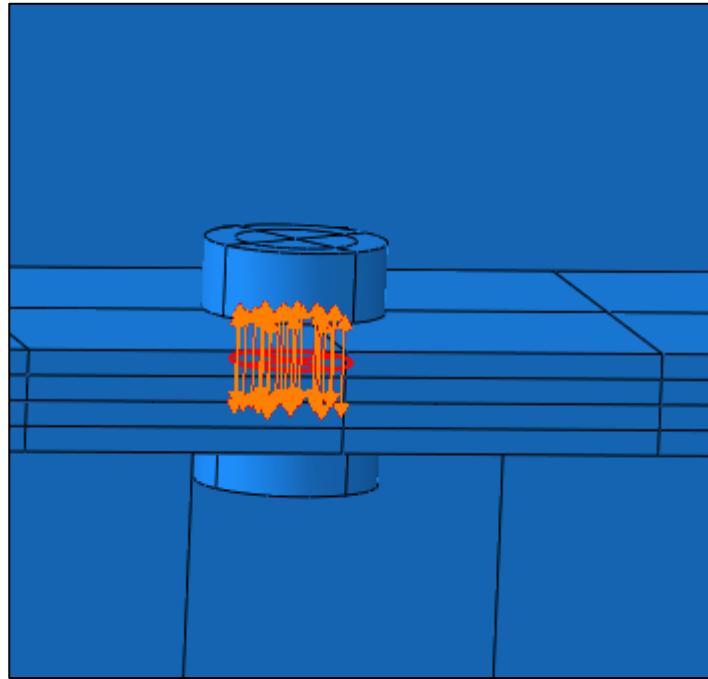


Figure 4.8. A typical bolt preload on the Simplified Helicopter Seat

Boundary condition phenomenon of this analysis is straightforward as the floor sections of the seat legs are fixed before bolt preload is applied. The boundary conditions, which exist on the floor sections of the seat legs, and the bolt preloads are shown in Figure 4.9.
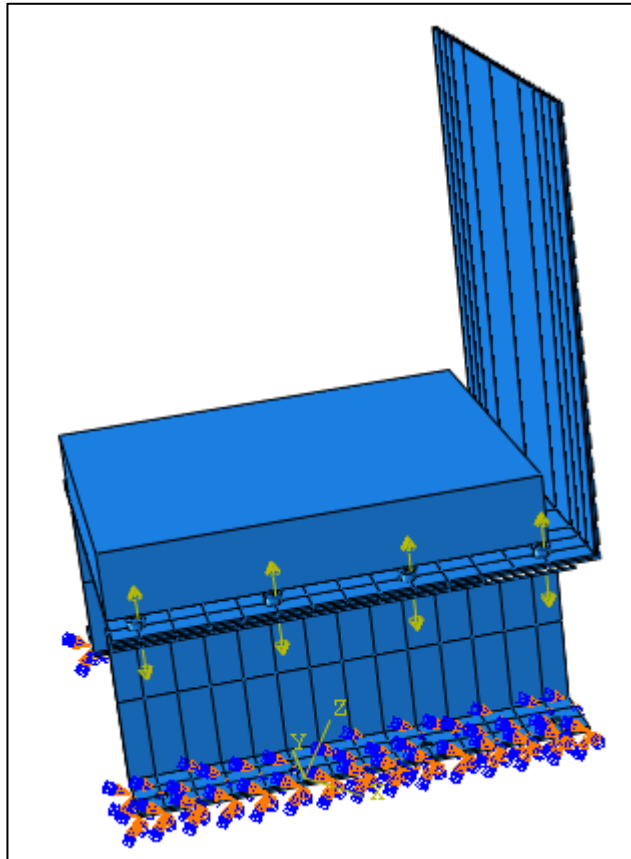
Figure 4.9. Boundary conditions of bolt preload analysis of the Simplified Helicopter Seat

As noted in Section 3.2.8, C3D8R meshing element is selected for all parts and fasteners. Therefore, this selection helps to reduce the run time of the analysis. Number of elements of all parts are less than $10^5$, which is desired as it is explained in Section 3.2.3. The mesh types are listed in Table 4.2.

Table 4.2. Mesh types of bolt preload analysis of the Simplified Helicopter Seat

| Part No | Number of Elements | Library | Element |
|---------|-------------------|---------|---------|
| P390A   | 3912              | Standard | C3D8R  |
| P460A   | 2240              | Standard | C3D8R  |
| P470    | 714               | Standard | C3D8R  |
| M12x10  | 1032              | Standard | C3D8R  |

After completing all input steps and processing the inputs, the analysis run is completed. The analysis lasts in only 3 minutes on the particular computer described

in Section 3.1, which is quite quick. The results of this analysis are evaluated in terms of von Mises failure criterion as follows [59].

The resulting von Mises stresses at the end of torque application are presented in Table 4.3. Factor of safeties with respect to yield ($n_Y$) are about 1.65 for fasteners, 3.86 for the seat legs, and 4.08 for the seat bucket as expected. DM is not investigated in the analysis since this part exists only for its mass effect. Figure 4.10 and Table 4.3 show the illustrative picture and the detailed results, respectively.
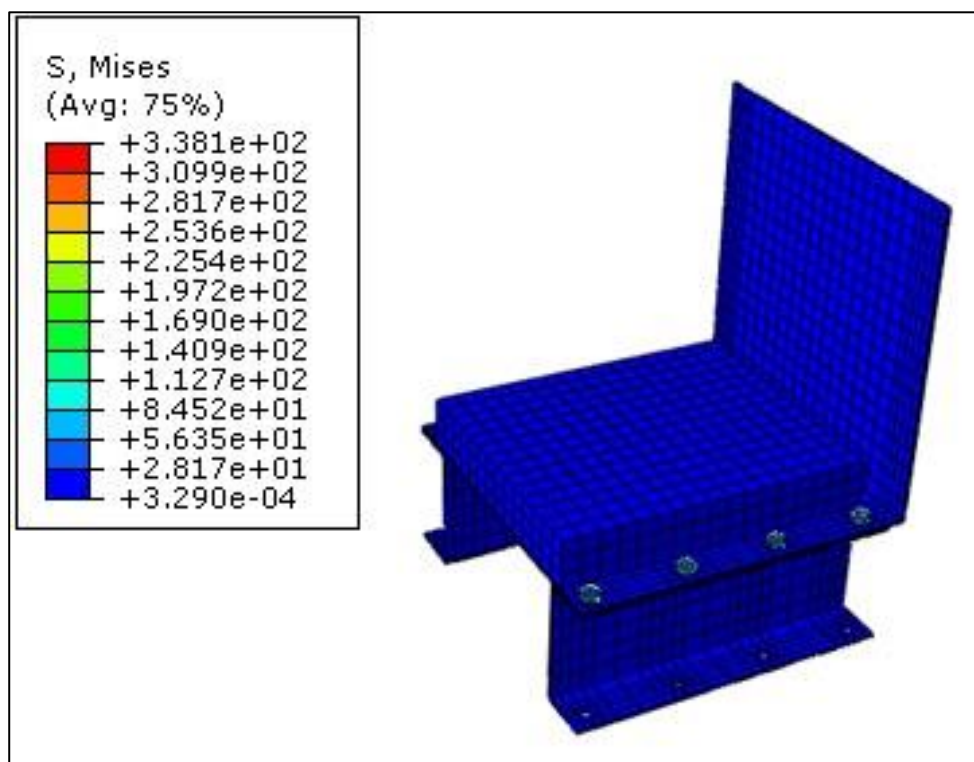


Figure 4.10. Results of bolt preload analysis of the Simplified Helicopter Seat

Table 4.3. von Mises stress results of bolt preload analysis of the Simplified Helicopter Seat

| Part No & Instances | Material | $S_Y$ [MPa] | $\sigma_{max}$ [MPa] | $n_Y$ |
|---|---|---|---|---|
| M12x10-1 | 8.8 Grade St | 543.9 | 338.1 | 1.61 |
| M12x10-2 | 8.8 Grade St | 543.9 | 327.5 | 1.66 |
| M12x10-3 | 8.8 Grade St | 543.9 | 324.4 | 1.68 |
| M12x10-4 | 8.8 Grade St | 543.9 | 327.7 | 1.66 |
| M12x10-5 | 8.8 Grade St | 543.9 | 327.2 | 1.66 |
| M12x10-6 | 8.8 Grade St | 543.9 | 335.1 | 1.62 |
| M12x10-7 | 8.8 Grade St | 543.9 | 322.1 | 1.69 |
| M12x10-8 | 8.8 Grade St | 543.9 | 327.3 | 1.66 |
| P390A-1 | Al 2024-T351 | 265.0 | 68.7 | 3.86 |
| P390A-2 | Al 2024-T351 | 265.0 | 68.7 | 3.86 |
| P460A-1 | Al 2024-T351 | 265.0 | 64.9 | 4.08 |

## 4.4. Crash Analysis of the Simplified Helicopter Seat

SHS must protects its structural integrity to be validated when it is applied to crash loads, which are expressed in Table 2.2. If SHS is not validated, the floor deformation effect upon SHS as seen in Chapter 5 cannot be investigated. To observe the effect of the 77 kg mass upon SHS, DM is utilized in this analysis. The aim of this analysis is to determine the behavior of SHS when the crash loads are applied. Since this is an impact case, it is done by using Abaqus/Explicit.

After the completion of the bolt preload analysis as discussed in Section 4.2, these stress results must be transferred into this analysis as an initial state, which is called mapping process as it is described in Section 3.2.8. In other words, after applying torque to the bolts, SHS with DM could be undergone to the crash loads applicable to the civilian passenger seat as stated in Table 2.2 which is a $30^0$ vertical impact to a rigid plane with 9.144 m/s initial velocity.

A vertical gap of 0.1 mm between the lowest point of the loaded SHS, which means SHS with DM, and the rigid plane is utilized to avoid the immediate impact. The initial condition of the loaded SHS against the rigid plane is pictured in Figure 4.11.
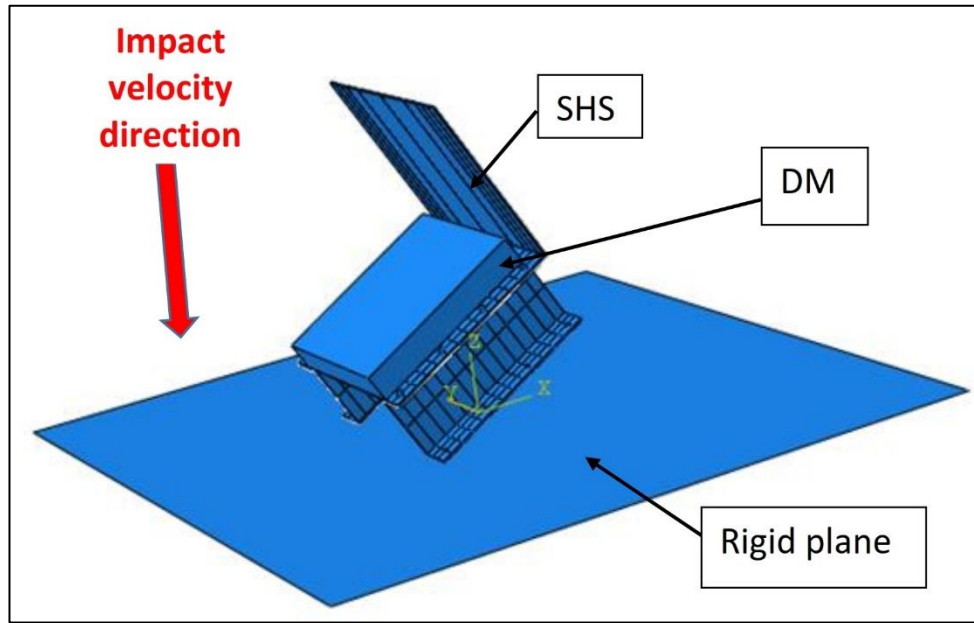
Figure 4.11. Initial condition of the crash analysis of the Simplified Helicopter Seat

The mesh types are the same with the one in Section 4.3 except the meshing library. By its nature, the explicit meshing library is selected instead of the standard library. The results are presented in Table 4.4.

Table 4.4. Mesh types of crash analysis of the Simplified Helicopter Seat

| Part No | Number of Elements | Library | Element |
|---------|--------------------|---------|---------|
| P390A | 3912 | Explicit | C3D8R |
| P460A | 2240 | Explicit | C3D8R |
| M12x10 | 1032 | Explicit | C3D8R |
| P470 | 714 | Explicit | C3D8R |

Two boundary conditions exist in this FEA as the fixation of the rigid plate and the initial speed of SHS. As known, the rigid plate is utilized as a contact plane for the impact of SHS. In addition, the initial speed of SHS, which is 9.144 m/s as indicated in Table 2.2, is the primary input of this analysis leading to the impact. When this initial speed is considered with the initial distance, which is 0.1 mm, the time for the onset of the impact is found as 0.011 ms. This value is about 0.2% of the unit time frame, which is 5 ms.

The crash analysis time of the FEA is 100 ms and which is explained in Section 3.2.5. This corresponds to 2 hours and 4 minutes on the particular computer described in Section 3.1 as the completion duration of the FEA. This analysis is investigated in terms of von Mises failure criterion [59]. Since the crash analysis is dynamic, the results are examined for all pre-crash, crash, and post-crash periods. Pre-crash period means the duration before SHS is contacted with the rigid plane. Crash period is time interval between the start and the end of the contacting of SHS and the rigid plane. Post-crash period is the duration after SHS and the rigid plane are separated. Resulting von Mises stresses can be observed in Figures 4.12 – 4.22 for twenty one different time steps.
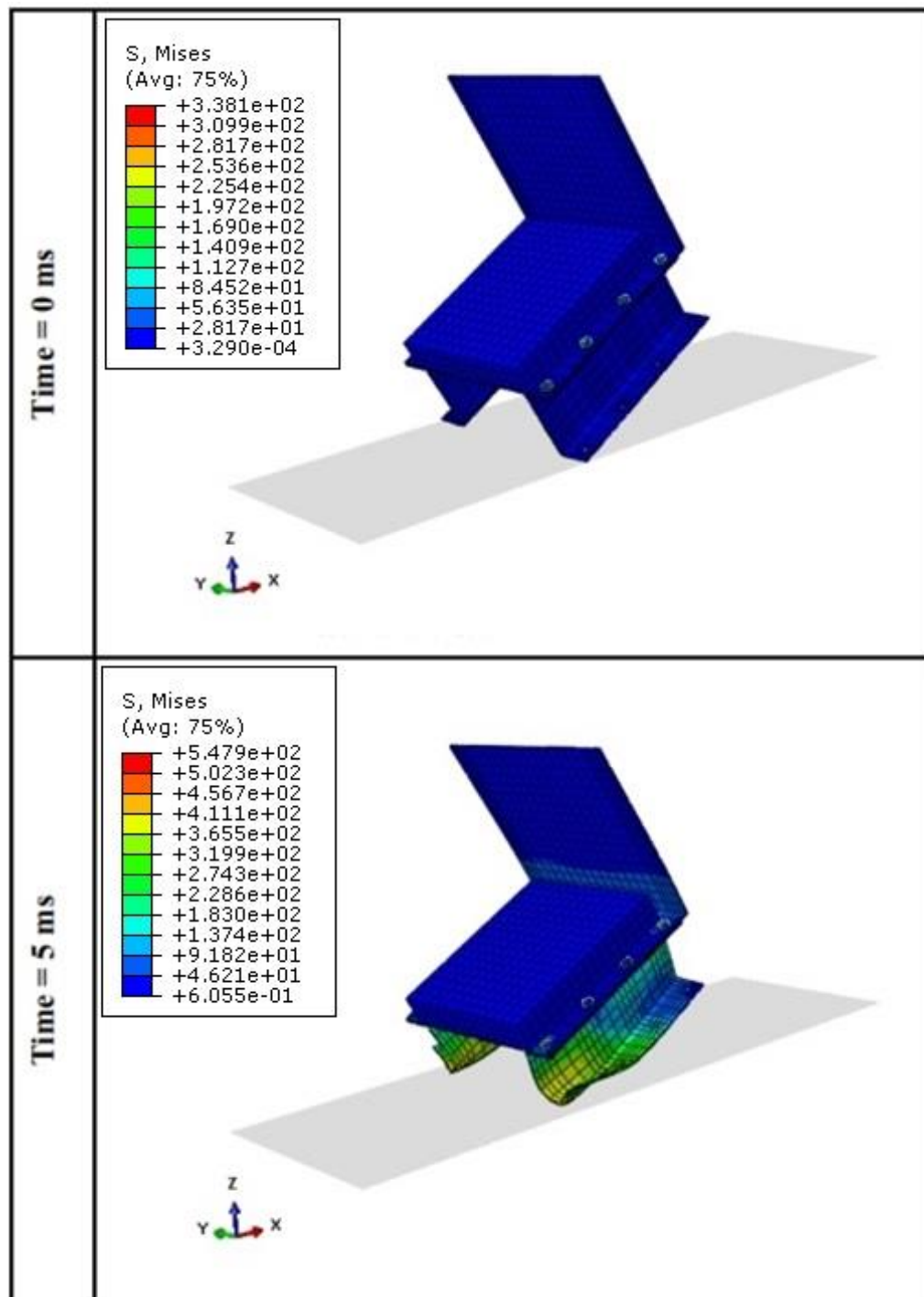
Figure 4.12. von Mises stress representation of the crash analysis of the Simplified Helicopter Seat at 0 ms and 5 ms
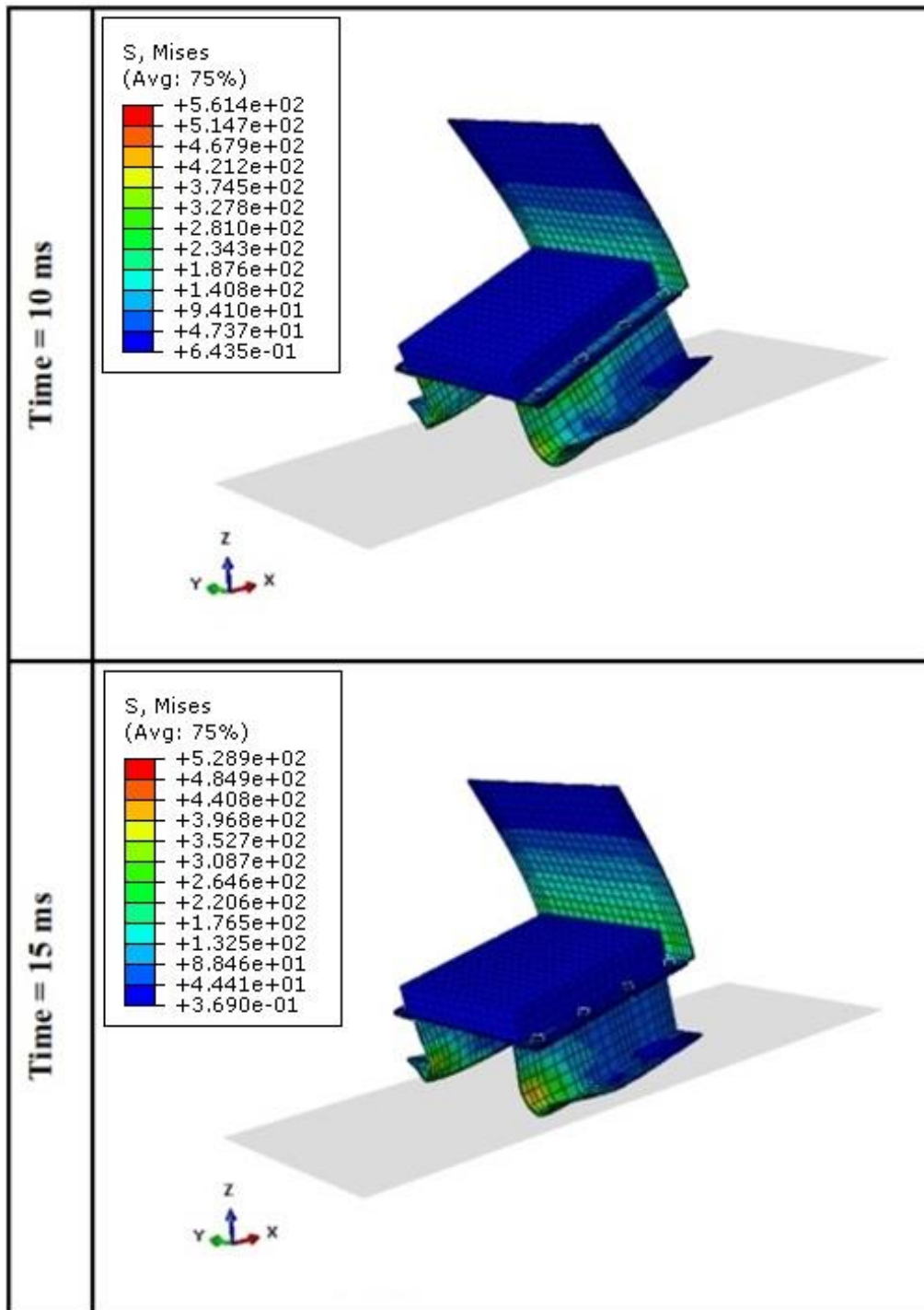
Figure 4.13. von Mises stress representation of the crash analysis of Simplified
Helicopter Seat at 10 ms and 15 ms
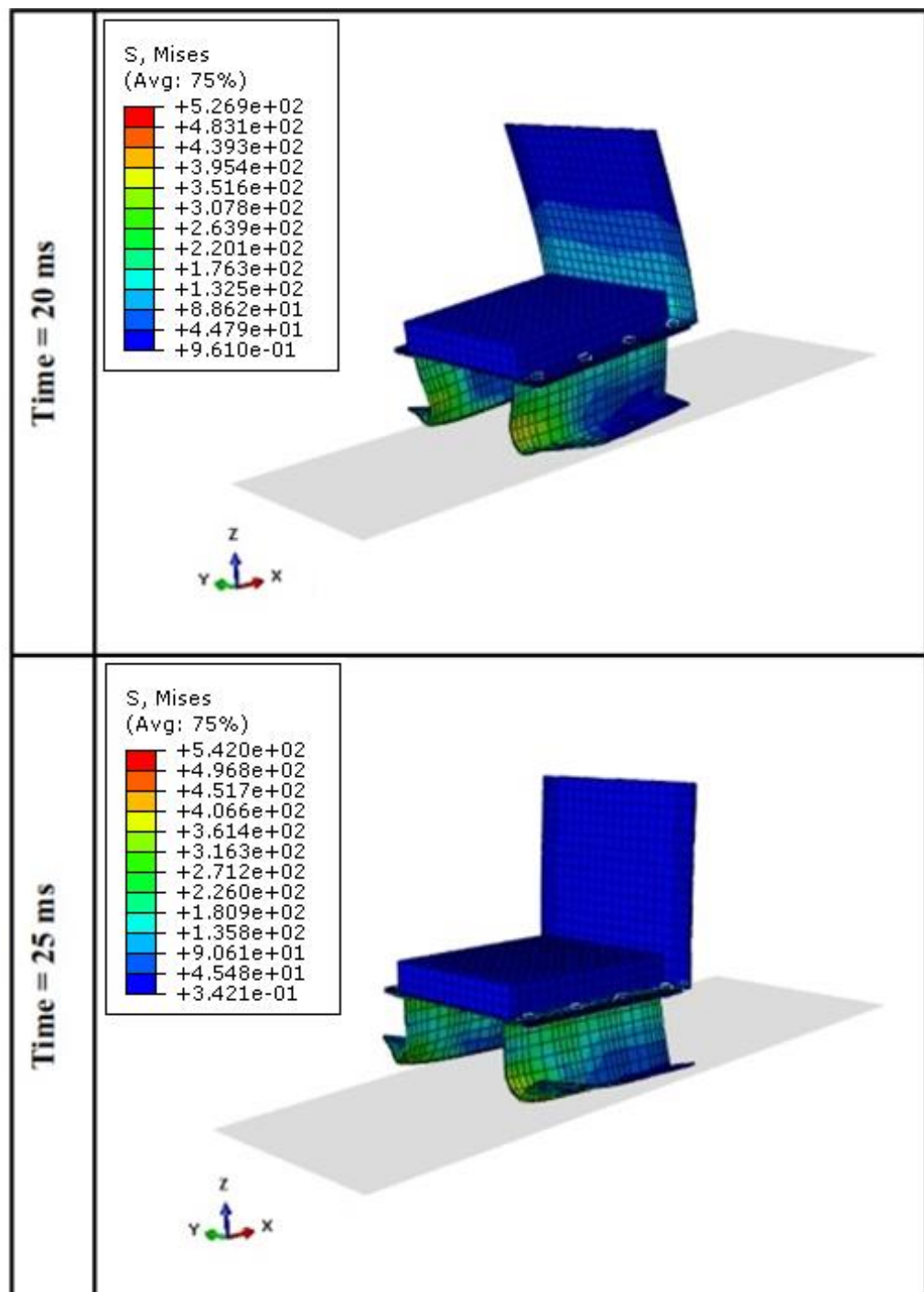
Figure 4.14. von Mises stress representation of the crash analysis of the Simplified Helicopter Seat at 20 ms and 25 ms

57
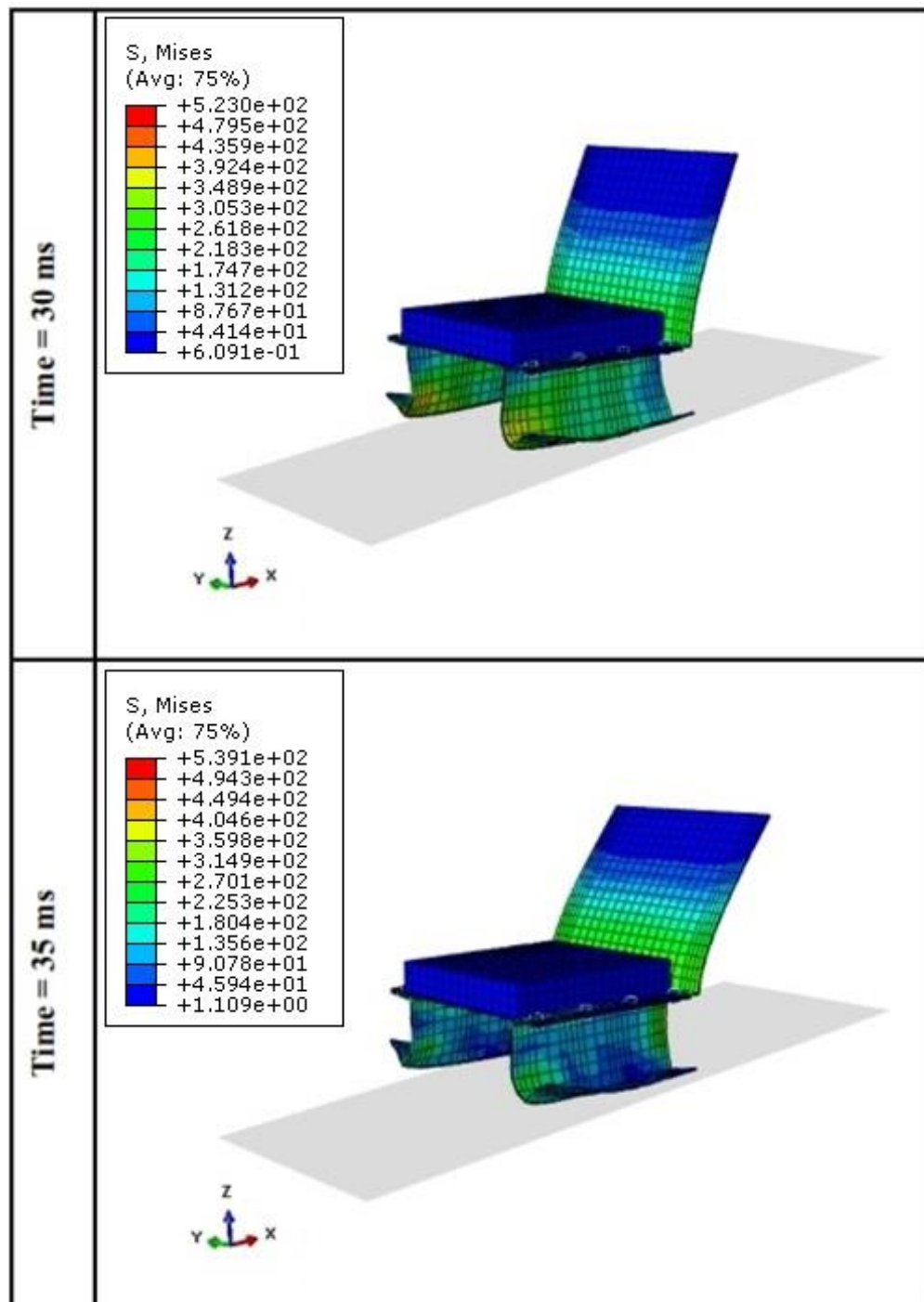
Figure 4.15. von Mises stress representation of the crash analysis of the Simplified
Helicopter Seat at 30 ms and 35 ms
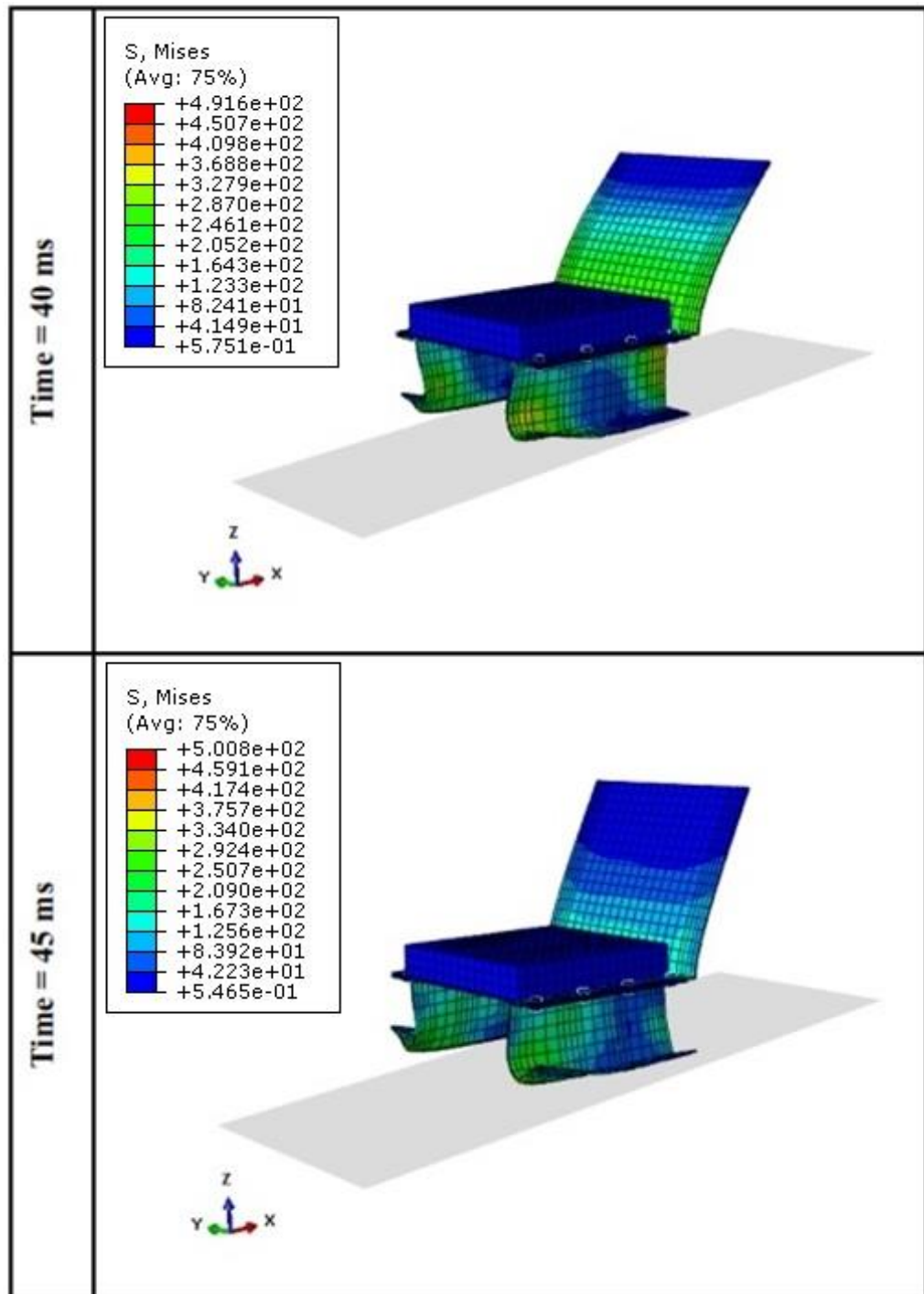
Figure 4.16. von Mises stress representation of the crash analysis of the Simplified Helicopter Seat at 40 ms and 45 ms
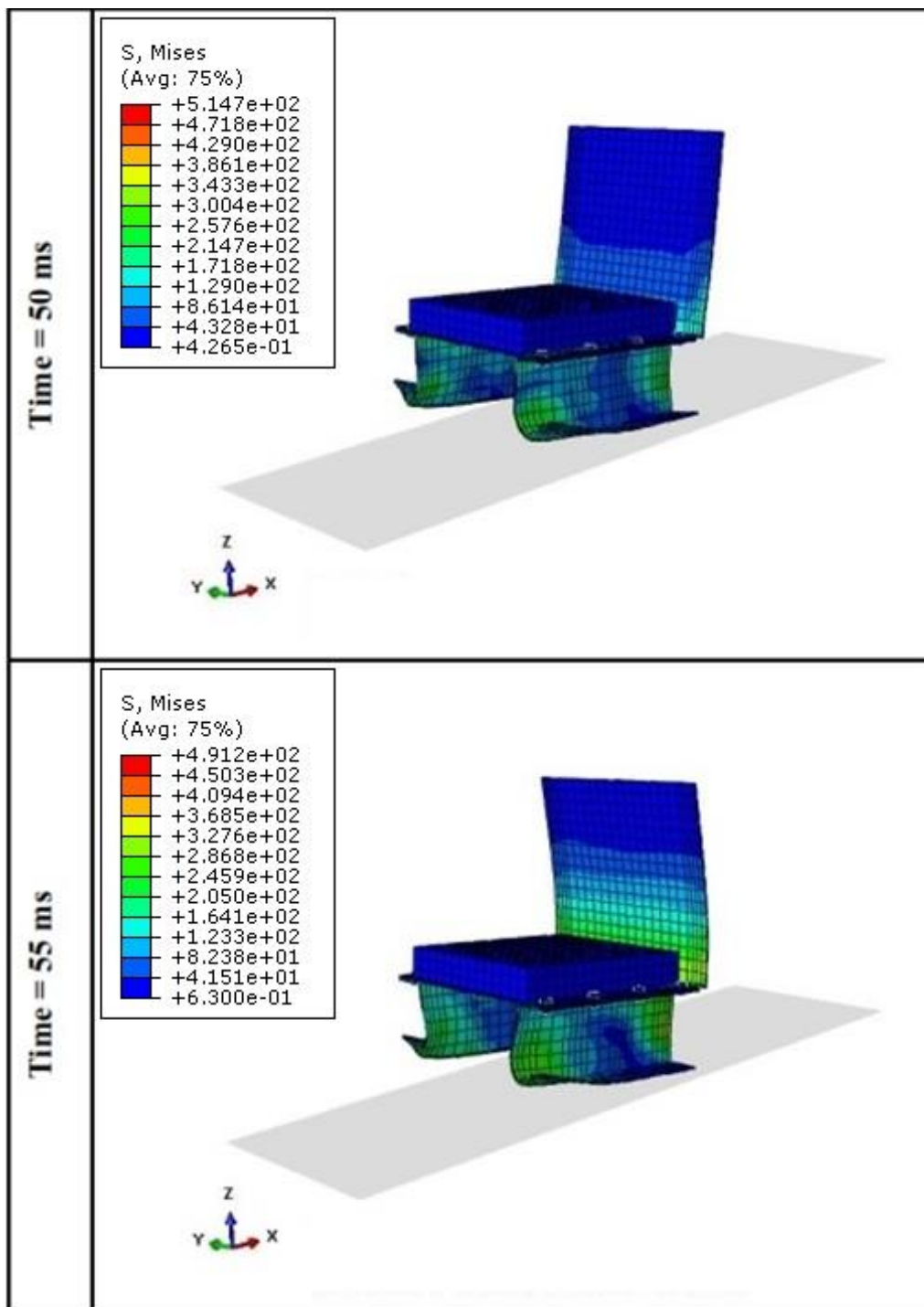
Figure 4.17. von Mises stress representation of the crash analysis of the Simplified Helicopter Seat at 50 ms and 55 ms

60
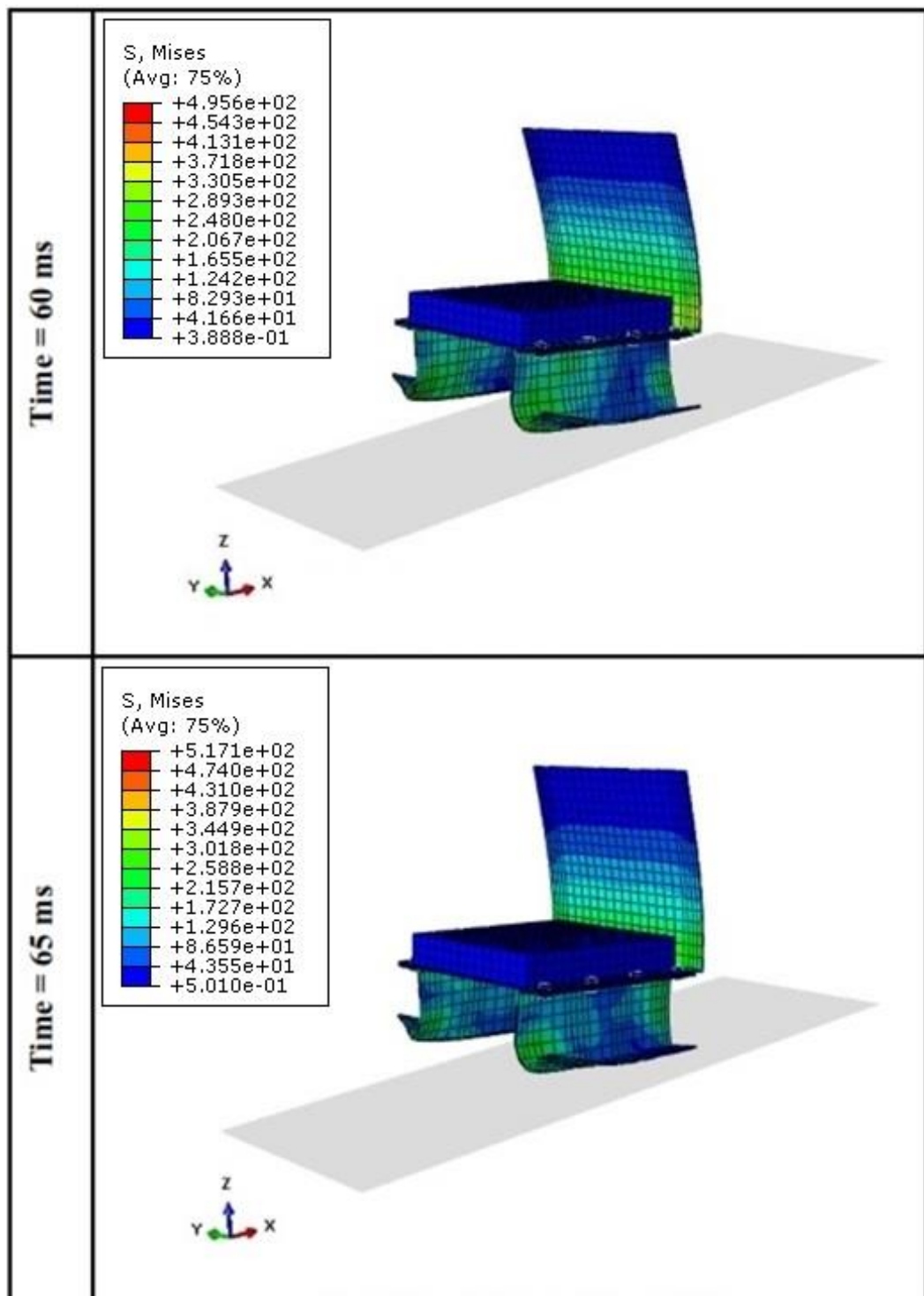
Figure 4.18. von Mises stress representation of the crash analysis of the Simplified Helicopter Seat at 60 ms and 65 ms
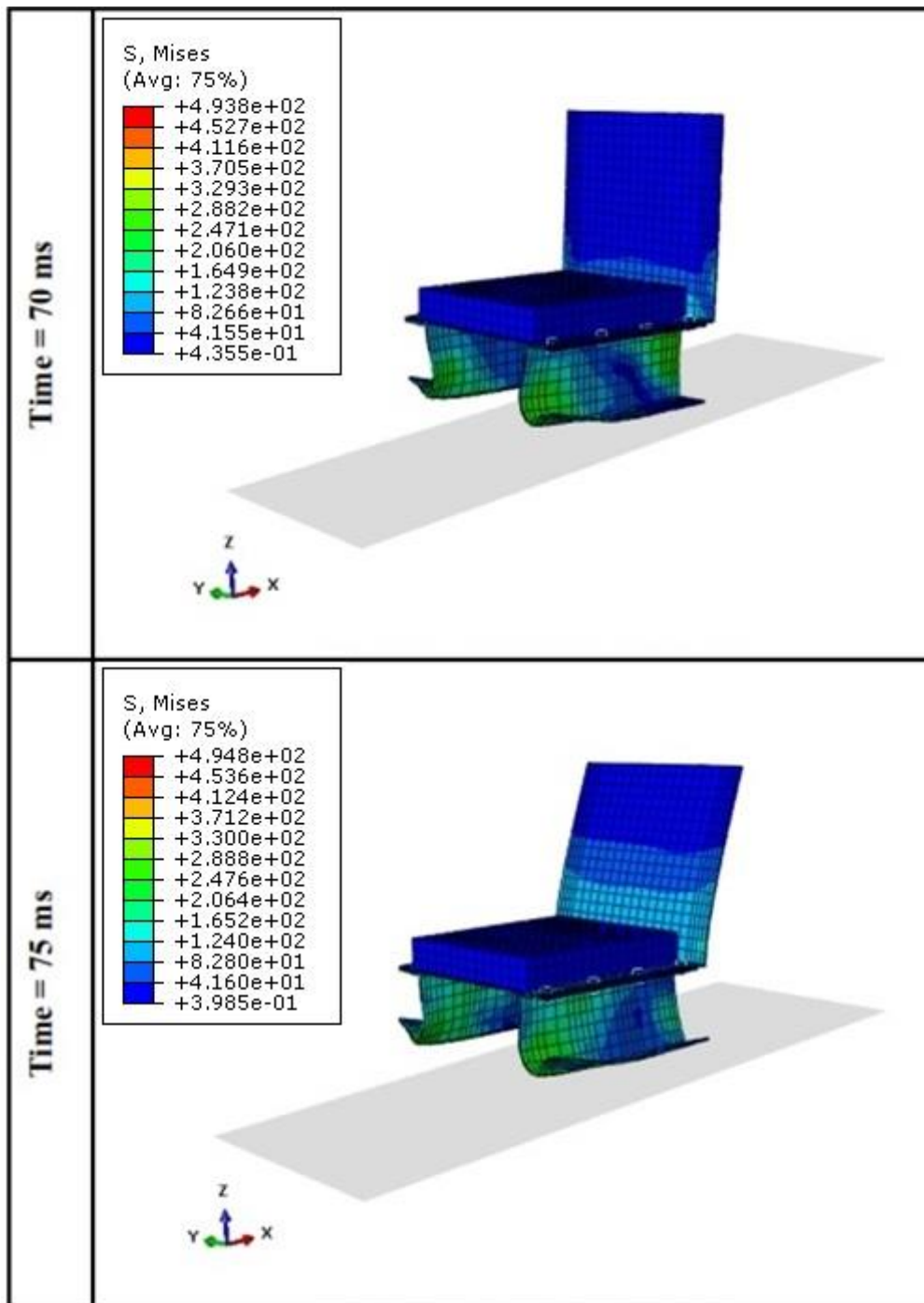
Figure 4.19. von Mises stress representation of the crash analysis of the Simplified Helicopter Seat at 70 ms and 75 ms
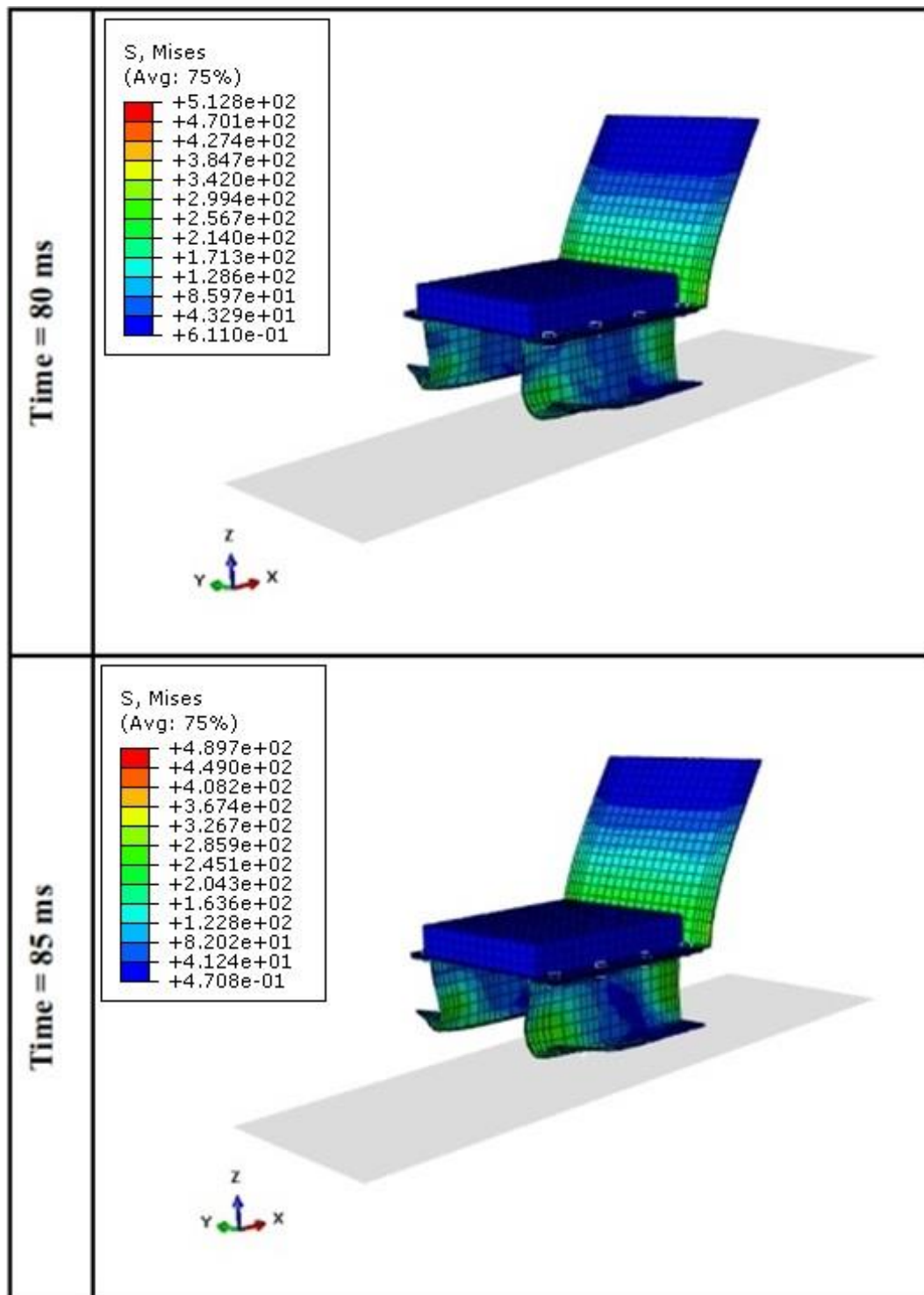
Figure 4.20. von Mises stress representation of the crash analysis of the Simplified Helicopter Seat at 80 ms and 85 ms
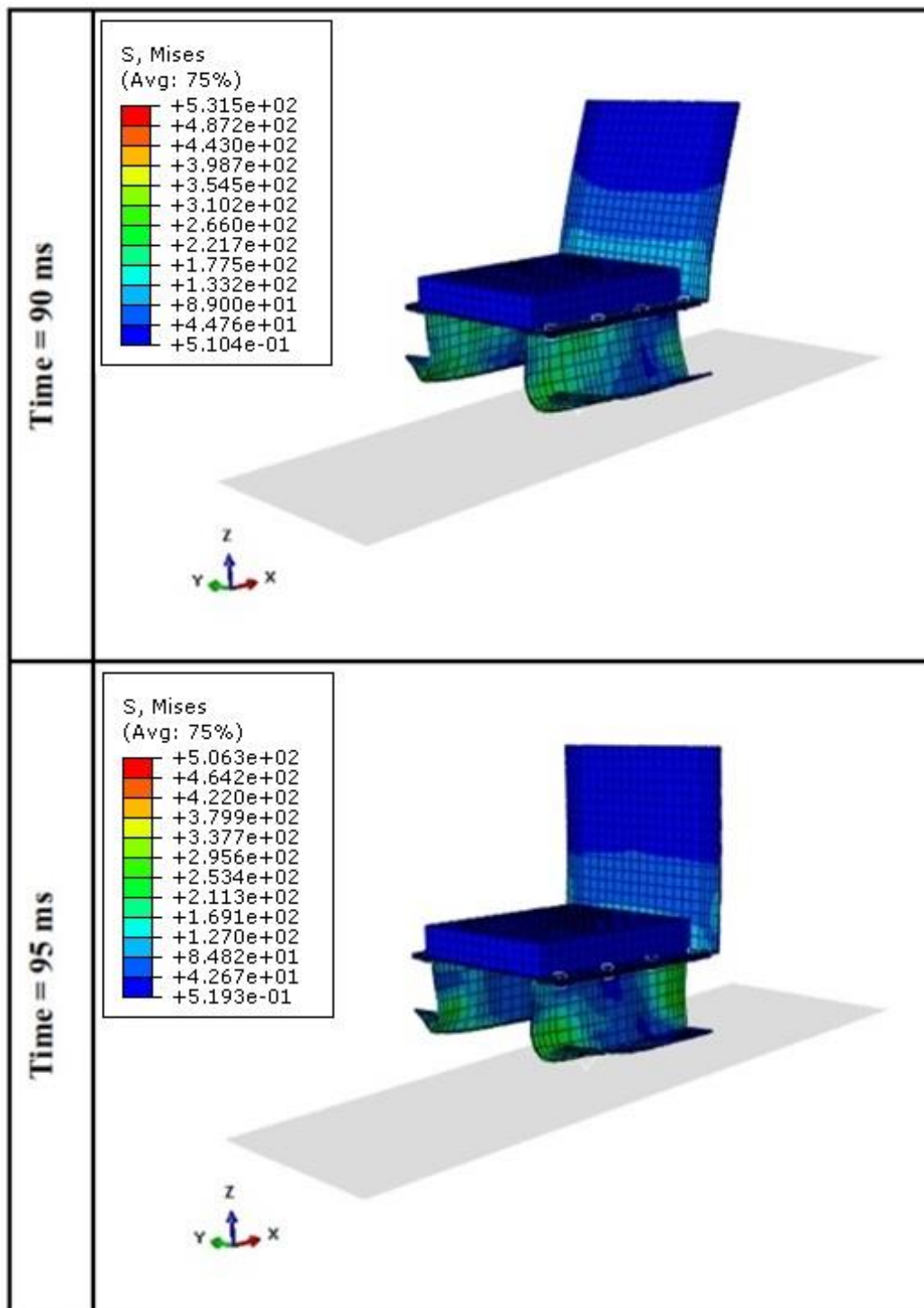
Figure 4.21. von Mises stress representation of the crash analysis of the Simplified Helicopter Seat at 90 ms and 95 ms
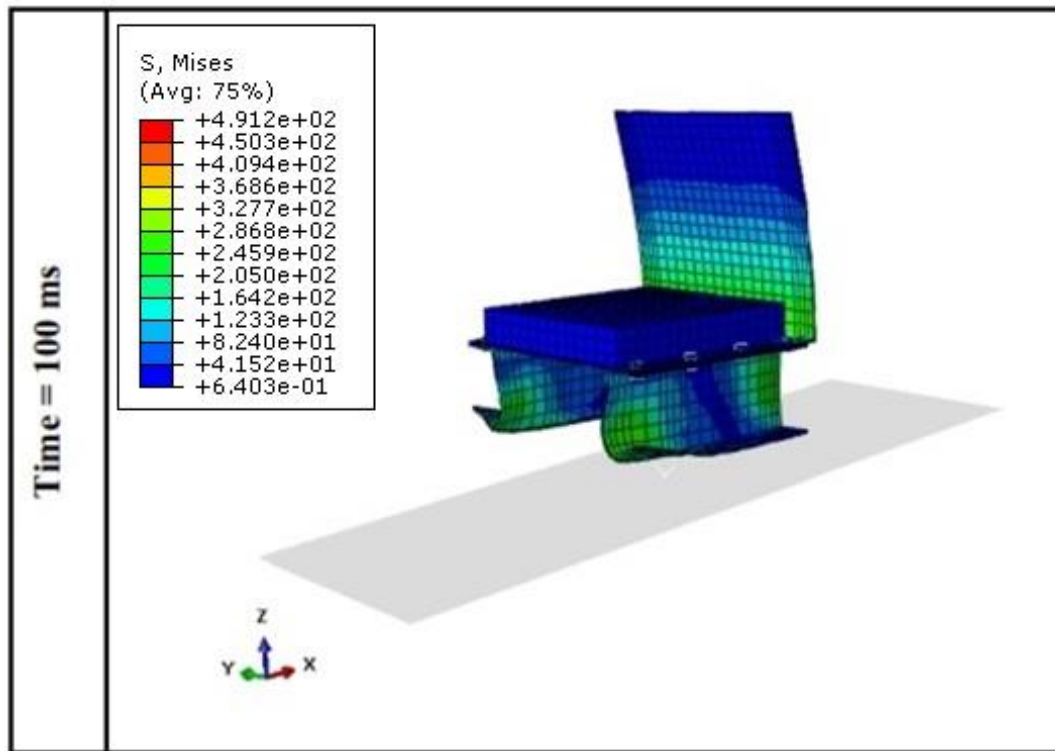
Figure 4.22. von Mises stress representation of the crash analysis of the Simplified Helicopter Seat at 100 ms

The following consequences can also be inferred from the results shown in Figures 4.12 – 4.22. The seat bucket behaves as a spring and oscillates about its corner axis. As expressed in Section 4.1, this is due to the geometry of the bucket that does not have an energy absorption system, which is not desired in real applications. Accordingly, the crash energy is absorbed by the seat legs, which are plastically deformed (PD). The separation of SHS from the floor starts about 35 ms. Although, separation is completed after that time, the acceleration on SHS and the stresses of SHS resume.

von Mises criterion of the parts and the fasteners are investigated as shown in Table 4.5 As it can be inferred from the table, nearly all fasteners are plastically deformed (PD) after the crash but none of them exceeds the ultimate tensile strength.

65

Table 4.5. von Mises stress results of crash analysis of the Simplified Helicopter Seat

| Part No & Instances | Material | $S_Y$ [MPa] | $\sigma_{max}$ [MPa] | $n_Y$ |
|---|---|---|---|---|
| M12x10-1 | 8.8 Grade St | 543.9 | 561.4 | PD |
| M12x10-2 | 8.8 Grade St | 543.9 | 544.6 | PD |
| M12x10-3 | 8.8 Grade St | 543.9 | 482.2 | 1.13 |
| M12x10-4 | 8.8 Grade St | 543.9 | 478.3 | 1.14 |
| M12x10-5 | 8.8 Grade St | 543.9 | 545.3 | PD |
| M12x10-6 | 8.8 Grade St | 543.9 | 560.9 | PD |
| M12x10-7 | 8.8 Grade St | 543.9 | 479.4 | 1.13 |
| M12x10-8 | 8.8 Grade St | 543.9 | 480.1 | 1.13 |
| P390A-1 | Al 2024-T351 | 265 | 543.1 | PD |
| P390A-2 | Al 2024-T351 | 265 | 543.1 | PD |
| P460A-1 | Al 2024-T351 | 265 | 365.5 | PD |

Nevertheless, the seat legs of SHS are the first parts that hit the rigid plate and they are heavily deformed being very close to the ultimate tensile strength point. However, these elements occur for the corner edges of the seat legs. This is quite acceptable since these cells are not in the vicinity of the bucket section of SHS. In other words, considerable impact energy could have been transferred to the seat bucket. To conclude, SHS with DM withstands the vertical impact criterion stated in Table 2.2.

# CHAPTER 5

# DESIGN AND ANALYSES OF THE INTERCHANGEABLE FLOOR DEFORMATION UNIT

## 5.1. Design Information of the Interchangeable Floor Deformation Unit

Design of Interchangeable Floor Deformation Unit (IFDU) is derived from the need of simulating the floor deformation of helicopters, which is explained in Section 2.1. Simplified Helicopter Seat (SHS) is located on the top of IFDU so as to be wrapped for the floor deformation, which is a prerequisite condition before impact. Likewise, IFDU is mounted to Sled Test Fixture (STF) from its bottom section.

Parts of IFDU are illustrated in Figure 5.1. At the left section of IFDU, the roll deformation mechanism is designed where the roll deformation is initiated with the rotation of the roll lever. At the right section of IFDU, the pitch deformation mechanism performs the tasks of the pitch deformation with the rotation of the pitch lever.
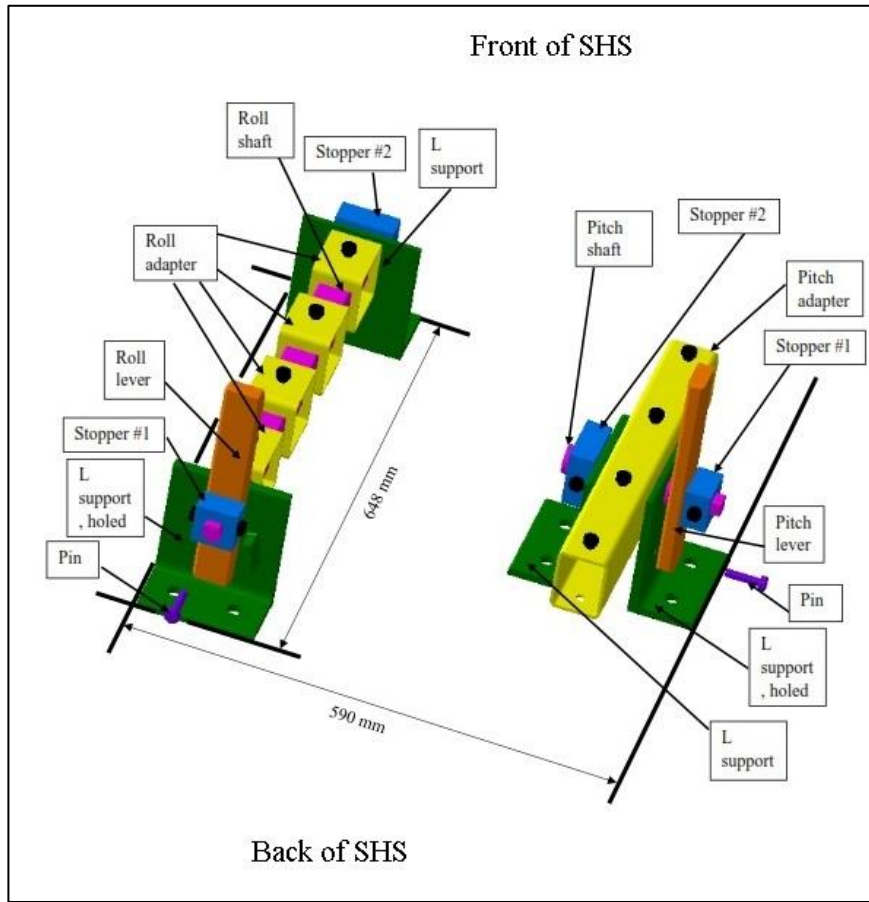
Figure 5.1. The model of the Interchangeable Floor Deformation Unit

IFDU is fixed to the floor or the floor representative item with the floor supports, which are selected as L-shaped parts. Two of L-shaped parts have mechanical stopper feature for limiting the angle of roll and pitch motion. They function to ensure and guide the rotation of the roll lever or pitch lever at $10^0$. After the roll lever and the pitch lever are rotated to their desired positions, the roll pin and the pitch pin are inserted into the holes into the floor supports to obtain the floor deformed shape of SHS. The roll pin and the pitch pin, and the roll lever and the pitch lever are geometrically and structurally the same. SHS is fixed to rotation transmitting parts. The mass data of IFDU is shown in Table 5.1, where all fasteners of IFDU have a total mass of 0.61 kg. Resultantly, IFDU has a mass of 30.11 kg.

68

Table 5.1. Mass data of the Interchangeable Floor Deformation Unit

| Part No | Part Name | Material | Unit Mass (kg) | Qty. | Total Mass (kg) |
|---------|-----------|----------|----------------|------|-----------------|
| P214A | Pitch Adapter | A284 St, Grade D | 3.29 | 1 | 3.29 |
| P224A | Roll Adapter | A284 St, Grade D | 0.45 | 4 | 1.80 |
| P234 | Pitch Shaft | A284 St, Grade D | 1.43 | 1 | 1.43 |
| P247A | L Support, Holed | A284 St, Grade D | 2.42 | 2 | 4.84 |
| P257A | L Support | A284 St, Grade D | 2.43 | 2 | 4.86 |
| P266 | Roll Shaft | A284 St, Grade D | 6.76 | 1 | 6.76 |
| P304 | Lever | A284 St, Grade D | 1.86 | 2 | 3.72 |
| P480 | Stopper #1 | A284 St, Grade D | 0.46 | 2 | 0.92 |
| P490 | Stopper #2 | A284 St, Grade D | 0.90 | 2 | 1.80 |
| P501 | Pin | A284 St, Grade D | 0.04 | 2 | 0.08 |

IFDU must have the function of interchangeability since helicopter seat dimensions of the industry varies. The width (590 mm) of IFDU can be adjusted with leaving the gap smaller or larger. On the other hand, the length (648 mm) of IFDU can be changed by making some modifications regarding to the pitch adapter, the roll adapter, and the roll shaft. For the same purpose, welding is avoided as a design procedure since it does not allow any flexibility regarding to the modification of IFDU.

## 5.2. Finite Element Analysis Information of the Interchangeable Floor Deformation Unit and the Simplified Helicopter Seat

The design of IFDU is obliged to many requirements such that it should withstand the static loads caused by floor deformation and it should withstand the downward impact loads. Quasi-static finite element analysis is done to verify IFDU for the floor deformation. On the other hand, dynamic finite element analysis is performed for simulating impact loads and observing the response of IFDU.

Before starting to analyses, IFDU is loaded with SHS and 77 kg dummy mass (DM), which has the part number of P470. Moreover, some means must exist underneath the L supports (P247A and P257A) so as to connect these parts prior to floor deformation and impact, consecutively. Dummy floor part (P322) is employed for the analyses. The parts and fasteners of IFDU and SHS with the 77 kg dummy mass (DM) is represented in Figure 5.2.
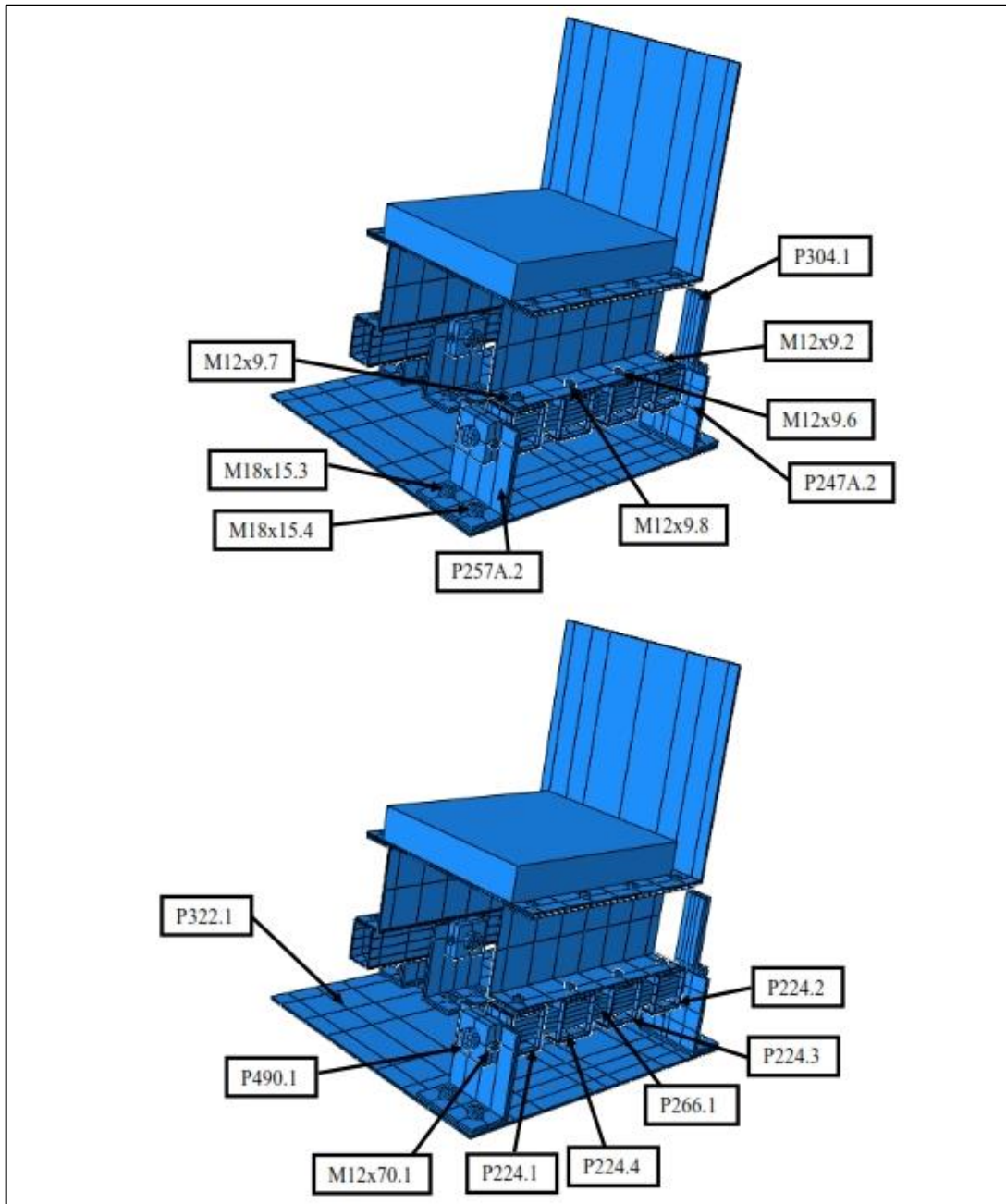
Figure 5.2. Parts and fasteners of the Interchangeable Floor Deformation Unit and the Simplified Helicopter Seat
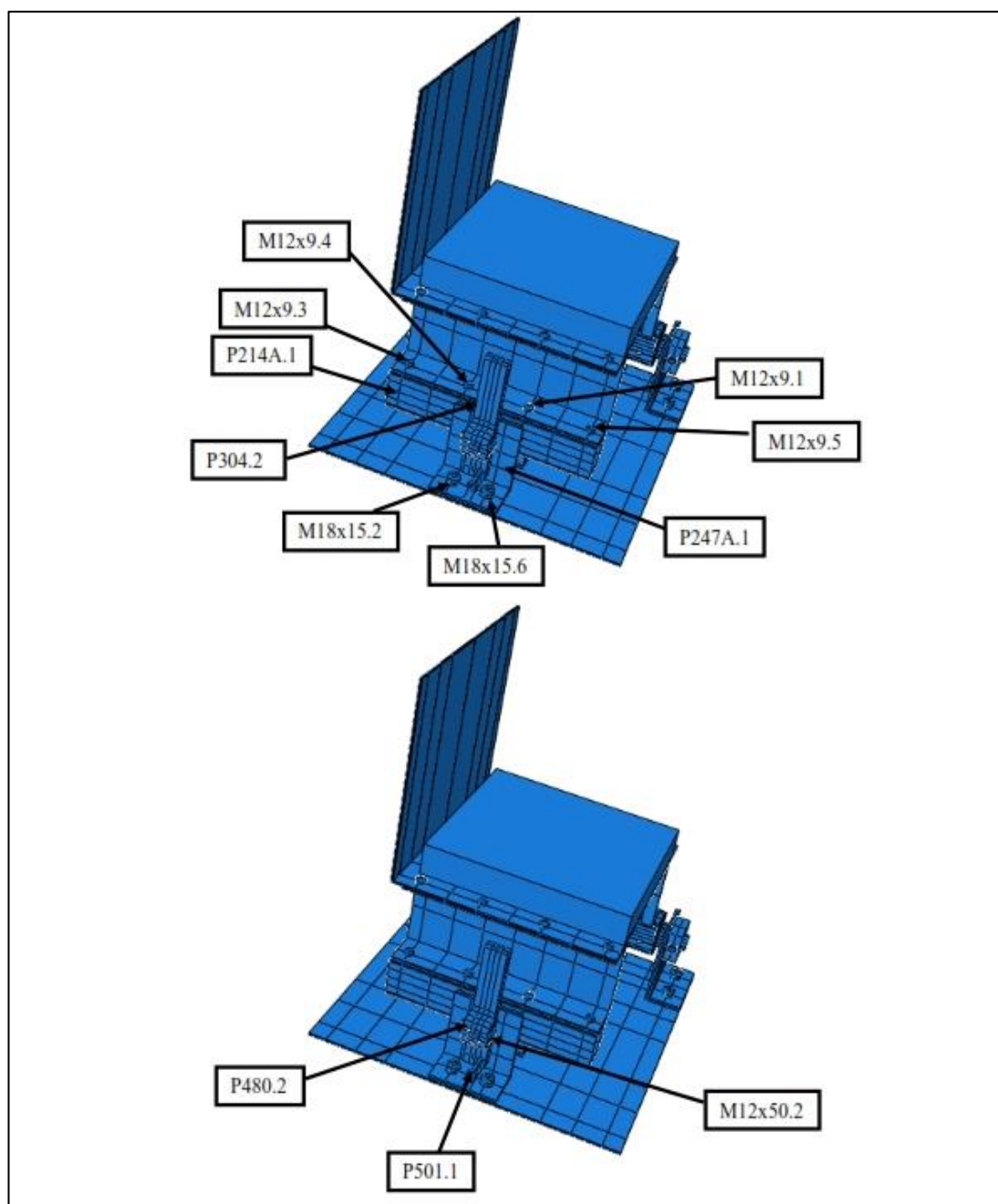
Figure 5.2. (continued)
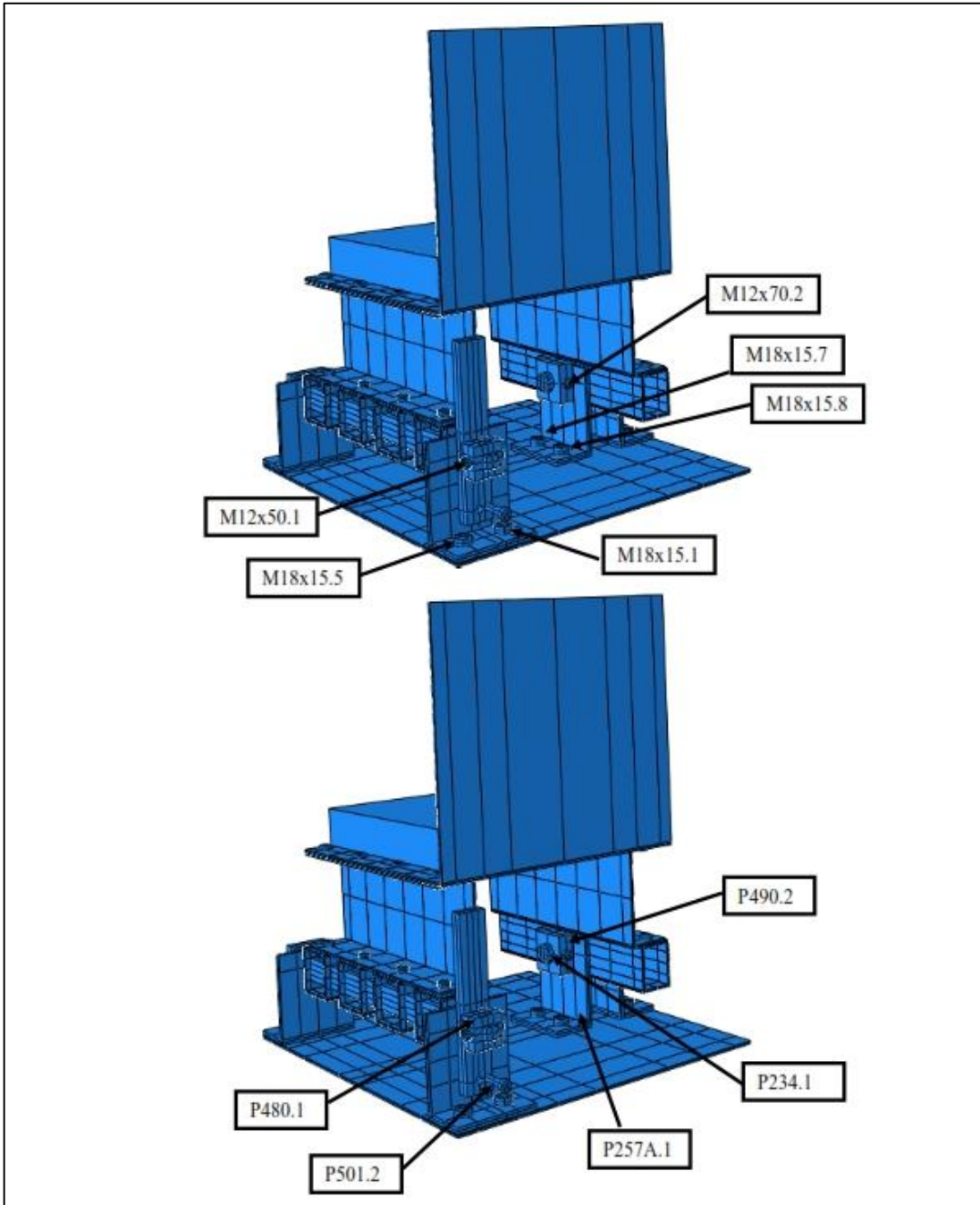
Figure 5.2. (continued)

**5.3. Bolt Preload Analysis of the Interchangeable Floor Deformation Unit and the Simplified Helicopter Seat**

The importance of the bolt preload analysis is explained in Section 3.2.10. Its effect must be included prior to the floor deformation and pin insertion analyses and the crash analyses of IFDU that are discussed in Section 5.4 and Section 5.5, respectively.

The connection of the seat bucket and the seat legs remain same with Section 4.3 as utilization of M12x10 bolts and nuts. On the other hand, M12x9 bolt and nut combination is preferred for the connection between the seat legs and IFDU interface. While the floor deformation mechanism is used in IFDU, there must be stoppers in order to prevent the inadvertent dislocation of the roll or pitch lever. The stoppers are connected to the roll and pitch shafts with M12x50 and M12x70 bolt and nuts, where M12x50 is used for the lever side, and M12x70 is used for the other side.

Furthermore, the mass data of IFDU and SHS combination are expressed in terms of quantities, material, and mass. The design data of the assembly is outlined in Table 5.1 and Table 4.1.

Since this a bolt preload analysis, which is explained in Section 3.2.10, the most important section of this analysis is the torque value input. All M12 bolts and all M18 bolts are torqued with 66.5 Nm and 270.7 Nm. These values are converted into 27,700 N axial bolt preload for M12 bolts and 75,200 N for M18 bolts.

Boundary conditions of this analysis consists of the fixation of the dummy floor part. This is necessary in order to make the assembly stationary prior to applying torque. The boundary conditions and the bolt preloads are shown in Figure 5.3.
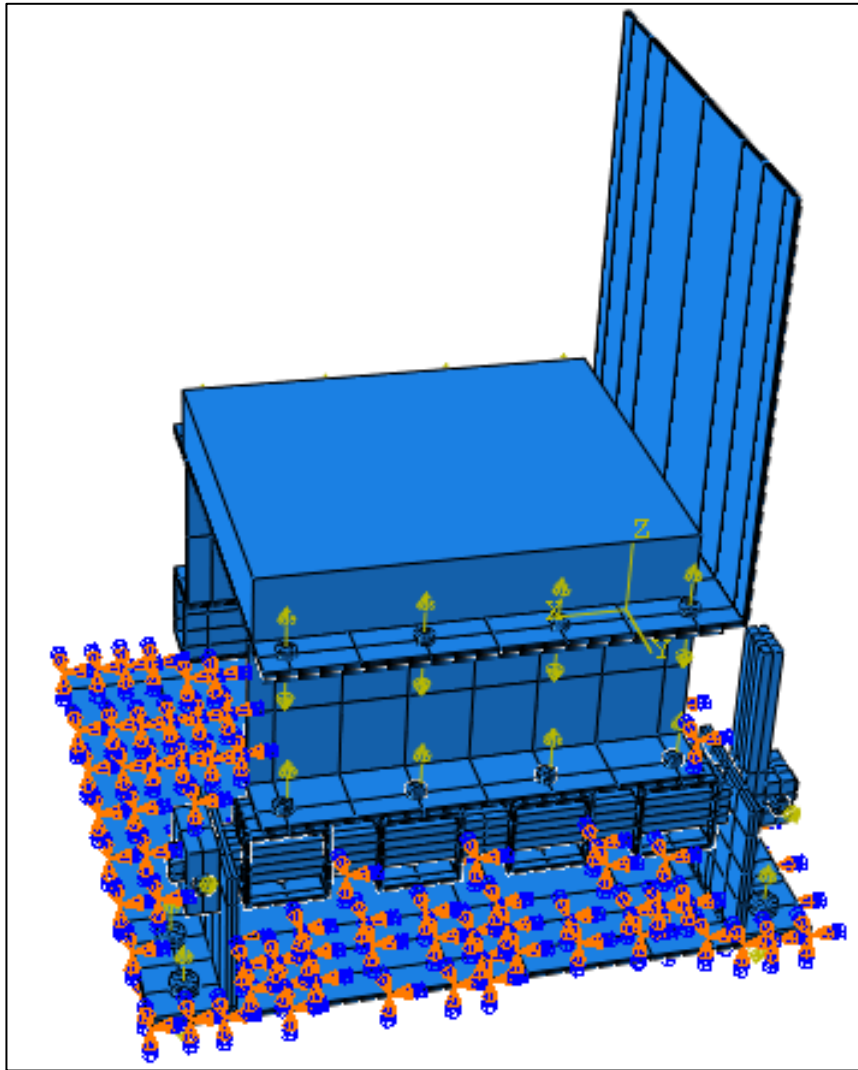
Figure 5.3. Boundary conditions and bolt preloads of the Interchangeable Floor Deformation Unit and the Simplified Helicopter Seat

The meshing of SHS and IFDU is outlined as explained in Section 3.2.8. C3D8R element type is utilized to improve the run time of the analysis. The mesh types are presented in Table 5.2.

Table 5.2. Mesh types of bolt preload analysis of the Interchangeable Floor
Deformation Unit and the Simplified Helicopter Seat

| Part No | Number of Elements | Library | Element |
|---------|--------------------|---------|---------|
| P214A   | 3680               | Standard | C3D8R  |
| P224A   | 1056               | Standard | C3D8R  |
| P234    | 1538               | Standard | C3D8R  |
| P247A   | 2324               | Standard | C3D8R  |
| P257A   | 2268               | Standard | C3D8R  |
| P266    | 7584               | Standard | C3D8R  |
| P304    | 2192               | Standard | C3D8R  |
| P322    | 4096               | Standard | C3D8R  |
| P390A   | 6160               | Standard | C3D8R  |
| P460A   | 5016               | Standard | C3D8R  |
| P470    | 1134               | Standard | C3D8R  |
| P480    | 2120               | Standard | C3D8R  |
| P490    | 4372               | Standard | C3D8R  |
| M12x9   | 912                | Standard | C3D8R  |
| M12x10  | 1032               | Standard | C3D8R  |
| M12x50  | 2232               | Standard | C3D8R  |
| M12x70  | 2832               | Standard | C3D8R  |
| M18x15  | 1224               | Standard | C3D8R  |

Consequently, the analysis is performed after satisfying all necessary steps. The analysis is completed in 37 minutes on the particular computer described in Section 3.1. Bolt preload analysis of SHS and IFDU is done with applying torque to the fasteners that connects the parts among SHS and IFDU. It is a preliminary step before the floor deformation is simulated with the turn of the roll lever and the pitch lever, respectively, which is explained in Section 5.3. The results after torque process are visualized in Figure 5.4.
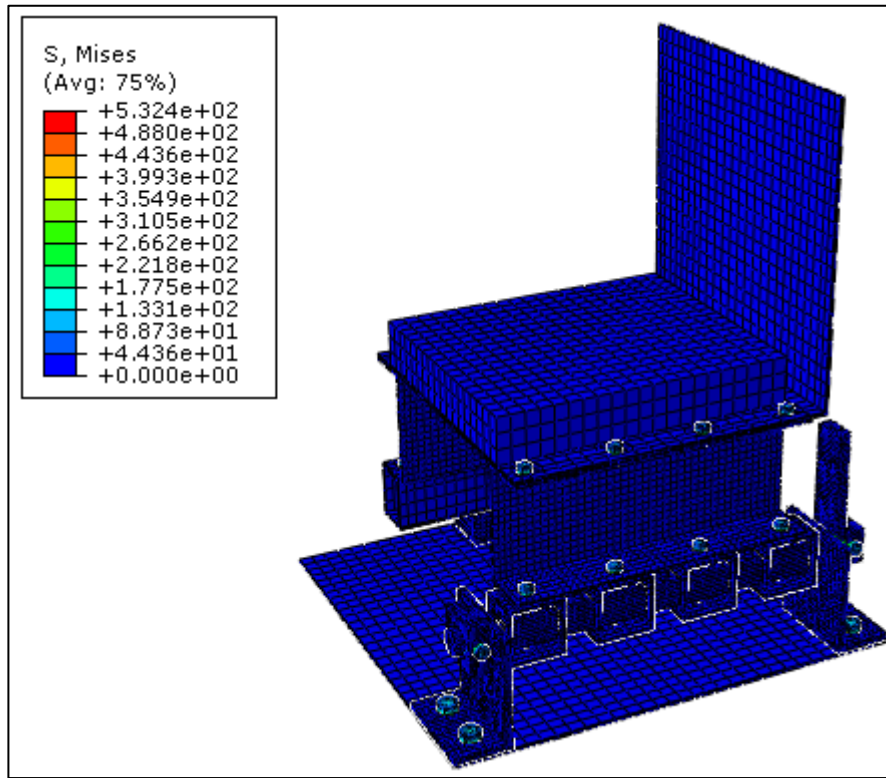
Figure 5.4. Results of bolt preload analysis of the Interchangeable Floor
Deformation Unit and the Simplified Helicopter Seat

At the end of torque application, the concluding stress values are shown in Table 5.3. Neither the parts nor the fasteners exceed the yield point. Therefore, their factor of safeties with respect to yield ($n_y$) range from 1.02 to 1.76. Other parts apart from the levers and the dummy floor part are stressed via torque application.

The 77 kg dummy mass (DM) is not investigated for this analysis since it only demonstrates the mass. In addition, the dummy floor part (P322-1) senses negligible bolting load since most of these loads are transferred to its mating parts (P247A-1, P247A-2, P257A-1, P257A-2). Furthermore, the pitch lever (P304-1) and the roll lever (P304-2) are not affected by bolt preload since they do not have bolt connections.

Table 5.3. von Mises stress results of bolt preload analysis of the Interchangeable Floor Deformation Unit and the Simplified Helicopter Seat

| Part No & Instances | Material | $S_Y$ [MPa] | $\sigma_{max}$ [MPa] | $n_Y$ |
|---|---|---|---|---|
| M12x9-1 | 8.8 Grade St | 543.9 | 308.8 | 1.76 |
| M12x9-2 | 8.8 Grade St | 543.9 | 368.6 | 1.48 |
| M12x9-3 | 8.8 Grade St | 543.9 | 312.0 | 1.74 |
| M12x9-4 | 8.8 Grade St | 543.9 | 310.5 | 1.75 |
| M12x9-5 | 8.8 Grade St | 543.9 | 318.6 | 1.71 |
| M12x9-6 | 8.8 Grade St | 543.9 | 367.6 | 1.48 |
| M12x9-7 | 8.8 Grade St | 543.9 | 373.7 | 1.46 |
| M12x9-8 | 8.8 Grade St | 543.9 | 367.4 | 1.48 |
| M12x10-1 | 8.8 Grade St | 543.9 | 330.1 | 1.65 |
| M12x10-2 | 8.8 Grade St | 543.9 | 336.7 | 1.62 |
| M12x10-3 | 8.8 Grade St | 543.9 | 331.2 | 1.64 |
| M12x10-4 | 8.8 Grade St | 543.9 | 332.1 | 1.64 |
| M12x10-5 | 8.8 Grade St | 543.9 | 336.6 | 1.62 |
| M12x10-6 | 8.8 Grade St | 543.9 | 345.0 | 1.58 |
| M12x10-7 | 8.8 Grade St | 543.9 | 333.6 | 1.63 |
| M12x10-8 | 8.8 Grade St | 543.9 | 332.2 | 1.64 |
| M12x50-1 | 8.8 Grade St | 543.9 | 324.3 | 1.68 |
| M12x50-2 | 8.8 Grade St | 543.9 | 325.4 | 1.67 |
| M12x70-1 | 8.8 Grade St | 543.9 | 324.0 | 1.68 |
| M12x70-2 | 8.8 Grade St | 543.9 | 324.1 | 1.68 |
| M18x15-1 | 8.8 Grade St | 543.9 | 531.0 | 1.02 |
| M18x15-2 | 8.8 Grade St | 543.9 | 530.2 | 1.03 |
| M18x15-3 | 8.8 Grade St | 543.9 | 532.1 | 1.02 |
| M18x15-4 | 8.8 Grade St | 543.9 | 530.7 | 1.02 |
| M18x15-5 | 8.8 Grade St | 543.9 | 530.9 | 1.02 |
| M18x15-6 | 8.8 Grade St | 543.9 | 532.4 | 1.02 |
| M18x15-7 | 8.8 Grade St | 543.9 | 532.2 | 1.02 |
| M18x15-8 | 8.8 Grade St | 543.9 | 531.4 | 1.02 |
| P214A-1 | A284 St, Grade D | 230.0 | 88.4 | 2.60 |
| P224A-1 | A284 St, Grade D | 230.0 | 89.0 | 2.58 |
| P224A-2 | A284 St, Grade D | 230.0 | 89.3 | 2.58 |
| P224A-3 | A284 St, Grade D | 230.0 | 88.5 | 2.60 |
| P224A-4 | A284 St, Grade D | 230.0 | 88.5 | 2.60 |
| P234-1 | A284 St, Grade D | 230.0 | 41.3 | 5.57 |
| P247A-1 | A284 St, Grade D | 230.0 | 179.5 | 1.28 |
| P247A-2 | A284 St, Grade D | 230.0 | 179.5 | 1.28 |
| P257A-1 | A284 St, Grade D | 230.0 | 153.3 | 1.50 |
| P257A-2 | A284 St, Grade D | 230.0 | 153.3 | 1.50 |
| P266-1 | A284 St, Grade D | 230.0 | 41.3 | 5.57 |
| P304-1 | A284 St, Grade D | 230.0 | 3.2 | 72.28 |
| P304-2 | A284 St, Grade D | 230.0 | 3.1 | 74.07 |
| P390A-1 | Al 2024-T351 | 265.0 | 85.4 | 3.10 |
| P390A-2 | Al 2024-T351 | 265.0 | 78.1 | 3.39 |
| P460A-1 | Al 2024-T351 | 265.0 | 57.9 | 4.58 |
| P480-1 | A284 St, Grade D | 230.0 | 158.4 | 1.45 |
| P480-2 | A284 St, Grade D | 230.0 | 160.7 | 1.43 |
| P490-1 | A284 St, Grade D | 230.0 | 168.4 | 1.37 |
| P490-2 | A284 St, Grade D | 230.0 | 167.8 | 1.37 |

## 5.4. Floor Deformation and Pin Insertion Analyses of the Interchangeable Floor Deformation Unit and the Simplified Helicopter Seat

The prerequisite of this analysis is the bolt preload analysis as discussed in Section 5.3 since the meshes change due to the bolt preloading. This mapping process is similar to the mapping of the bolt preload analysis of SHS as described in Section 4.2 into the crash analysis of SHS as described in Section 4.3.

The floor deformation and the pin insertion analyses are performed to be consistent with CS 29.562 as outlined in Section 2.1. Henceforth, Abaqus/Explicit is used for this analysis as explained in Section 3.1. The analyses involves two steps called floor deformation and pin insertion.

The floor deformation and the pin insertion analyses last in 50 ms consisting of three different phases as the roll deformation, the pitch deformation, and the pin insertion. The roll deformation occurs via turning the roll lever $10^0$ between 0 ms and 20 ms. The pitch deformation starts in a similar condition where the pitch lever is rotated between 20 ms and 40 ms. The pin insertion phase begins while the roll lever and the pitch lever are stagnant at their $10^0$ positions.

The pin insertion phase is necessary to hold the roll lever and the pitch lever in their positions. In real life, the roll pin and the pitch pin should be used for restraining the spring back of the levers. The last step is the steady state step where all lever loads are allowed to be relieved to observe the final behavior of the levers. They must be intact after this analysis. The roll pin (P501-2) and the pitch pin (P501-1) have diameters of 10 mm, and the unit mass of 0.04 kg. The fasters are made of 8.8 Grade Steels. Mesh type of the pin, either roll or pitch, is presented in Table 5.4.

Table 5.4. Mesh type of the pin

| Part No | Number of Elements | Library | Element |
|---------|--------------------|---------|---------|
| P501 | 896 | Standard | C3D8R |

As mentioned in Section 2.1, the roll deformation includes the deformation of IFDU and SHS assembly when the roll lever is rotated $10^0$. This is shown in Figure 5.5. The

roll deformation is occurred between 0 ms and 20 ms. The pitch deformation is performed just after the roll deformation as it is stated in Section 2.1. The pitch deformation occurs due to the pitch rotation, which is between 20 and 40 ms. This situation is illustrated in Figure 5.6.
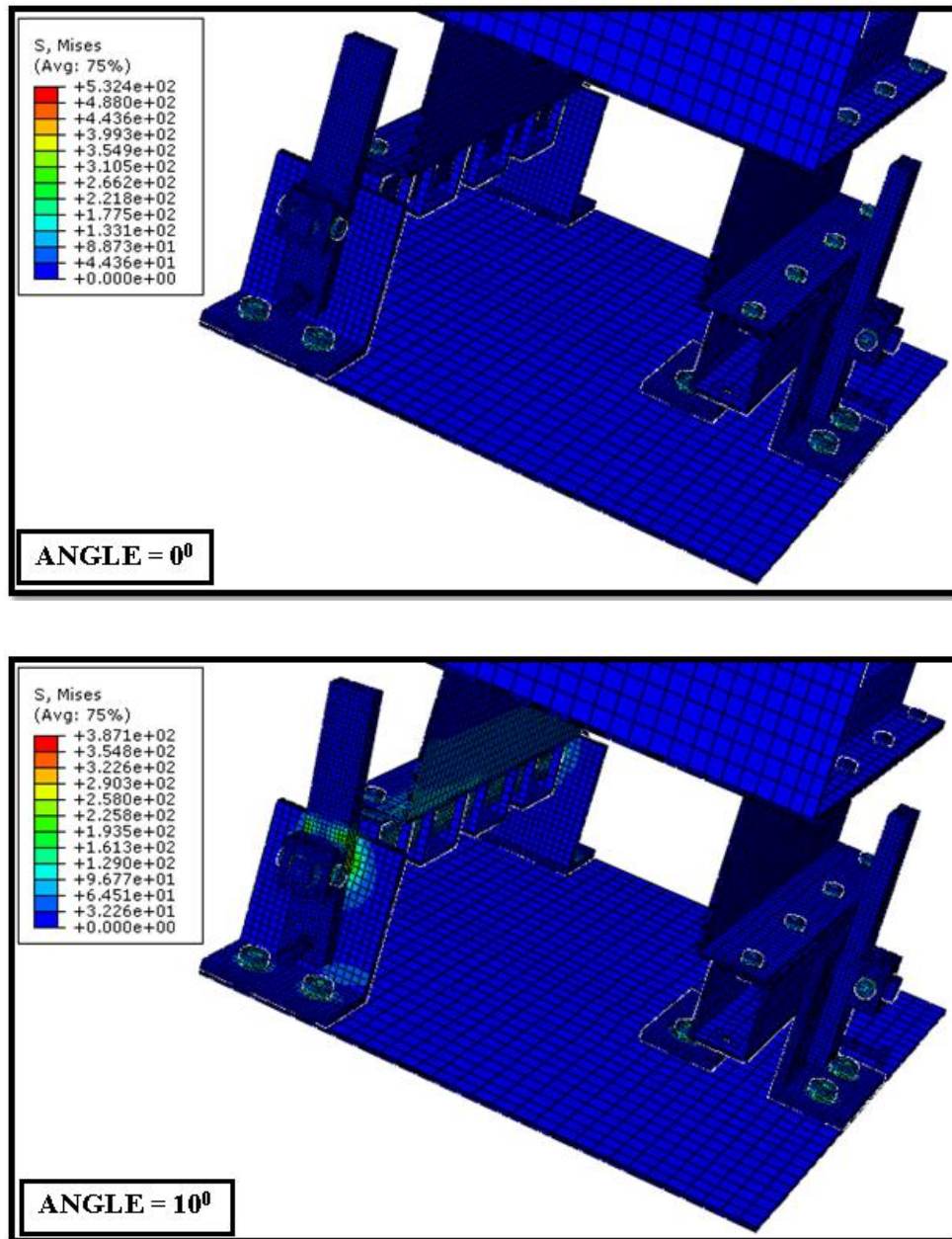


Figure 5.5. Roll rotation of the roll lever
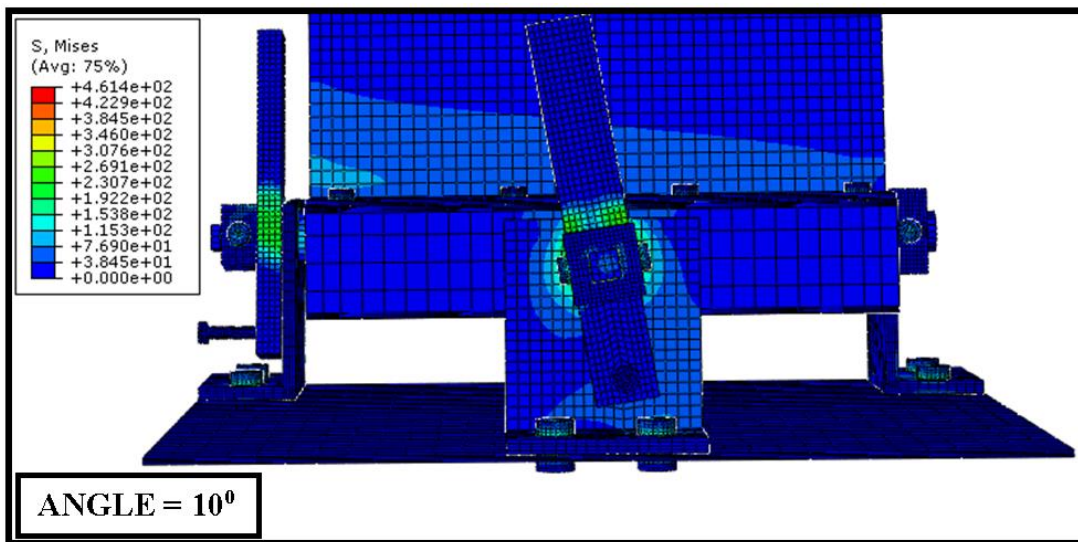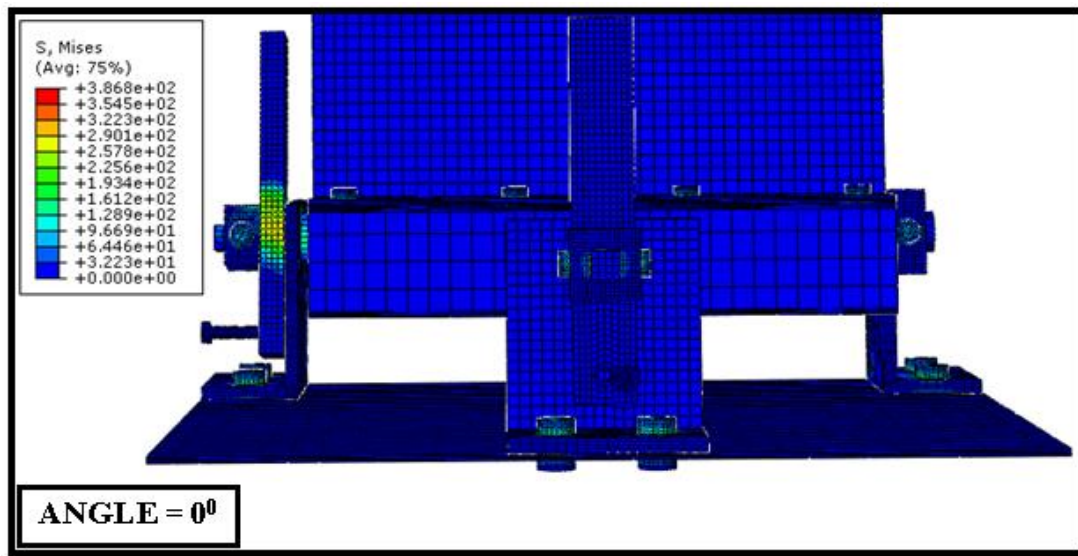
Figure 5.6. Pitch rotation of the pitch lever

Thereupon, the pin insertion phase starts. It is performed between 40 ms and 50 ms. The first half of this step involves the motion of the pitch pin and the roll pin. This motion is the linear displacement of the pin into the lever and the L support. This pin works as the fixation of the mechanism after the levers are turned. Finally, the steady state step starts to achieve a steady state condition. The initial and final states of the pins are shown in Figure 5.7.
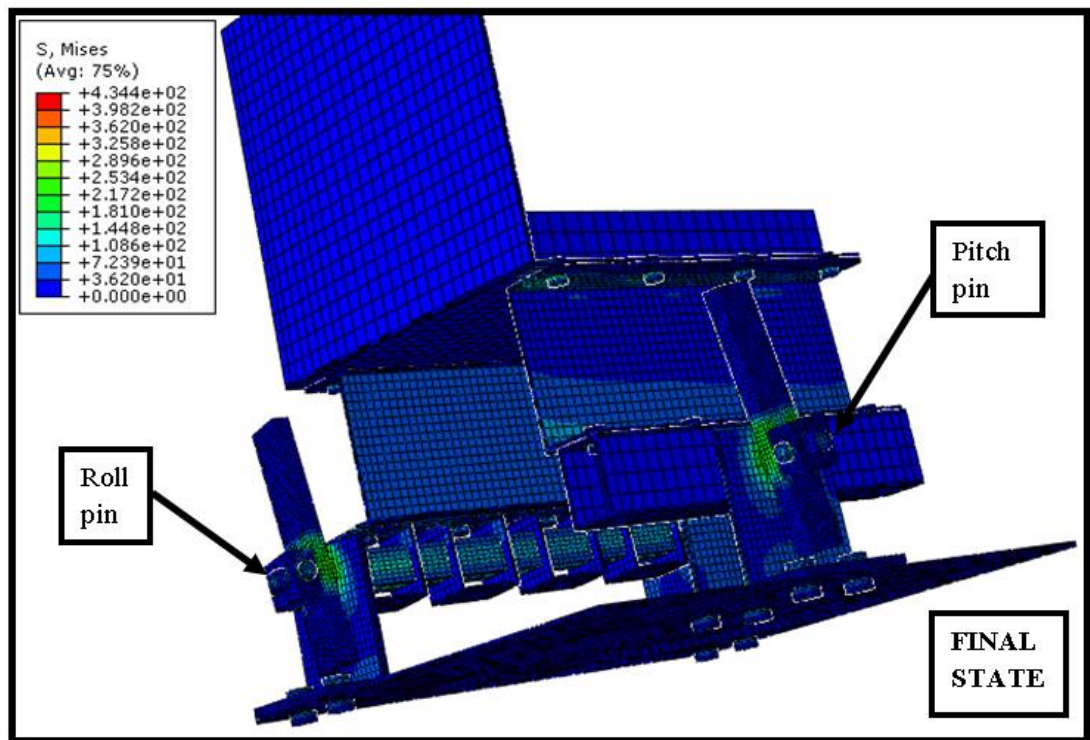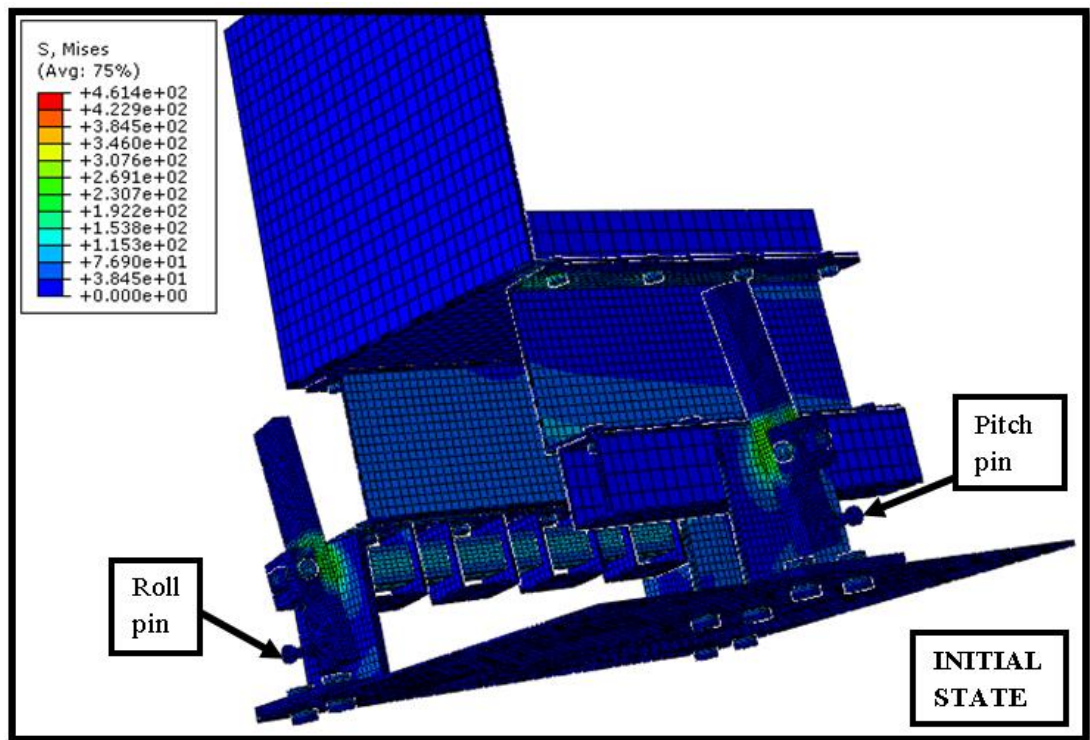
Figure 5.7. Initial and final position of the roll pin and the pitch pin

The analysis results in 3 hours and 38 minutes on the particular computer described in Section 3.1. Although, this is a quasi-static process Abaqus/Explicit is used for this analysis since it can handle many contacts during this analysis. The success criteria of the utilization of Abaqus/Explicit are explained in Appendix B.

The resulting von Mises stresses are tabulated in Table 5.5. The dummy floor part (P322-1) does have any loads, it does have only negligible stress value. In addition, none of the fasteners exceeds the yield strength limit. Their factor of safeties with respect to yield ($n_y$) are between 1.02 and 1.76.

On the other hand, some parts experiences plastic deformation. This situation is reasonable because considerable amount of the torsional loads are exerted to this parts due to the rotational motions. Noting that this may happen prior to the crash of a helicopter. In other words, the supporting parts holding the helicopter seat may experience plastic deformation prior to the impact. Another result of this situation is the fact that the plastically deformed (PD) parts should be replaced if the floor deformation test is repeated. On the contrary, the all of the parts or the fasteners of SHS are stressed within their elastic limit as shown in Table 5.5.

Table 5.5. von Mises stress results of floor deformation and pin insertion analyses of the Interchangeable Floor Deformation Unit and the Simplified Helicopter Seat

| Part No & Instances | Material | $S_Y$ [MPa] | $S_U$ [MPa] | $\sigma_{max}$ [MPa] | $n_Y$ | $n_U$ |
|---|---|---|---|---|---|---|
| M12x9-1 | 8.8 Grade St | 543.9 | 800.0 | 308.8 | 1.76 | 2.59 |
| M12x9-2 | 8.8 Grade St | 543.9 | 800.0 | 368.6 | 1.48 | 2.17 |
| M12x9-3 | 8.8 Grade St | 543.9 | 800.0 | 312.0 | 1.74 | 2.56 |
| M12x9-4 | 8.8 Grade St | 543.9 | 800.0 | 310.5 | 1.75 | 2.58 |
| M12x9-5 | 8.8 Grade St | 543.9 | 800.0 | 318.6 | 1.71 | 2.51 |
| M12x9-6 | 8.8 Grade St | 543.9 | 800.0 | 367.6 | 1.48 | 2.18 |
| M12x9-7 | 8.8 Grade St | 543.9 | 800.0 | 373.7 | 1.46 | 2.14 |
| M12x9-8 | 8.8 Grade St | 543.9 | 800.0 | 367.4 | 1.48 | 2.18 |
| M12x10-1 | 8.8 Grade St | 543.9 | 800.0 | 461.4 | 1.18 | 1.73 |
| M12x10-2 | 8.8 Grade St | 543.9 | 800.0 | 393.5 | 1.38 | 2.03 |
| M12x10-3 | 8.8 Grade St | 543.9 | 800.0 | 377.6 | 1.44 | 2.12 |
| M12x10-4 | 8.8 Grade St | 543.9 | 800.0 | 383.5 | 1.42 | 2.09 |
| M12x10-5 | 8.8 Grade St | 543.9 | 800.0 | 387.2 | 1.40 | 2.07 |
| M12x10-6 | 8.8 Grade St | 543.9 | 800.0 | 420.1 | 1.29 | 1.90 |
| M12x10-7 | 8.8 Grade St | 543.9 | 800.0 | 395.9 | 1.37 | 2.02 |
| M12x10-8 | 8.8 Grade St | 543.9 | 800.0 | 405.5 | 1.34 | 1.97 |
| M12x50-1 | 8.8 Grade St | 543.9 | 800.0 | 385.2 | 1.41 | 2.08 |

Table 5.5. (continued)

| Part No & Instances | Material | $S_Y$ [MPa] | $S_U$ [MPa] | $\sigma_{max}$ [MPa] | $n_Y$ | $n_U$ |
|---|---|---|---|---|---|---|
| M12x50-2 | 8.8 Grade St | 543.9 | 800.0 | 428.8 | 1.27 | 1.87 |
| M12x70-1 | 8.8 Grade St | 543.9 | 800.0 | 339.6 | 1.60 | 2.36 |
| M12x70-2 | 8.8 Grade St | 543.9 | 800.0 | 349.9 | 1.55 | 2.29 |
| M18x15-1 | 8.8 Grade St | 543.9 | 800.0 | 531.0 | 1.02 | 1.51 |
| M18x15-2 | 8.8 Grade St | 543.9 | 800.0 | 530.2 | 1.03 | 1.51 |
| M18x15-3 | 8.8 Grade St | 543.9 | 800.0 | 532.1 | 1.02 | 1.50 |
| M18x15-4 | 8.8 Grade St | 543.9 | 800.0 | 530.7 | 1.02 | 1.51 |
| M18x15-5 | 8.8 Grade St | 543.9 | 800.0 | 530.9 | 1.02 | 1.51 |
| M18x15-6 | 8.8 Grade St | 543.9 | 800.0 | 532.4 | 1.02 | 1.50 |
| M18x15-7 | 8.8 Grade St | 543.9 | 800.0 | 532.2 | 1.02 | 1.50 |
| M18x15-8 | 8.8 Grade St | 543.9 | 800.0 | 531.4 | 1.02 | 1.51 |
| P214A-1 | A284 St, Grade D | 230.0 | 338.3 | 230.0 | PD | 1.47 |
| P224A-1 | A284 St, Grade D | 230.0 | 338.3 | 133.9 | 1.72 | 2.53 |
| P224A-2 | A284 St, Grade D | 230.0 | 338.3 | 178.9 | 1.29 | 1.89 |
| P224A-3 | A284 St, Grade D | 230.0 | 338.3 | 143.0 | 1.61 | 2.37 |
| P224A-4 | A284 St, Grade D | 230.0 | 338.3 | 131.8 | 1.75 | 2.57 |
| P234-1 | A284 St, Grade D | 230.0 | 338.3 | 295.6 | PD | 1.14 |
| P247A-1 | A284 St, Grade D | 230.0 | 338.3 | 261.1 | PD | 1.30 |
| P247A-2 | A284 St, Grade D | 230.0 | 338.3 | 265.5 | PD | 1.27 |
| P257A-1 | A284 St, Grade D | 230.0 | 338.3 | 267.4 | PD | 1.27 |
| P257A-2 | A284 St, Grade D | 230.0 | 338.3 | 264.6 | PD | 1.28 |
| P266-1 | A284 St, Grade D | 230.0 | 338.3 | 295.7 | PD | 1.14 |
| P304-1 | A284 St, Grade D | 230.0 | 338.3 | 280.5 | PD | 1.21 |
| P304-2 | A284 St, Grade D | 230.0 | 338.3 | 314.0 | PD | 1.08 |
| P390A-1 | Al 2024-T351 | 265.0 | 547.9 | 207.6 | 1.28 | 2.64 |
| P390A-2 | Al 2024-T351 | 265.0 | 547.9 | 141.1 | 1.88 | 3.88 |
| P460A-1 | Al 2024-T351 | 265.0 | 547.9 | 128.6 | 2.06 | 4.26 |
| P480-1 | A284 St, Grade D | 230.0 | 338.3 | 224.7 | 1.02 | 1.51 |
| P480-2 | A284 St, Grade D | 230.0 | 338.3 | 222.3 | 1.03 | 1.52 |
| P490-1 | A284 St, Grade D | 230.0 | 338.3 | 228.4 | 1.01 | 1.48 |
| P490-2 | A284 St, Grade D | 230.0 | 338.3 | 227.7 | 1.01 | 1.47 |
| P501-1 | 8.8 Grade St | 543.9 | 800.0 | 667.5 | PD | 1.20 |
| P501-2 | 8.8 Grade St | 543.9 | 800.0 | 641.1 | PD | 1.25 |

## 5.5. Crash Analysis of the Interchangeable Floor Deformation Unit and the Simplified Helicopter Seat

The crash analysis begins after the completion of the bolt preload analysis as discussed in Section 5.3 and the floor deformation and the pin insertions analyses as discussed in Section 5.4. This is accomplished by using the mapping process in Abaqus/Explicit. After deforming IFDU and SHS with $10^0$ roll and pitch deformations, 9.144 ms/s initial impact velocity is applied to the assembly of IFDU and SHS with DM as stated in Table 2.2.

The crash does not start immediately as mentioned in Section 4.4. Likewise, 0.1 mm vertical gap between the lowest point of the assembly and the rigid plane is employed to avoid the immediate crash due to the establishment of the continuous data.

The goal of this analysis is to figure the response of IFDU and SHS when the crash loads are applied while they are affected with the floor deformation at the onset of this analysis. The initial condition of this analysis is illustrated in Figure 5.8 where the 77 kg dummy mass (DM) is applied on the seat bucket.



Figure 5.8.  Initial condition of the crash analysis of the Interchangeable Floor Deformation Unit and the Simplified Helicopter Seat

The boundary condition of this analysis is the same with the crash analysis of SHS as seen in Section 4.3 as two boundary conditions are used. The first one is the fixation of the rigid plane, which form the basis of the impacted surface. The second one is the initial speed of 9.144 m/s for IFDU and SHS with 77 kg mass (DM) is on.

Since SHS and IFDU are the same with the floor deformation and the pin insertion analyses as seen in Section 5.3, design data is not changed. On the other hand, the

mesh types are selected from the explicit library while all information is the same with Table 5.2.

Eventually, the analysis inputs are processed with the crash simulation. The total step times of analysis occurs in 100 ms. This time equals to 6 hours and 12 minutes on the particular computer described in Section 3.1. This analysis is studied in terms of von Mises criterion [59]. As known, the outcomes of the crash analysis are dynamic. Outcomes of von Mises stresses can be observed in Figure 5.9 − 5.19 where twenty linear time points are utilized in this analysis.

Figure 5.9. von Mises stress representation of the crash analysis of the
Interchangeable Floor Deformation Unit and the Simplified Helicopter Seat at 0 ms
and 5 ms

86

Figure 5.10. von Mises stress representation of the crash analysis of the Interchangeable Floor Deformation Unit and the Simplified Helicopter Seat at 10 ms and 15 ms

Figure 5.11. von Mises stress representation of the crash analysis of the
Interchangeable Floor Deformation Unit and the Simplified Helicopter Seat at 20 ms
and 25 ms

88

Figure 5.12. von Mises stress representation of the crash analysis of the Interchangeable Floor Deformation Unit and the Simplified Helicopter Seat at 30 ms and 35 ms

Figure 5.13. von Mises stress representation of the crash analysis of the Interchangeable Floor Deformation Unit and the Simplified Helicopter Seat at 40 ms and 45 ms

90

Figure 5.14. von Mises stress representation of the crash analysis of the
Interchangeable Floor Deformation Unit and the Simplified Helicopter Seat at 50 ms
and 55 ms
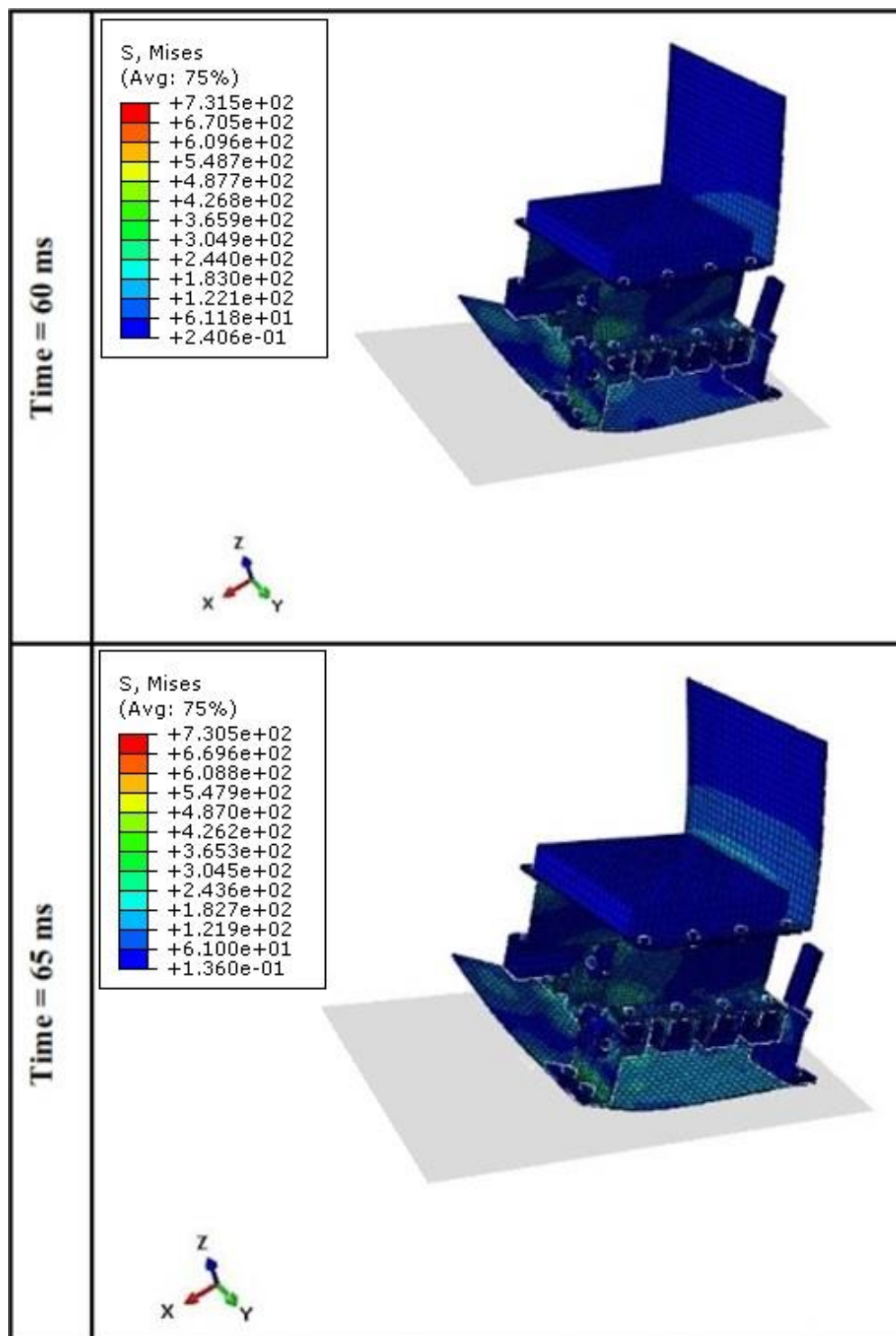
Figure 5.15. von Mises stress representation of the crash analysis of the Interchangeable Floor Deformation Unit and the Simplified Helicopter Seat at 60 ms and 65 ms

92
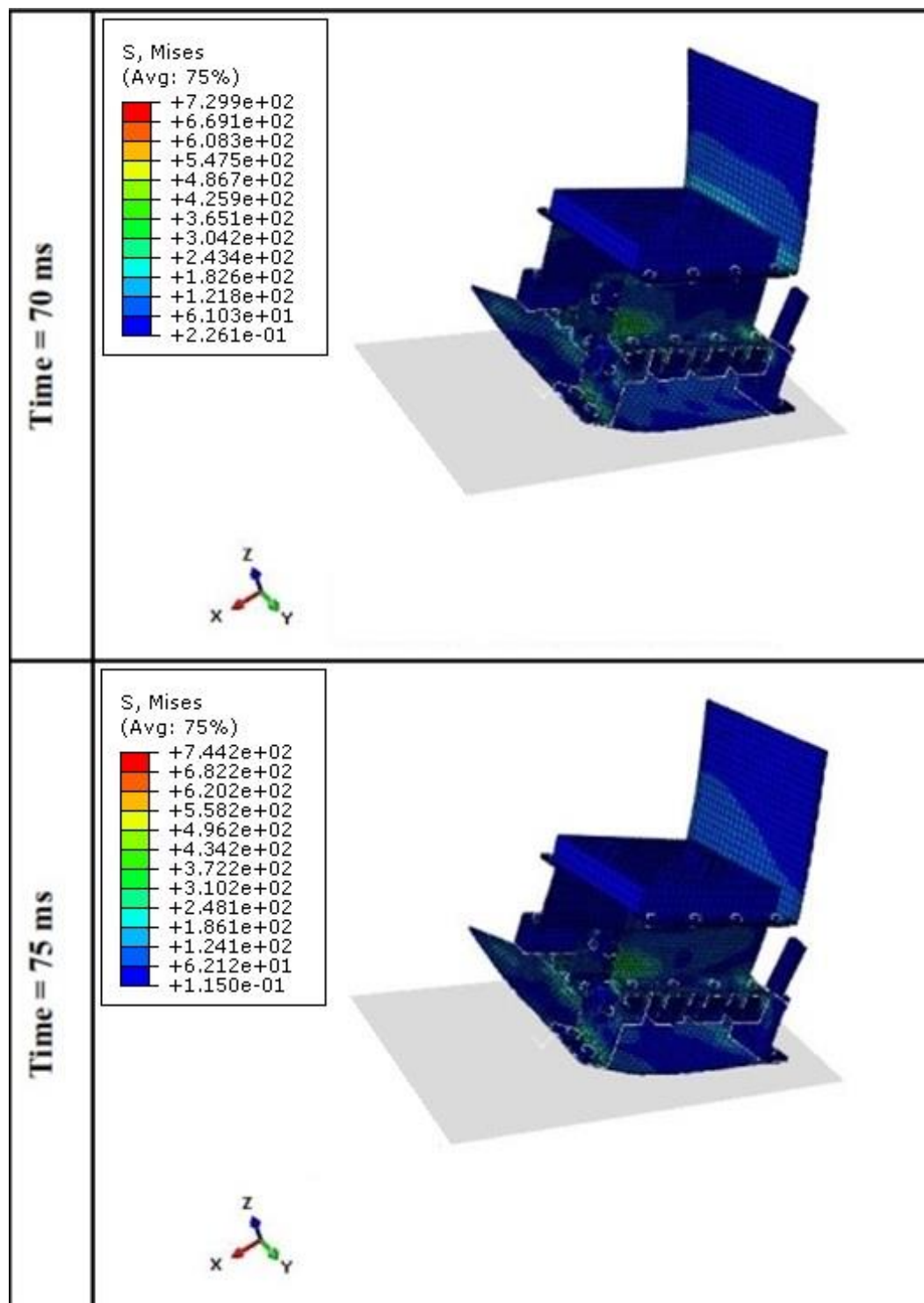
Figure 5.16. von Mises stress representation of the crash analysis of the Interchangeable Floor Deformation Unit and the Simplified Helicopter Seat at 70 ms and 75 ms

93
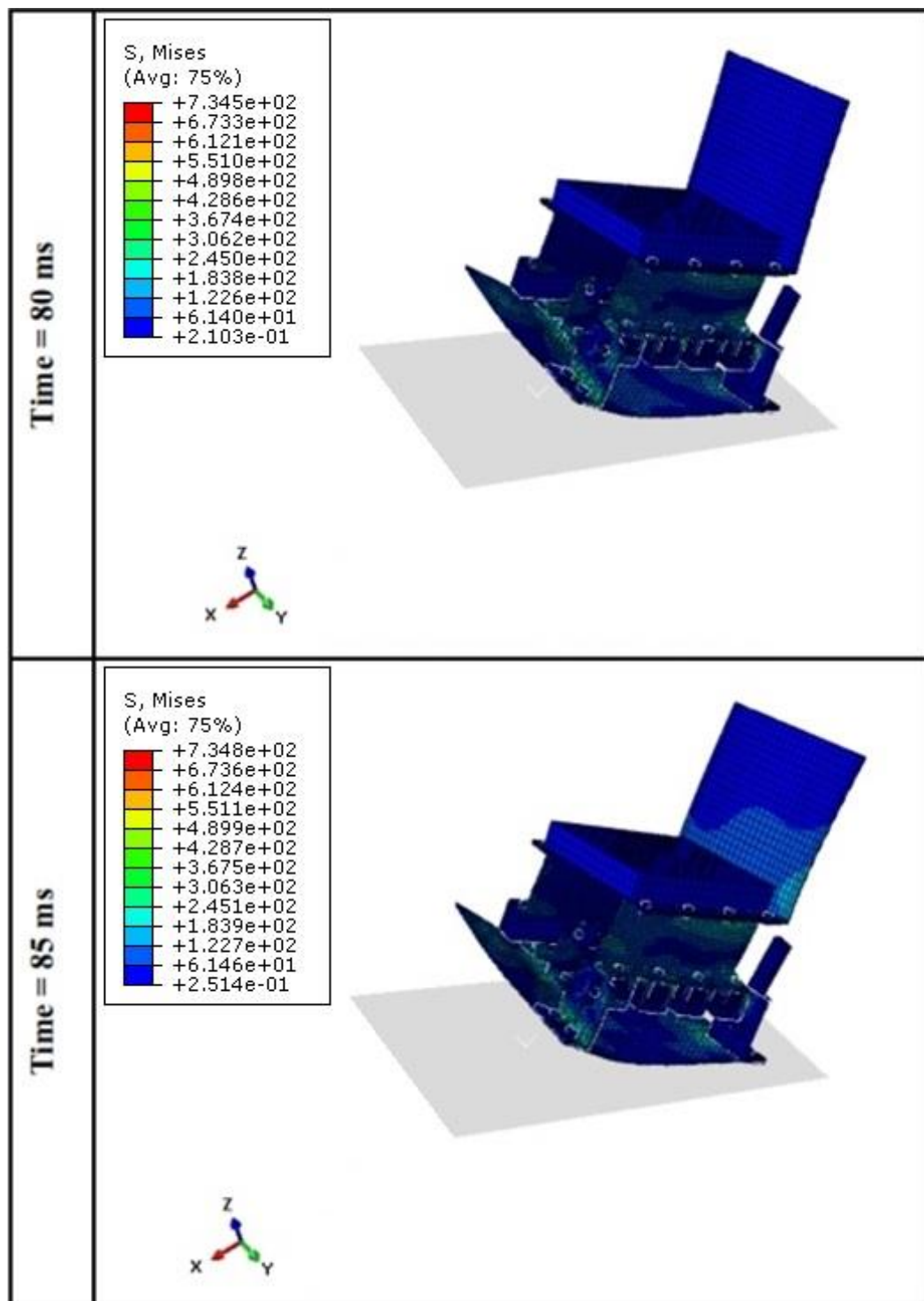
Figure 5.17. von Mises stress representation of the crash analysis of the
Interchangeable Floor Deformation Unit and the Simplified Helicopter Seat at 80 ms
and 85 ms

94
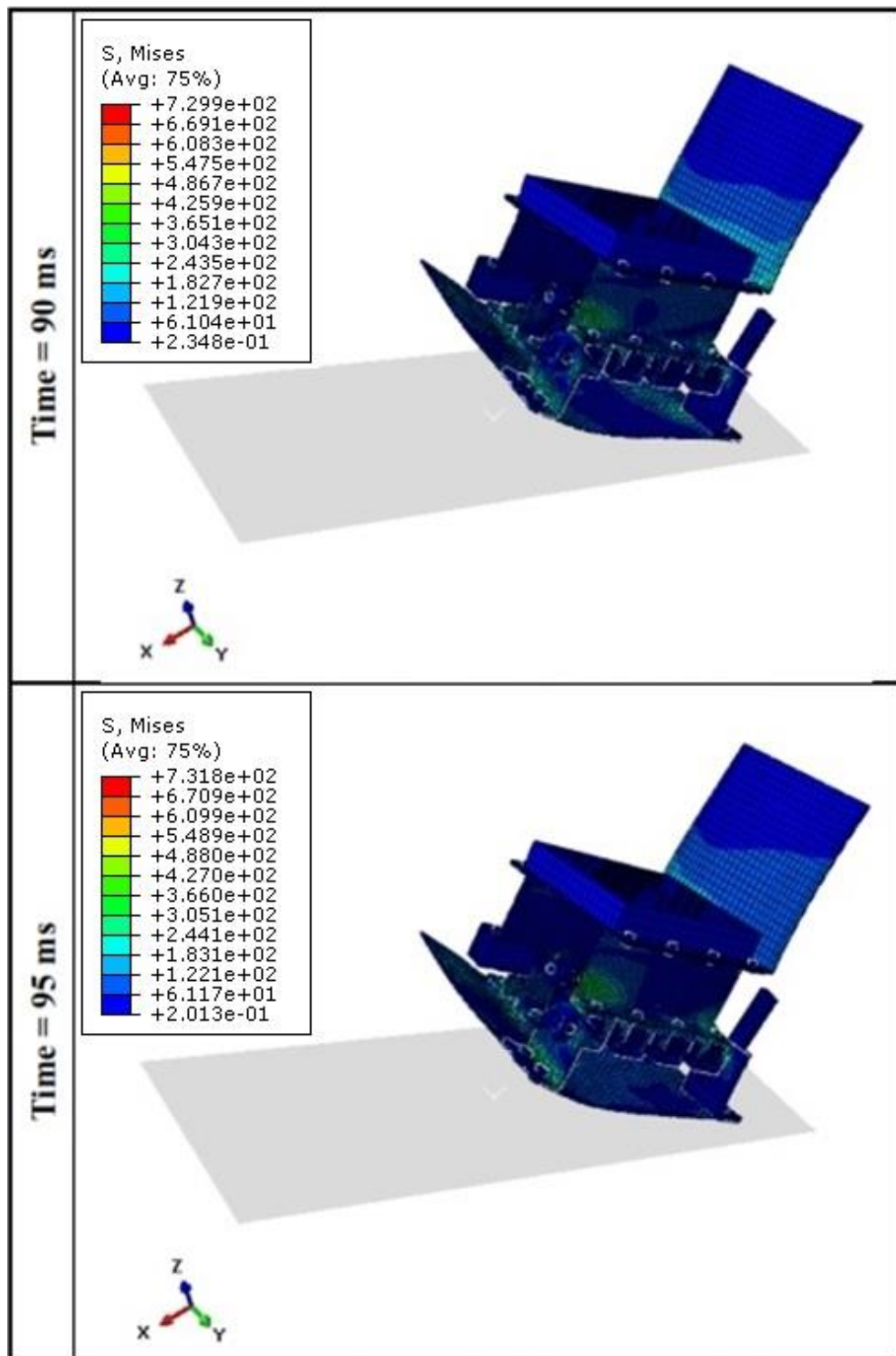
Figure 5.18. von Mises stress representation of the crash analysis of the
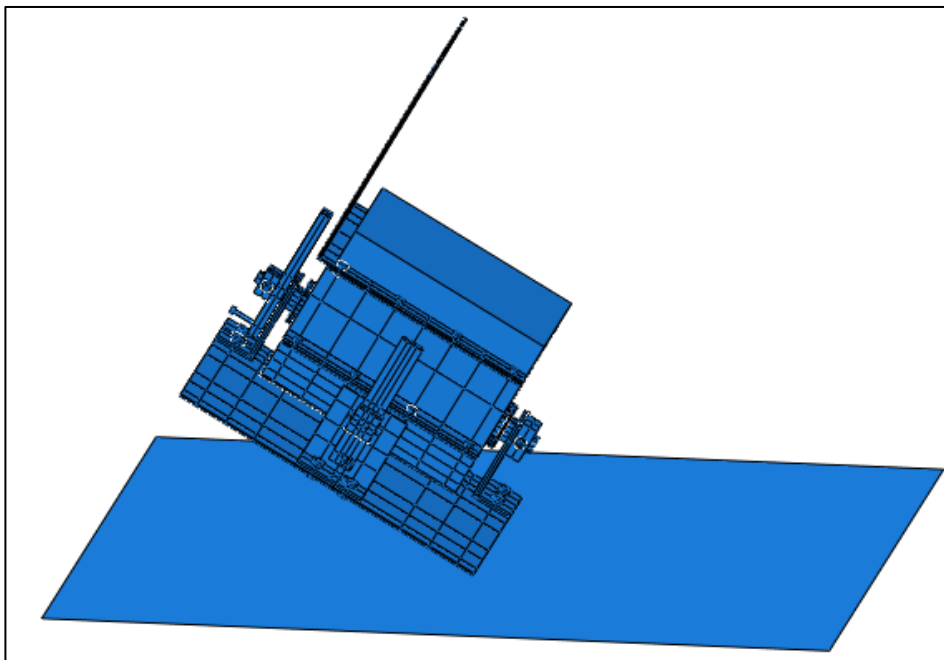Interchangeable Floor Deformation Unit and the Simplified Helicopter Seat at 90 ms
and 95 ms
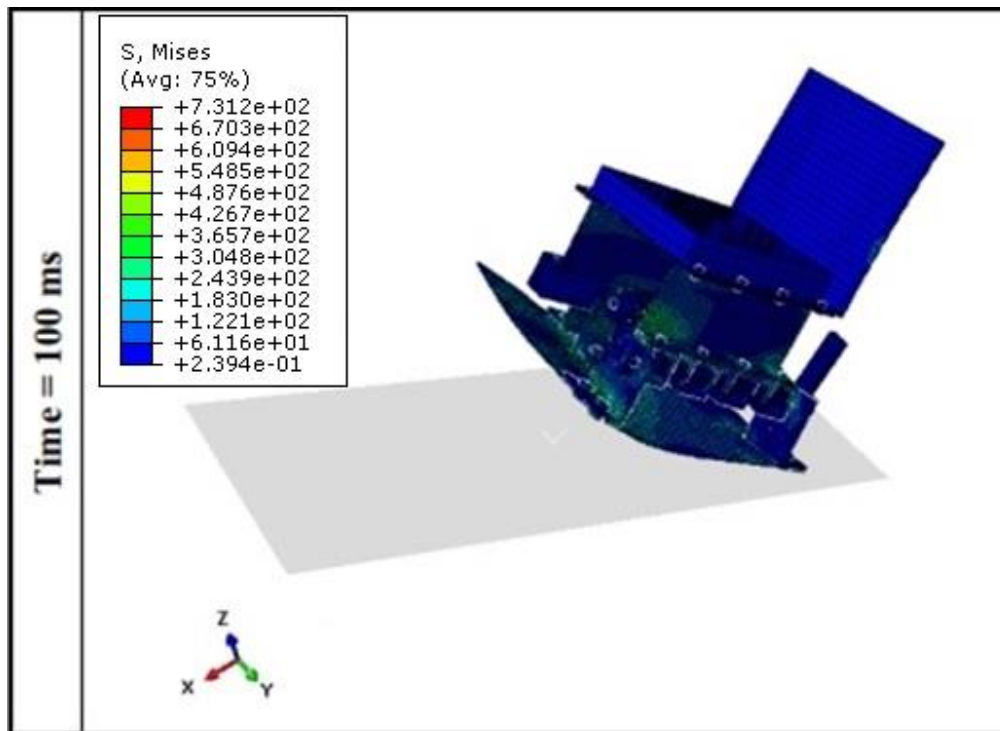
Figure 5.19. von Mises stress representation of the crash analysis of the Interchangeable Floor Deformation Unit and the Simplified Helicopter Seat at 100 ms

To summarize, the subsequent consequences can be derived from Figure 5.9 – 5.19. IFDU and SHS maintain their structural integrity after the impact. In other words, none of the parts or the fasteners are separated from the assembly. Contrary, since SHS does not have any energy absorption system, the impact energy is absorbed by both IFDU and SHS. The impact energy is converted to the kinetic energy and the internal energy of SHS and IFDU. The impact finishes about 45 ms and after which the separation of the assembly from the rigid plate starts.

After the general review of the outcomes, the von Mises criterion of all parts and fasteners are reviewed via examining all figures from Figure 5.9 – 5.19. The maximum stresses of each part or fastener are shown in Table 5.6. Due to impact loads, nearly all parts and fasteners plastically deformed (PD) exceeding the yield point. On the contrary, none of the parts or fasteners exceed the ultimate tensile strength that means the structural integrity of the assembly resumes after the crash.
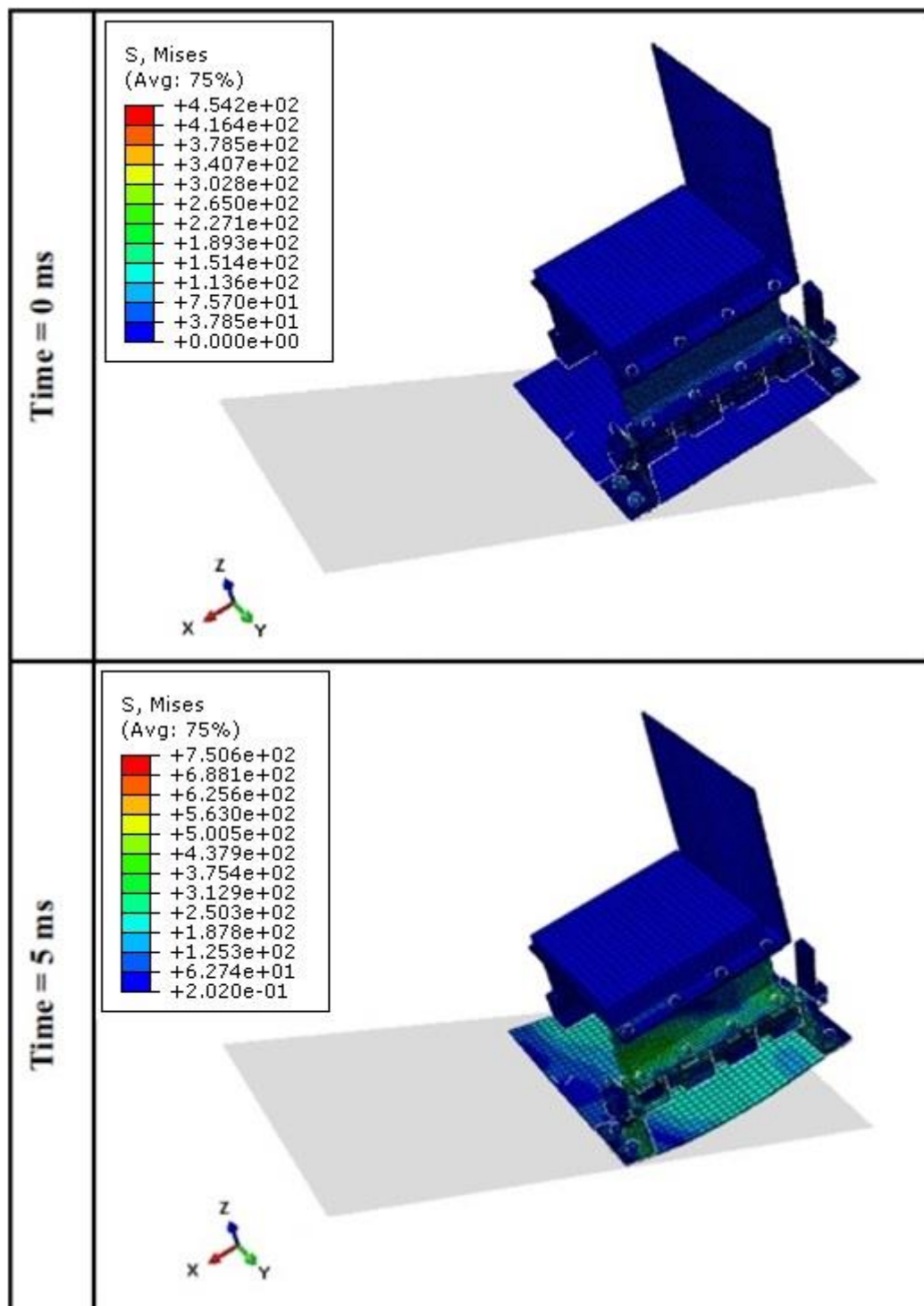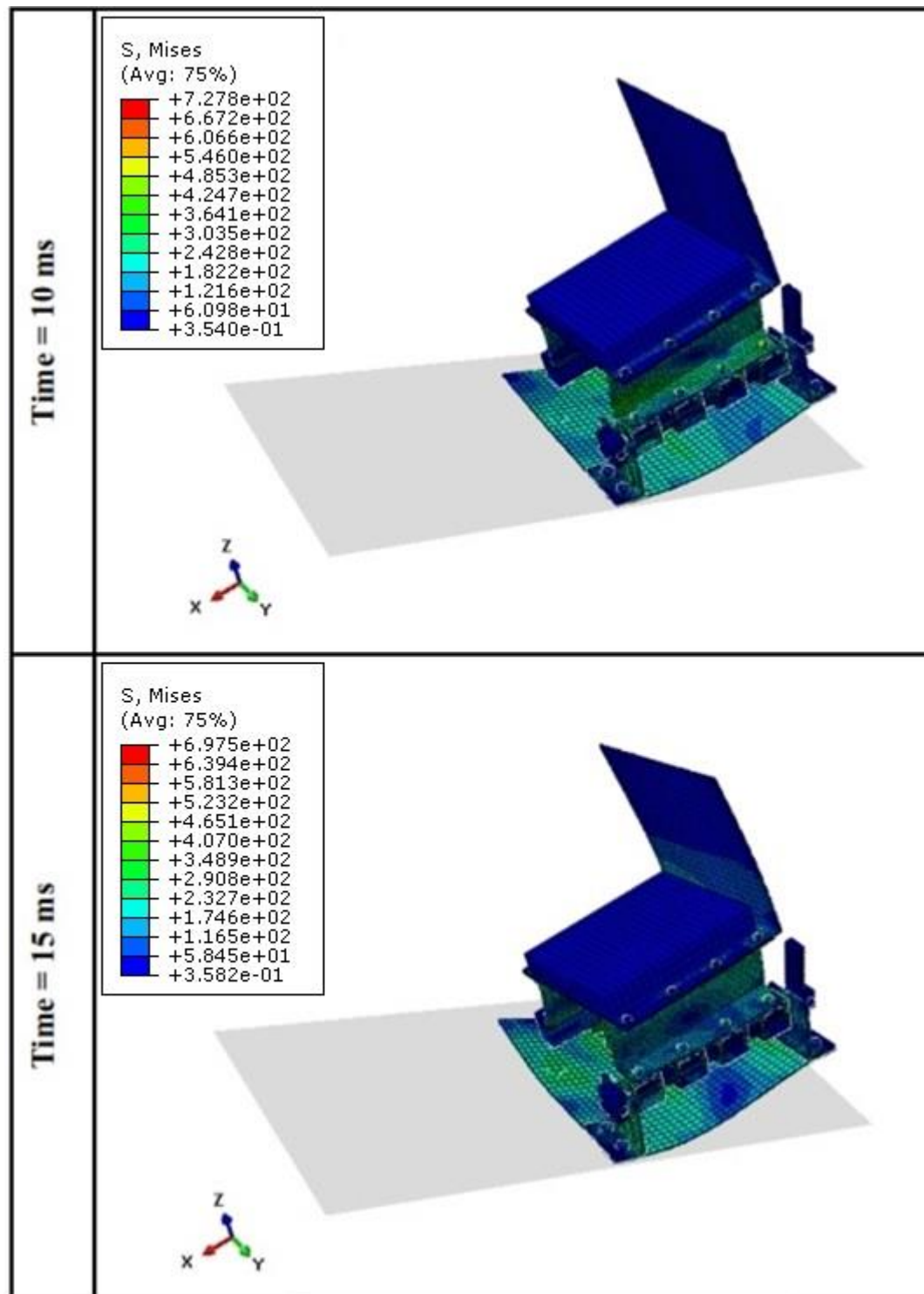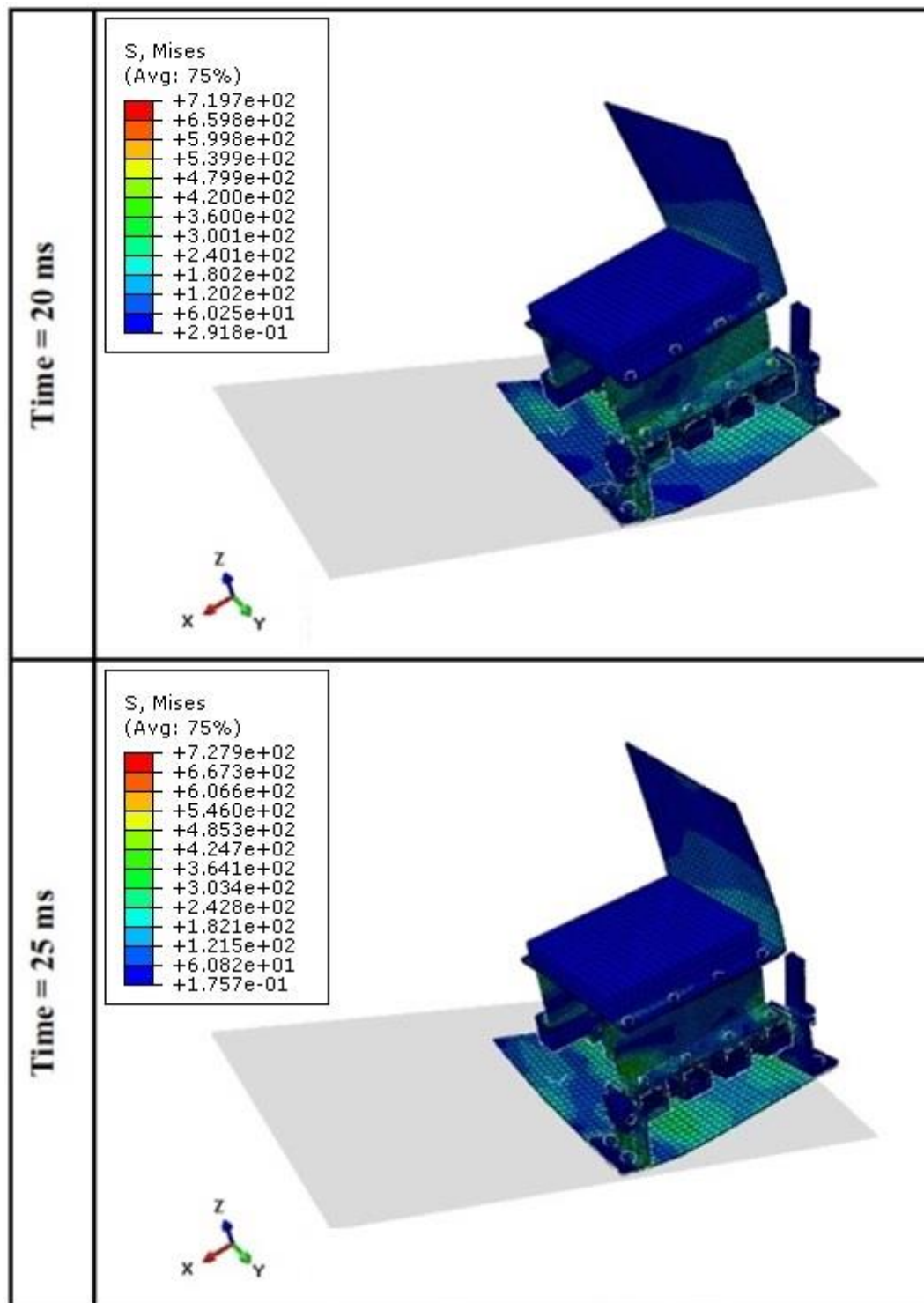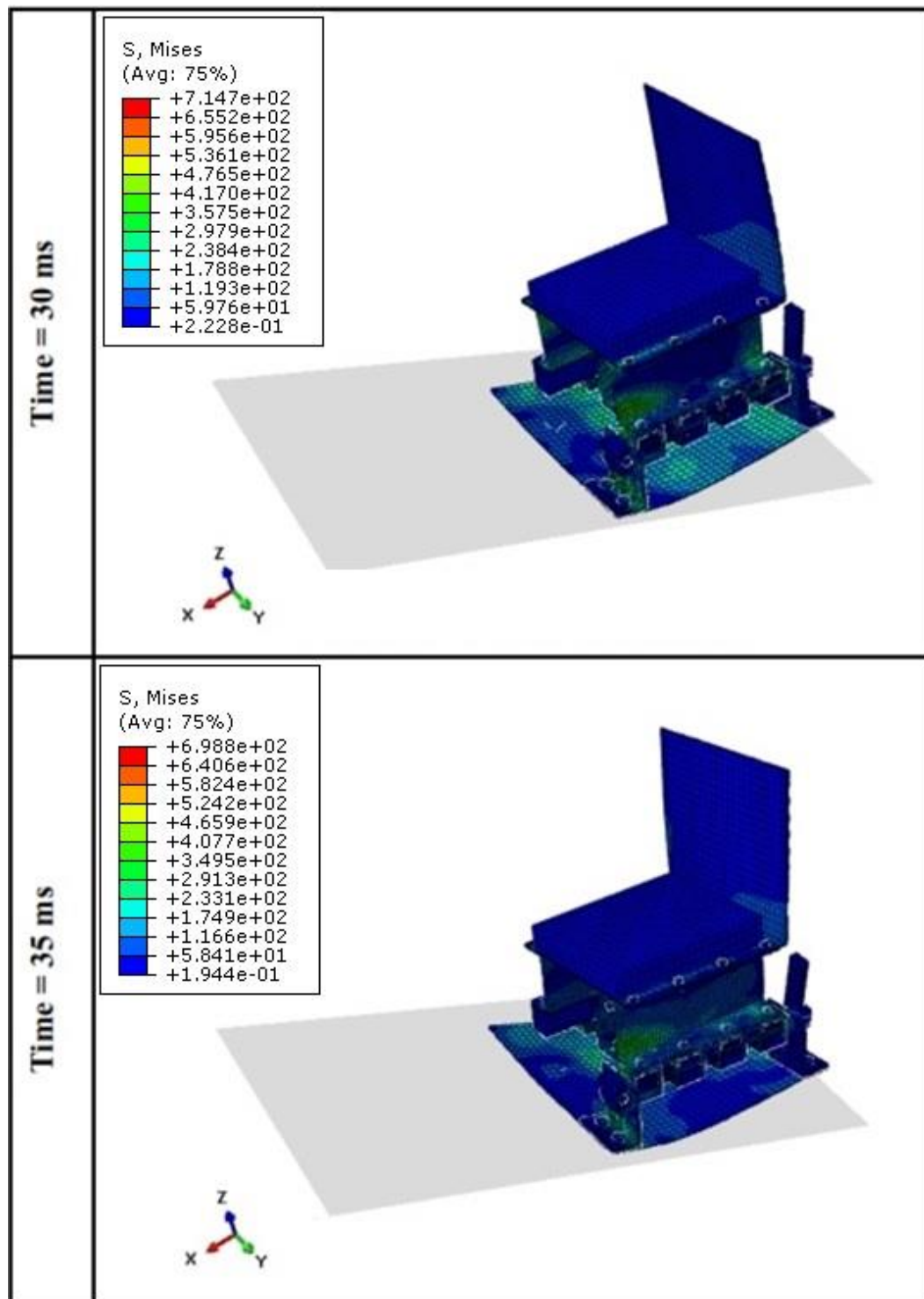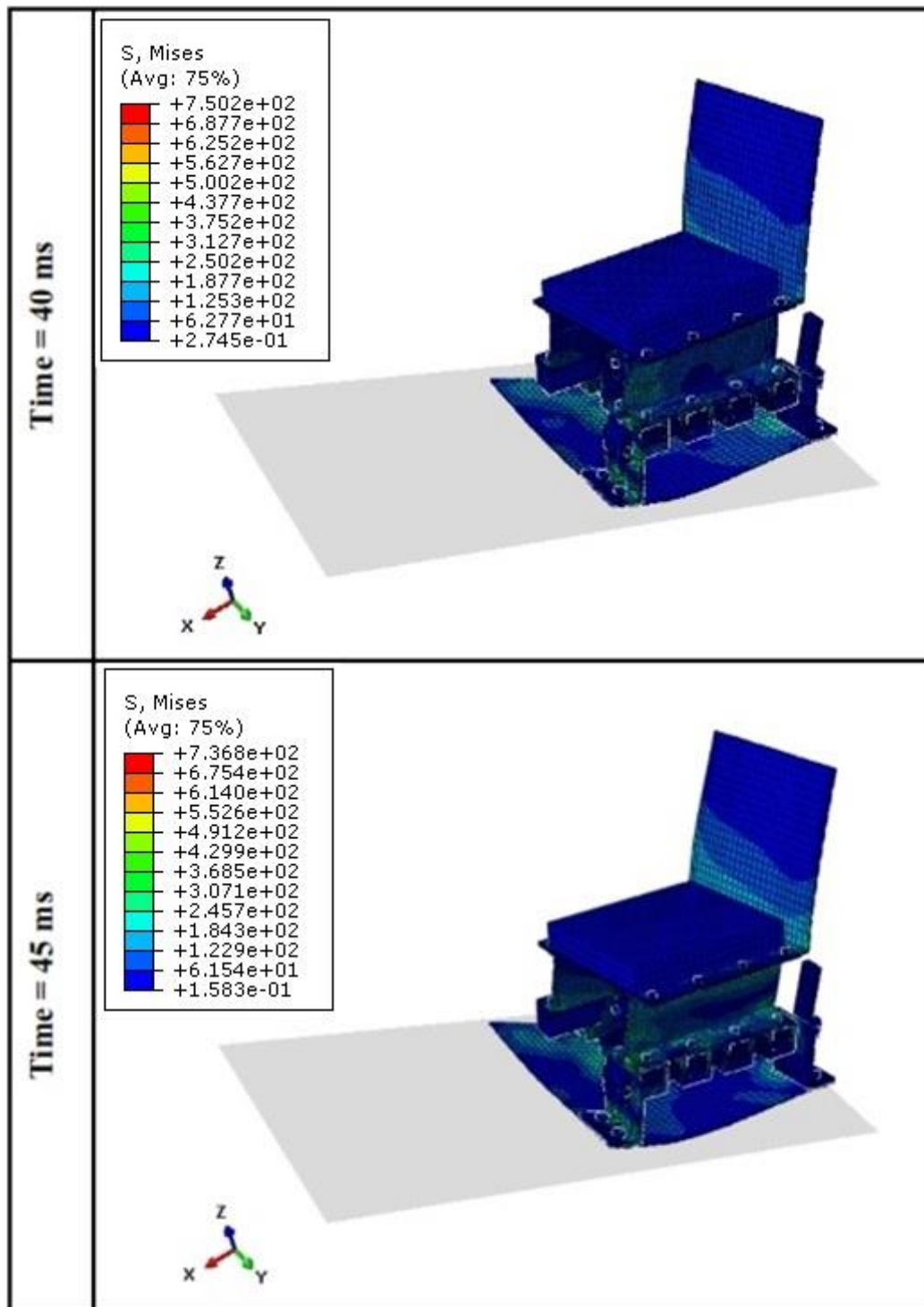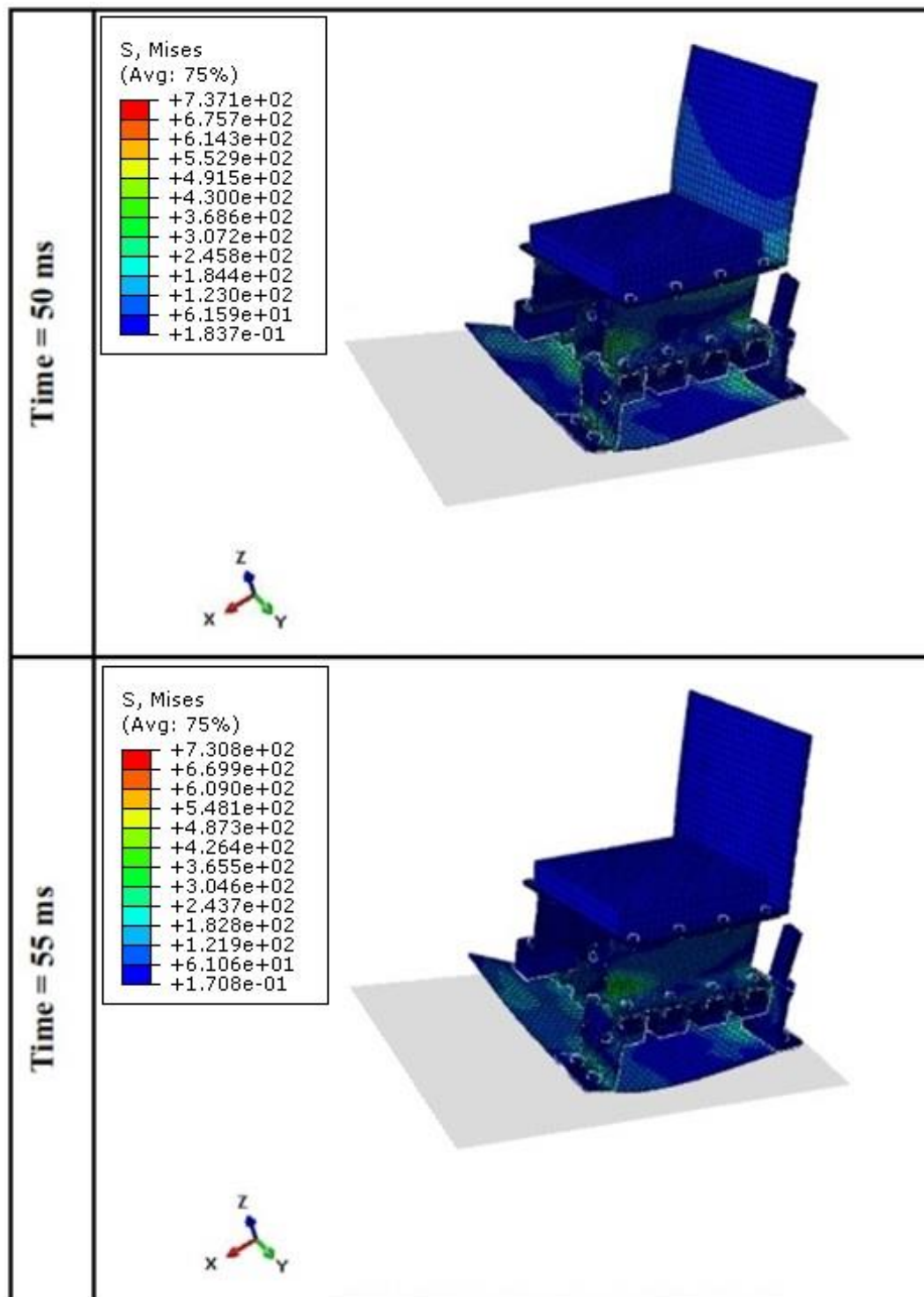
96

Table 5.6. von Mises stress results of crash analysis of the Interchangeable Floor Deformation Unit and the Simplified Helicopter Seat

| Part No & Instances | Material | $S_Y$ [MPa] | $\sigma_{max}$ [MPa] | $n_Y$ |
|---|---|---|---|---|
| M12x9-1 | 8.8 Grade St | 543.9 | 473.3 | 1.15 |
| M12x9-2 | 8.8 Grade St | 543.9 | 700.1 | PD |
| M12x9-3 | 8.8 Grade St | 543.9 | 550.8 | PD |
| M12x9-4 | 8.8 Grade St | 543.9 | 545.8 | PD |
| M12x9-5 | 8.8 Grade St | 543.9 | 503.3 | 1.08 |
| M12x9-6 | 8.8 Grade St | 543.9 | 653.9 | PD |
| M12x9-7 | 8.8 Grade St | 543.9 | 602.8 | PD |
| M12x9-8 | 8.8 Grade St | 543.9 | 536.2 | 1.01 |
| M12x10-1 | 8.8 Grade St | 543.9 | 531.1 | 1.02 |
| M12x10-2 | 8.8 Grade St | 543.9 | 571.4 | PD |
| M12x10-3 | 8.8 Grade St | 543.9 | 549.1 | PD |
| M12x10-4 | 8.8 Grade St | 543.9 | 544.1 | PD |
| M12x10-5 | 8.8 Grade St | 543.9 | 540.2 | 1.01 |
| M12x10-6 | 8.8 Grade St | 543.9 | 621.8 | PD |
| M12x10-7 | 8.8 Grade St | 543.9 | 514.3 | 1.06 |
| M12x10-8 | 8.8 Grade St | 543.9 | 540.0 | 1.01 |
| M12x50-1 | 8.8 Grade St | 543.9 | 558.0 | PD |
| M12x50-2 | 8.8 Grade St | 543.9 | 532.4 | 1.02 |
| M12x70-1 | 8.8 Grade St | 543.9 | 573.9 | PD |
| M12x70-2 | 8.8 Grade St | 543.9 | 565.5 | PD |
| M18x15-1 | 8.8 Grade St | 543.9 | 648.9 | PD |
| M18x15-2 | 8.8 Grade St | 543.9 | 609.5 | PD |
| M18x15-3 | 8.8 Grade St | 543.9 | 750.6 | PD |
| M18x15-4 | 8.8 Grade St | 543.9 | 727.8 | PD |
| M18x15-5 | 8.8 Grade St | 543.9 | 651.1 | PD |
| M18x15-6 | 8.8 Grade St | 543.9 | 750.2 | PD |
| M18x15-7 | 8.8 Grade St | 543.9 | 588.1 | PD |
| M18x15-8 | 8.8 Grade St | 543.9 | 582.8 | PD |
| P214A-1 | A284 St, Grade D | 230.0 | 276.6 | PD |
| P224A-1 | A284 St, Grade D | 230.0 | 302.7 | PD |
| P224A-2 | A284 St, Grade D | 230.0 | 308.6 | PD |
| P224A-3 | A284 St, Grade D | 230.0 | 289.0 | PD |
| P224A-4 | A284 St, Grade D | 230.0 | 298.8 | PD |
| P234-1 | A284 St, Grade D | 230.0 | 300.0 | PD |
| P247A-1 | A284 St, Grade D | 230.0 | 307.4 | PD |
| P247A-2 | A284 St, Grade D | 230.0 | 276.0 | PD |
| P257A-1 | A284 St, Grade D | 230.0 | 312.1 | PD |
| P257A-2 | A284 St, Grade D | 230.0 | 303.0 | PD |
| P266-1 | A284 St, Grade D | 230.0 | 301.5 | PD |
| P304-1 | A284 St, Grade D | 230.0 | 285.6 | PD |
| P304-2 | A284 St, Grade D | 230.0 | 314.0 | PD |
| P390A-1 | Al 2024-T351 | 265.0 | 374.9 | PD |
| P390A-2 | Al 2024-T351 | 265.0 | 446.3 | PD |
| P460A-1 | Al 2024-T351 | 265.0 | 316.3 | PD |
| P480-1 | A284 St, Grade D | 230.0 | 242.1 | PD |
| P480-2 | A284 St, Grade D | 230.0 | 227.4 | 1.01 |
| P490-1 | A284 St, Grade D | 230.0 | 255.1 | PD |
| P490-2 | A284 St, Grade D | 230.0 | 313.1 | PD |

97

Table 5.6. (continued)

| Part No & Instances | Material | $S_Y$ [MPa] | $\sigma_{max}$ [MPa] | $n_Y$ |
|---|---|---|---|---|
| P501-1 | 8.8 Grade St | 543.9 | 685.0 | PD |
| P501-2 | 8.8 Grade St | 543.9 | 694.2 | PD |

The results of Table 5.5 and Table 5.6 are compared since they both involve the crash of the helicopter seat. The seat bucket (P460A-1) and the seat legs (P390A-1 and P390A-2) have lower factor of safeties as shown in Table 5.7. The main reason for this outcome is the lack of the energy absorption system in SHS. Henceforth, IFDU that is directly mounted to SHS behaves some sort of energy absorption mechanism. Since IFDU absorbs some impact energy, SHS deals with less impact energy comparing its impact as a single assembly as described in Section 4.4.

Table 5.7. Comparison of von Mises results of Table 4.5 and Table 5.6

| Part No & Instances | Material | $S_U$ [MPa] | $\sigma_{max}$ [MPa] (Table 4.5) | $\sigma_{max}$ [MPa] (Table 5.6) |
|---|---|---|---|---|
| M12x10-1 | 8.8 Grade St | 800.0 | 561.4 | 531.1 |
| M12x10-2 | 8.8 Grade St | 800.0 | 544.6 | 571.4 |
| M12x10-3 | 8.8 Grade St | 800.0 | 482.2 | 549.1 |
| M12x10-4 | 8.8 Grade St | 800.0 | 478.3 | 544.1 |
| M12x10-5 | 8.8 Grade St | 800.0 | 545.3 | 540.2 |
| M12x10-6 | 8.8 Grade St | 800.0 | 560.9 | 621.8 |
| M12x10-7 | 8.8 Grade St | 800.0 | 479.4 | 514.3 |
| M12x10-8 | 8.8 Grade St | 800.0 | 480.1 | 540.0 |
| P390A-1 | Al 2024-T351 | 547.9 | 543.1 | 374.9 |
| P390A-2 | Al 2024-T351 | 547.9 | 543.1 | 446.3 |
| P460A-1 | Al 2024-T351 | 547.9 | 365.5 | 316.3 |

# CHAPTER 6

# DESIGN AND ANALYSIS OF THE SLED TEST FIXTURE

## 6.1. Design Information of the Sled Test Fixture

The Sled Test Fixture (STF) is necessary in order to perform sled tests of helicopter seats on a sled test equipment. Hence, it is designed as an adapter between the sled test facility of METU-BILTIR Center Vehicle Safety Unit and the Interchangeable Floor Deformation Unit (IFDU). It is shown in Figure 6.1. The dimensions between the axes of outer holes of STF must be aligned with the holes on the sled since they are fastened through these holes.
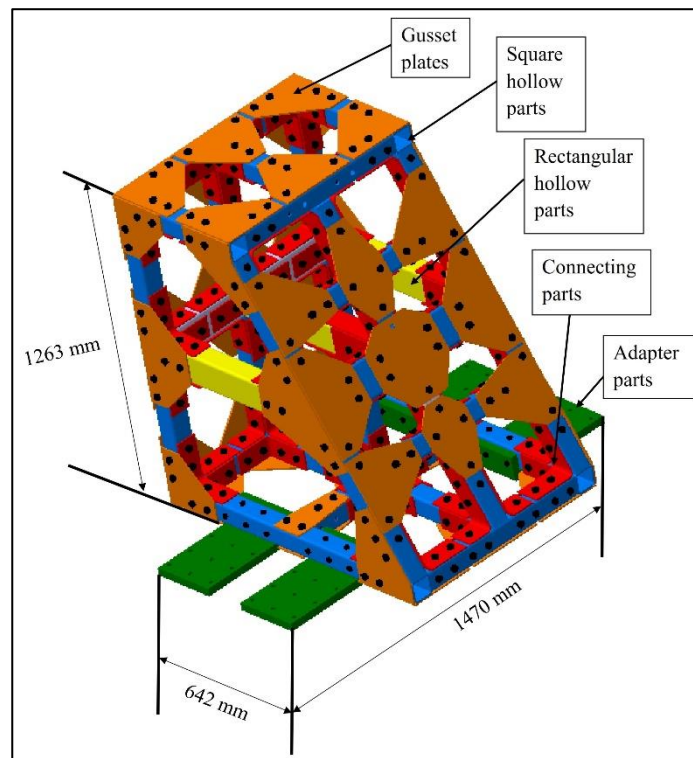


Figure 6.1. The model of the Sled Test Fixture

STF consists of adapter parts, square hollow parts, rectangular hollow parts, and connecting parts. The adapter parts are used for mounting STF to the sled. Square hollow parts and rectangular hollow parts construct the outer section of STF. They are connected to each other with L-shaped connecting parts and C-shaped connecting parts.

STF consists of 67 unique parts and 7 different type fasteners, which corresponds to a total number of 494 items. The mass data of STF is tabulated in Table 6.1, where all fasteners of STF have a total mass of 88.95 kg. Total mass of STF is 709.89 kg.

Table 6.1. Mass data of the Sled Test Fixture

| Part No | Part Name | Material | Unit Mass (kg) | Qty. | Total Mass (kg) |
|---------|-----------|----------|----------------|------|-----------------|
| P114A | Mounting Plate | A284 St, Grade D | 27.15 | 4 | 108.60 |
| P126A | Square Hollow Part | A284 St, Grade D | 14.06 | 2 | 28.13 |
| P135A | Square Hollow Part | A284 St, Grade D | 15.85 | 2 | 31.70 |
| P146A | Square Hollow Part | A284 St, Grade D | 15.89 | 2 | 31.78 |
| P342A | Square Hollow Part | A284 St, Grade D | 6.11 | 2 | 12.21 |
| P352A | Square Hollow Part | A284 St, Grade D | 8.79 | 5 | 43.97 |
| P363A | Square Hollow Part | A284 St, Grade D | 5.74 | 1 | 5.74 |
| P373A | Rect. Hollow Part | A284 St, Grade D | 12.70 | 1 | 12.70 |
| P401A | Square Hollow Part | A284 St, Grade D | 8.84 | 2 | 17.68 |
| P531A | C-shaped Part | A284 St, Grade D | 2.33 | 1 | 2.33 |
| P531SA | C-shaped Part | A284 St, Grade D | 2.33 | 1 | 2.33 |
| P540A | L-shaped Part | A284 St, Grade D | 1.39 | 5 | 6.94 |
| P551 | Gusset Plate | A284 St, Grade D | 2.59 | 2 | 5.18 |
| P560 | Gusset Plate | A284 St, Grade D | 2.82 | 2 | 5.64 |
| P570A | L-shaped Part | A284 St, Grade D | 1.13 | 21 | 23.67 |
| P580A | L-shaped Part | A284 St, Grade D | 1.25 | 12 | 15.05 |
| P590A | L-shaped Part | A284 St, Grade D | 0.99 | 14 | 13.89 |
| P600 | Gusset Plate | A284 St, Grade D | 2.09 | 4 | 8.35 |
| P610 | Gusset Plate | A284 St, Grade D | 1.83 | 4 | 7.32 |
| P620 | Gusset Plate | A284 St, Grade D | 2.38 | 4 | 9.50 |
| P621 | Gusset Plate | A284 St, Grade D | 2.30 | 2 | 4.60 |
| P630A | L-shaped Part | A284 St, Grade D | 1.28 | 3 | 3.84 |
| P641A | C-shaped Part | A284 St, Grade D | 2.20 | 1 | 2.20 |
| P641SA | C-shaped Part | A284 St, Grade D | 2.20 | 1 | 2.20 |
| P650A | Gusset Plate | A284 St, Grade D | 2.17 | 2 | 4.34 |
| P660A | Square Hollow Part | A284 St, Grade D | 5.05 | 1 | 5.05 |
| P670A | Square Hollow Part | A284 St, Grade D | 6.21 | 1 | 6.21 |
| P680A | Square Hollow Part | A284 St, Grade D | 13.73 | 1 | 13.73 |
| P690A | Rect. Hollow Part | A284 St, Grade D | 11.61 | 2 | 23.22 |

Table 6.1. (continued)

| P700A | L-shaped Part | A284 St, Grade D | 1.68 | 2 | 3.36 |
|-------|---------------|------------------|------|-----|-------|
| P710A | Square Hollow Part | A284 St, Grade D | 6.01 | 1 | 6.01 |
| P720A | Square Hollow Part | A284 St, Grade D | 3.94 | 1 | 3.94 |
| P730A | Square Hollow Part | A284 St, Grade D | 2.25 | 2 | 4.49 |
| P740A | Square Hollow Part | A284 St, Grade D | 3.49 | 1 | 3.49 |
| P750A | Rect. Hollow Part | A284 St, Grade D | 5.02 | 2 | 10.04 |
| P760 | Gusset Plate | A284 St, Grade D | 1.27 | 4 | 5.08 |
| P770A | C-shaped Part | A284 St, Grade D | 1.81 | 1 | 1.81 |
| P770SA | C-shaped Part | A284 St, Grade D | 1.81 | 1 | 1.81 |
| P780 | Gusset Plate | A284 St, Grade D | 2.98 | 1 | 2.98 |
| P790 | Gusset Plate | A284 St, Grade D | 3.60 | 1 | 3.60 |
| P800 | Gusset Plate | A284 St, Grade D | 3.22 | 2 | 6.44 |
| P810A | L-shaped Part | A284 St, Grade D | 0.87 | 10 | 8.68 |
| P820 | Gusset Plate | A284 St, Grade D | 2.35 | 1 | 2.35 |
| P830A | L-shaped Part | A284 St, Grade D | 1.69 | 1 | 1.69 |
| P830SA | L-shaped Part | A284 St, Grade D | 1.69 | 1 | 1.69 |
| P840A | C-shaped Part | A284 St, Grade D | 1.69 | 2 | 3.38 |
| P850A | C-shaped Part | A284 St, Grade D | 1.69 | 2 | 3.38 |
| P860A | C-shaped Part | A284 St, Grade D | 1.42 | 2 | 2.83 |
| P870A | C-shaped Part | A284 St, Grade D | 1.42 | 2 | 2.83 |
| P880A | Rect. Hollow Part | A284 St, Grade D | 11.61 | 1 | 11.61 |
| P890A | L-shaped Part | A284 St, Grade D | 1.80 | 1 | 1.80 |
| P890SA | L-shaped Part | A284 St, Grade D | 1.80 | 1 | 1.80 |
| P900A | Bended Support | A284 St, Grade D | 2.61 | 1 | 2.61 |
| P900SA | Bended Support | A284 St, Grade D | 2.61 | 1 | 2.61 |
| P910A | C-shaped Part | A284 St, Grade D | 1.99 | 1 | 1.99 |
| P920 | Gusset Plate | A284 St, Grade D | 3.26 | 2 | 6.52 |
| P930 | Gusset Plate | A284 St, Grade D | 4.22 | 2 | 8.44 |
| P940 | Gusset Plate | A284 St, Grade D | 3.78 | 2 | 7.55 |
| P950 | Gusset Plate | A284 St, Grade D | 5.96 | 1 | 5.96 |
| P960 | Gusset Plate | A284 St, Grade D | 2.67 | 2 | 5.33 |
| P970A | L-shaped Part | A284 St, Grade D | 1.84 | 1 | 1.84 |
| P980 | Gusset Plate | A284 St, Grade D | 2.57 | 2 | 5.13 |
| P990 | Gusset Plate | A284 St, Grade D | 2.03 | 1 | 2.03 |
| PA00 | Gusset Plate | A284 St, Grade D | 3.09 | 2 | 6.18 |
| PA10 | Gusset Plate | A284 St, Grade D | 3.73 | 1 | 3.73 |
| PA20 | Gusset Plate | A284 St, Grade D | 2.65 | 2 | 5.30 |
| PA30 | Gusset Plate | A284 St, Grade D | 2.53 | 1 | 2.53 |

## 6.2. Finite Element Analysis Information of the Sled Test Fixture

The analysis model consists of STF and unique parts (PA40, PA51) and 1 different fastener type (M16x60) which totally corresponds to STF and 39 items (3 part, 36 fasteners). These are the simplifications performed on the assembly of analysis model as the implementation of a representative mass (RM), which has the part number of PA40, and dummy sled parts (PA51).

The representative mass (RM), which is displayed in Figure 6.2, is used instead of SHS, IFDU, and representative 77 kg mass. Crash results of SHS show that SHS is not suitable for the verification of STF due to the oscillations of the seat bucket as it is explained in Section 4.4. The representative mass (RM) has the same connection properties with IFDU when it is mounted to STF. It also has the same mass with of SHS, IFDU, and representative 77 kg mass, which is 115.94 kg.
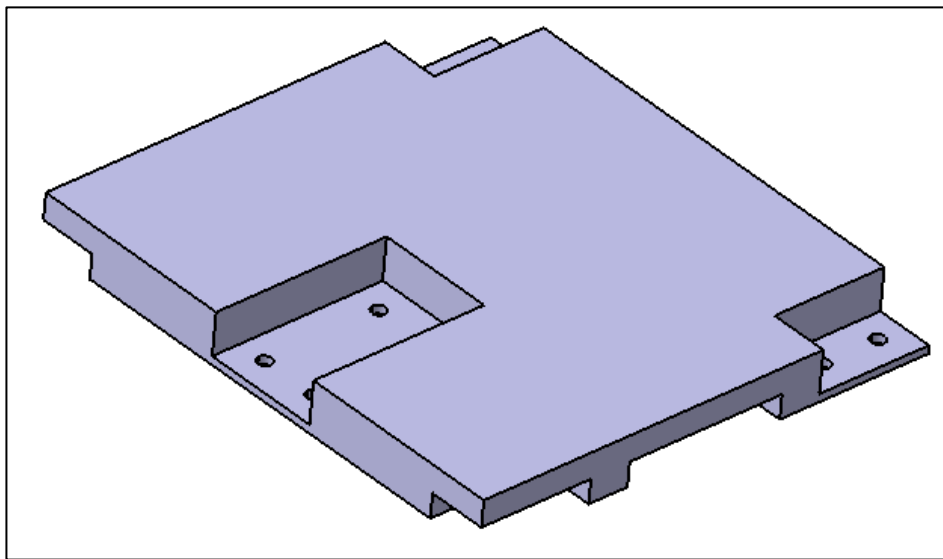


Figure 6.2. The representative mass (RM)

Dummy sled parts (PA51) are necessary since STF with RM needs to be accelerated as if they are on the accelerating sled test facility of METU-BILTIR Center Vehicle Safety Unit. Dummy sled parts play the role of mating floor part of STF. Moreover, it

initiates the crash simulation when the impulse shown in Figure 2.3 is applied on itself. It is visualized in Figure 6.3.
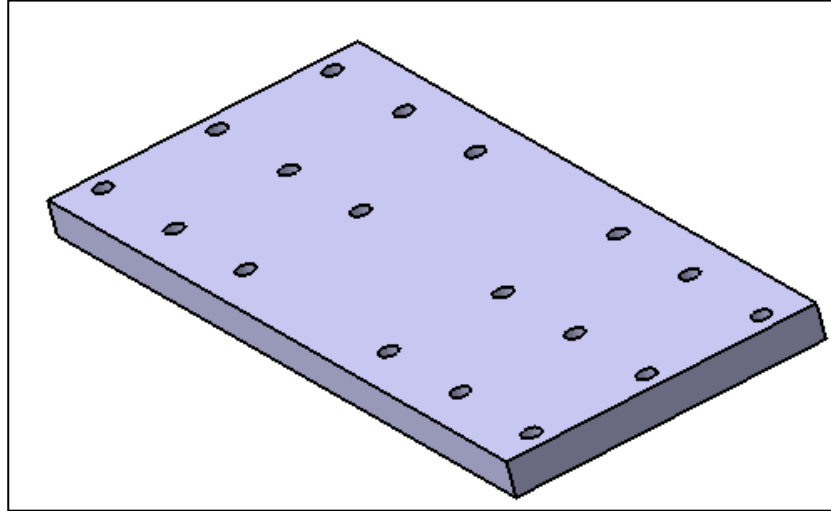


Figure 6.3. Dummy sled part (PA51)

The mass info of this analysis is displayed in Table 6.2. The total mass of the assembly is 911.59 kg. This value is sufficient for the mass capability of the sled test facility in BILTIR, which can carry 2500 kg [54]. The assembly includes STF, one representative mass (RM, numbered as PA40) and two dummy sled parts (PA51) as illustrated in Figure 6.4.

Table 6.2. Mass info of crash test analysis of the Sled Test Fixture

| Part No | Part Name | Material | Unit Mass (kg) | Qty. | Total Mass (kg) |
|---------|-----------|----------|----------------|------|-----------------|
| P027 | STF | - | 709.89 | 1 | 709.89 |
| PA40 | Representative mass | A284, Grade D | 115.94 | 1 | 115.94 |
| PA51 | Dummy sled part | A284, Grade D | 40.02 | 2 | 80.04 |
| M16x60 fasteners | | 8.8 Grade St | 0.16 | 36 | 5.72 |
| P005 | STF + mating parts | - | 911.59 | 4 | 911.59 |
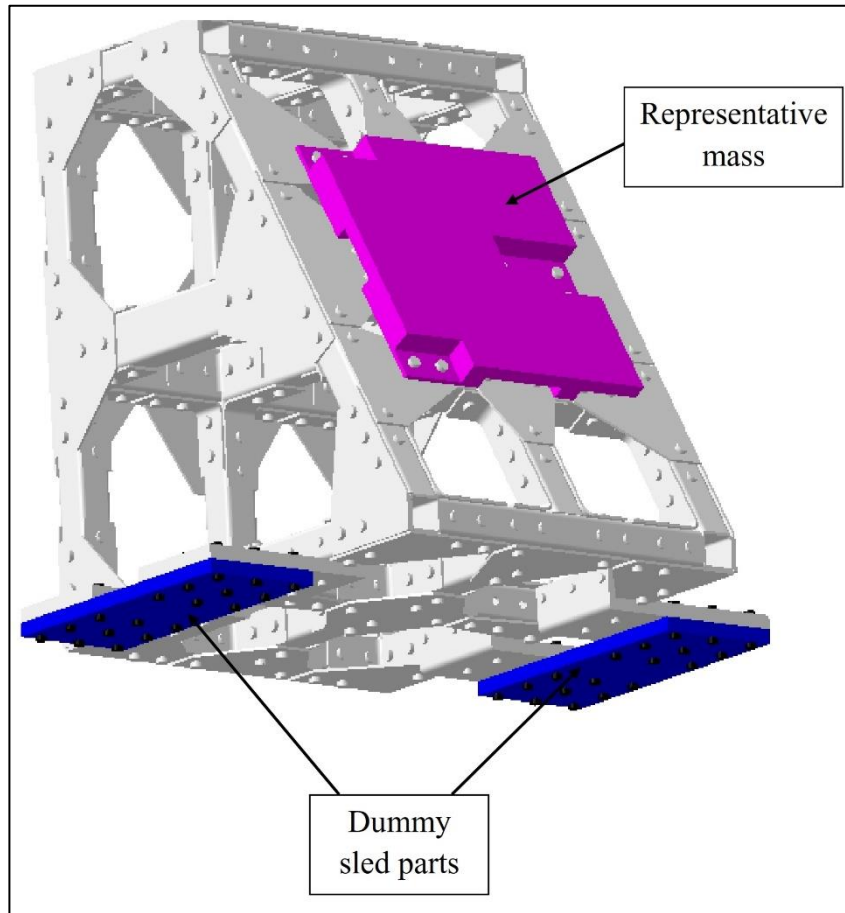
Figure 6.4. The model of the crash analysis of the Sled Test Fixture

## 6.3. Crash Analysis of the Sled Test Fixture

Unlike the crash analysis of SHS as discussed in Section 4.4 and the crash analysis of IFDU as discussed in Section 5.5, STF do not have vertical initial velocity of impact. Nevertheless, it has the horizontal impact impulse as explained above so as to make better simulation with the accelerating sled test facility of METU-BILTIR Center Vehicle Safety Unit.

The only boundary condition of this crash analysis is the horizontal impact impulse, which is at +x direction. It is shown in Figure 2.3. This boundary condition, which is displayed in Figure 6.5 is applied to both dummy sled parts (PA51).
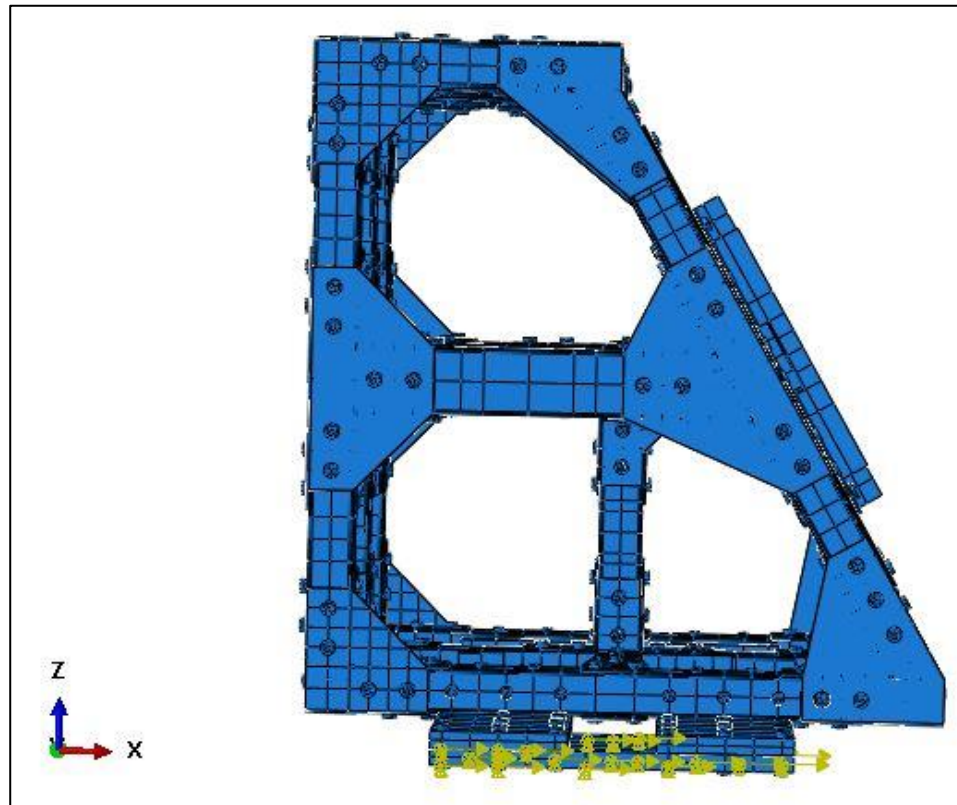
Figure 6.5.  Boundary conditions of the crash analysis of the Sled Test Fixture

All mesh elements used in this analysis are made from C3D8R element as it is explained in Section 3.2.8. The accuracy and the duration of this FEA are balanced with this type of mesh. Number of elements for all parts and fasteners do not exceed $10^5$ elements. Table 6.3 shows the mesh types.

Table 6.3. Mesh types of the crash analysis of the Sled Test Fixture

| Part No | Number of Elements | Library | Element |
|---------|--------------------|---------|---------|
| M14x110 | 1360 | Explicit | C3D8R |
| M16x60 | 1392 | Explicit | C3D8R |
| M18x86 | 1088 | Explicit | C3D8R |
| M18x92 | 1152 | Explicit | C3D8R |
| M18x96 | 1152 | Explicit | C3D8R |
| M18x102 | 1216 | Explicit | C3D8R |
| M18x132 | 1472 | Explicit | C3D8R |
| M18x152 | 1600 | Explicit | C3D8R |
| P114A | 2400 | Explicit | C3D8R |
| P126A | 6912 | Explicit | C3D8R |
| P135A | 7680 | Explicit | C3D8R |

105

Table 6.3. (continued)

| Part No | Number of Elements | Library | Element |
| --- | --- | --- | --- |
| P146A | 7712 | Explicit | C3D8R |
| P342A | 3072 | Explicit | C3D8R |
| P352A | 4800 | Explicit | C3D8R |
| P363A | 3072 | Explicit | C3D8R |
| P373A | 5568 | Explicit | C3D8R |
| P401A | 4736 | Explicit | C3D8R |
| P531A | 2780 | Explicit | C3D8R |
| P531SA | 2684 | Explicit | C3D8R |
| P540A | 976 | Explicit | C3D8R |
| P551 | 2928 | Explicit | C3D8R |
| P560 | 1700 | Explicit | C3D8R |
| P570A | 808 | Explicit | C3D8R |
| P580A | 832 | Explicit | C3D8R |
| P590A | 712 | Explicit | C3D8R |
| P600 | 1112 | Explicit | C3D8R |
| P610 | 1128 | Explicit | C3D8R |
| P620 | 1352 | Explicit | C3D8R |
| P621 | 2748 | Explicit | C3D8R |
| P630A | 880 | Explicit | C3D8R |
| P641A | 2376 | Explicit | C3D8R |
| P641SA | 2404 | Explicit | C3D8R |
| P650A | 2372 | Explicit | C3D8R |
| P660A | 2816 | Explicit | C3D8R |
| P670A | 3456 | Explicit | C3D8R |
| P680A | 6912 | Explicit | C3D8R |
| P690A | 3712 | Explicit | C3D8R |
| P700A | 1072 | Explicit | C3D8R |
| P710A | 3584 | Explicit | C3D8R |
| P720A | 2080 | Explicit | C3D8R |
| P730A | 1408 | Explicit | C3D8R |
| P740A | 1664 | Explicit | C3D8R |
| P750A | 2816 | Explicit | C3D8R |
| P760 | 512 | Explicit | C3D8R |
| P770A | 2012 | Explicit | C3D8R |
| P770SA | 2088 | Explicit | C3D8R |
| P780 | 3572 | Explicit | C3D8R |
| P790 | 5160 | Explicit | C3D8R |
| P800 | 4444 | Explicit | C3D8R |
| P810A | 648 | Explicit | C3D8R |
| P820 | 2908 | Explicit | C3D8R |
| P830A | 1832 | Explicit | C3D8R |
| P830SA | 1792 | Explicit | C3D8R |
| P840A | 1248 | Explicit | C3D8R |

Table 6.3. (continued)

| Part No | Number of Elements | Library | Element |
|---------|-------------------|---------|---------|
| P850A | 1248 | Explicit | C3D8R |
| P860A | 1048 | Explicit | C3D8R |
| P870A | 1024 | Explicit | C3D8R |
| P880A | 5008 | Explicit | C3D8R |
| P890A | 2084 | Explicit | C3D8R |
| P890SA | 2168 | Explicit | C3D8R |
| P900A | 3080 | Explicit | C3D8R |
| P900SA | 3104 | Explicit | C3D8R |
| P910A | 1048 | Explicit | C3D8R |
| P920 | 2132 | Explicit | C3D8R |
| P930 | 2532 | Explicit | C3D8R |
| P940 | 2376 | Explicit | C3D8R |
| P950 | 5280 | Explicit | C3D8R |
| P960 | 1448 | Explicit | C3D8R |
| P970A | 1224 | Explicit | C3D8R |
| P980 | 3132 | Explicit | C3D8R |
| P990 | 2668 | Explicit | C3D8R |
| PA00 | 1820 | Explicit | C3D8R |
| PA10 | 4272 | Explicit | C3D8R |
| PA20 | 2976 | Explicit | C3D8R |
| PA30 | 3128 | Explicit | C3D8R |
| PA40 | 6072 | Explicit | C3D8R |
| PA51 | 2976 | Explicit | C3D8R |

The aim of this analysis is to determine the suitability of STF since it must protect its integrity with no plastic deformation. STF is designed to have the repeatability feature since many sled tests can be performed upon the helicopter seats.

After determining all the input regarding to the analysis, the processing section of the analysis begins. The time needed for the completion of the analysis is 33 hours and 59 minutes on the particular computer described in Section 3.1. The von Mises stresses of whole model are visualized from Figures 6.6 – Figure 6.16.

Figure 6.6. von Mises stress representation of the crash analysis of the Sled Test Fixture at 0 ms and 5 ms

108

Figure 6.7. von Mises stress representation of the crash analysis of the Sled Test Fixture at 10 ms and 15 ms

Figure 6.8. von Mises stress representation of the crash analysis of the Sled Test Fixture at 20 ms and 25 ms

110

Figure 6.9. von Mises stress representation of the crash analysis of the Sled Test Fixture at 30 ms and 35 ms

Figure 6.10. von Mises stress representation of the crash analysis of the Sled Test Fixture at 40 ms and 45 ms

112

Figure 6.11. von Mises stress representation of the crash analysis of the Sled Test Fixture at 50 ms and 55 ms

113
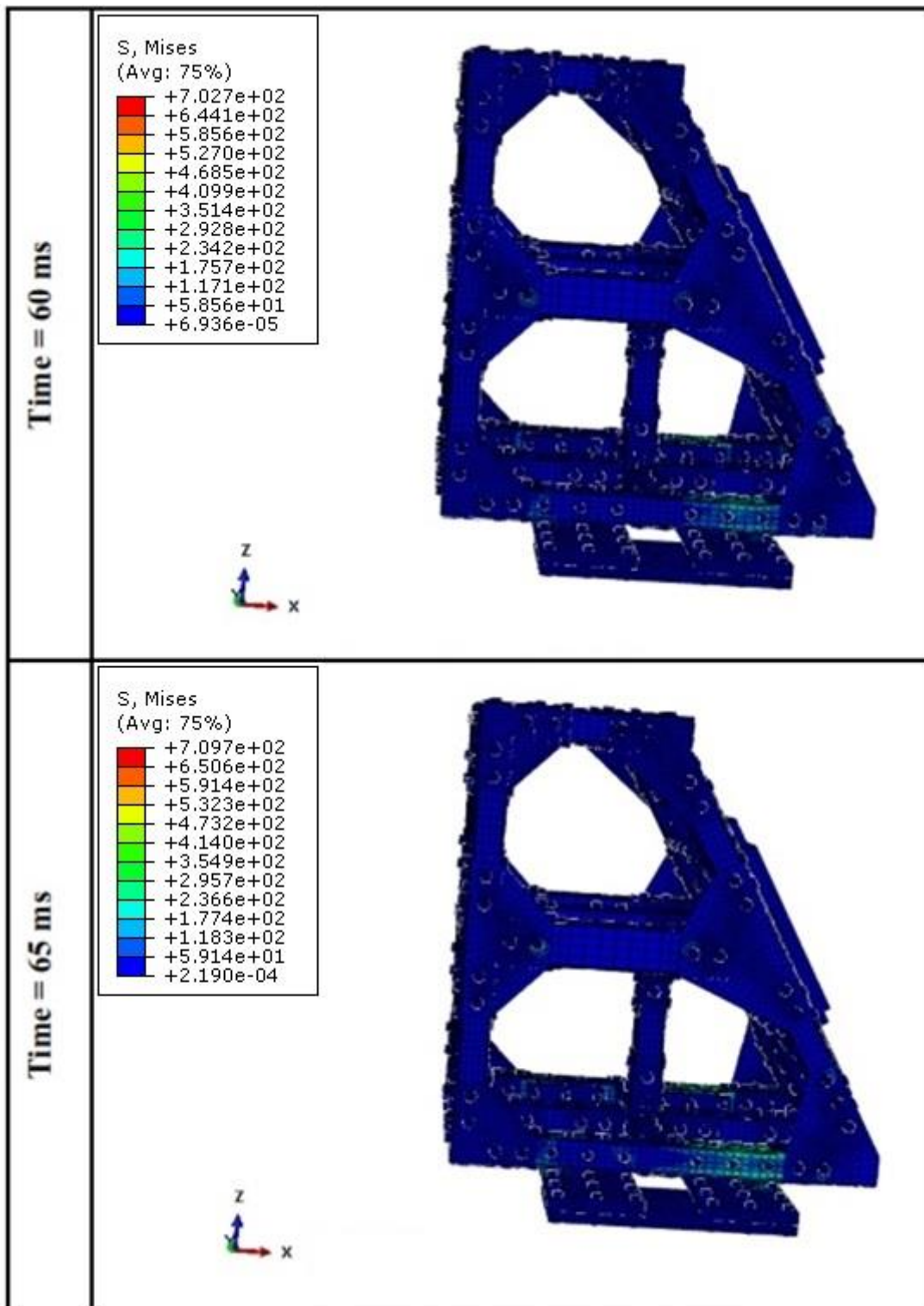
Figure 6.12. von Mises stress representation of the crash analysis of the Sled Test Fixture at 60 ms and 65 ms

114
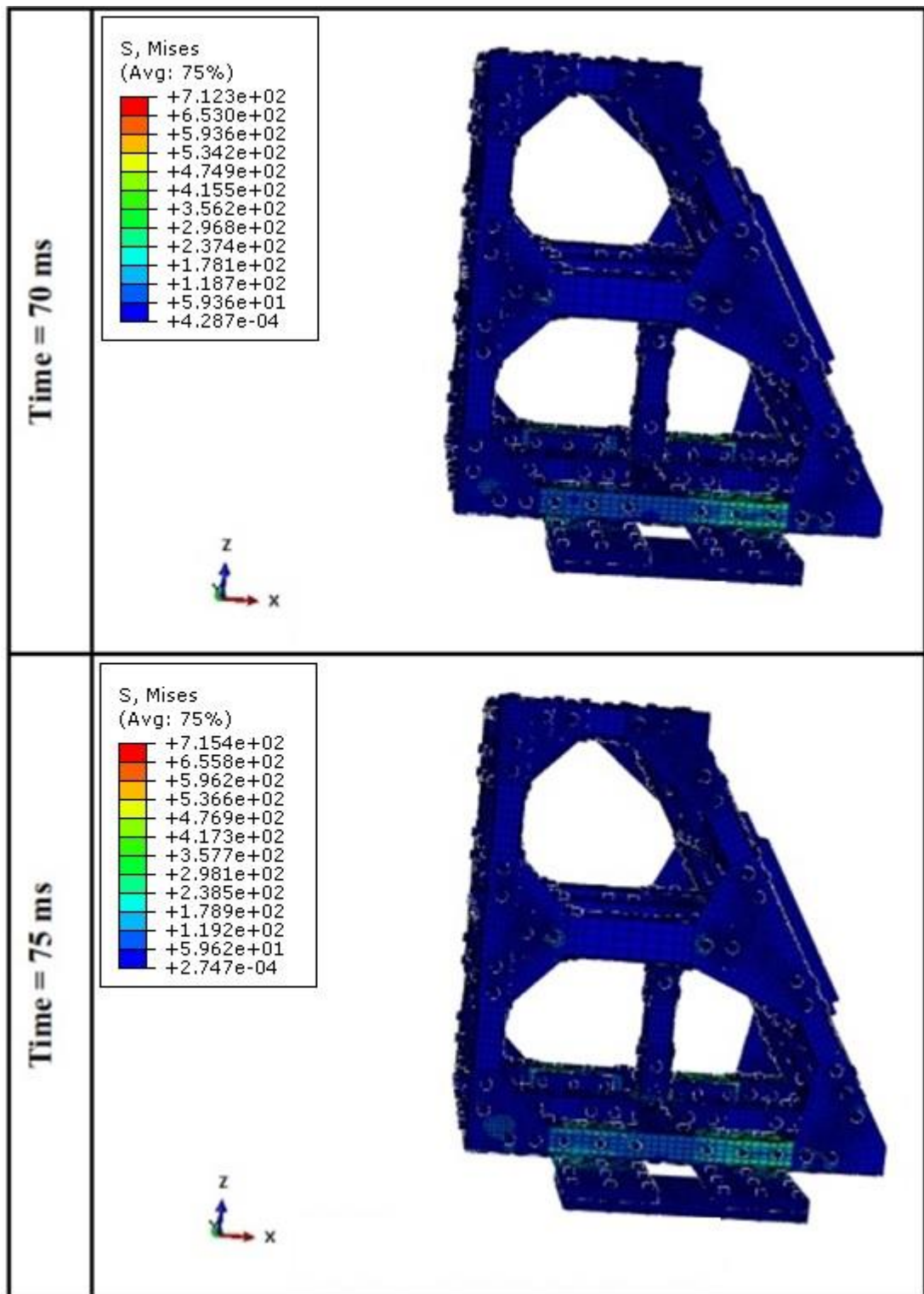
Figure 6.13. von Mises stress representation of the crash analysis of the Sled Test Fixture at 70 ms and 75 ms
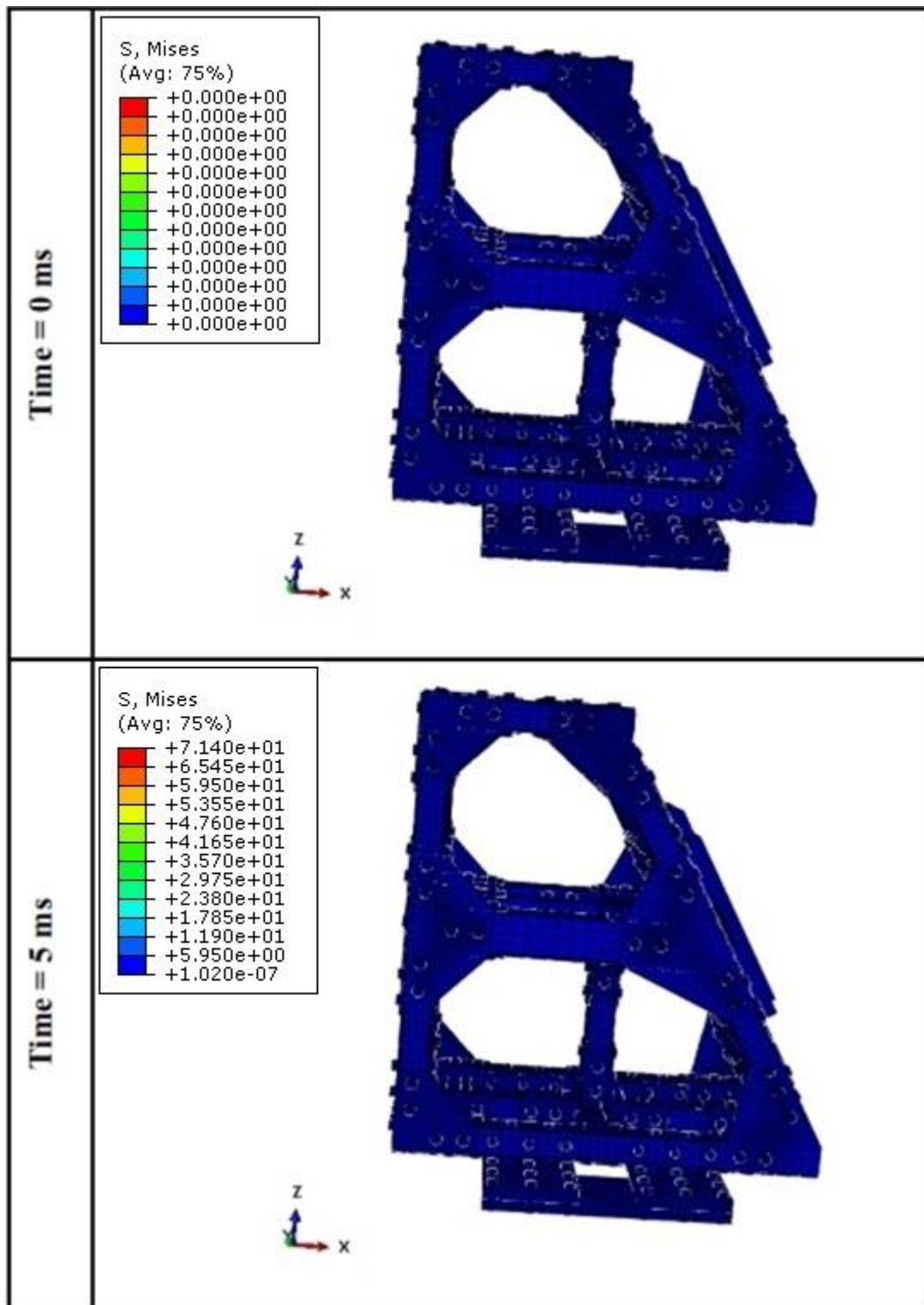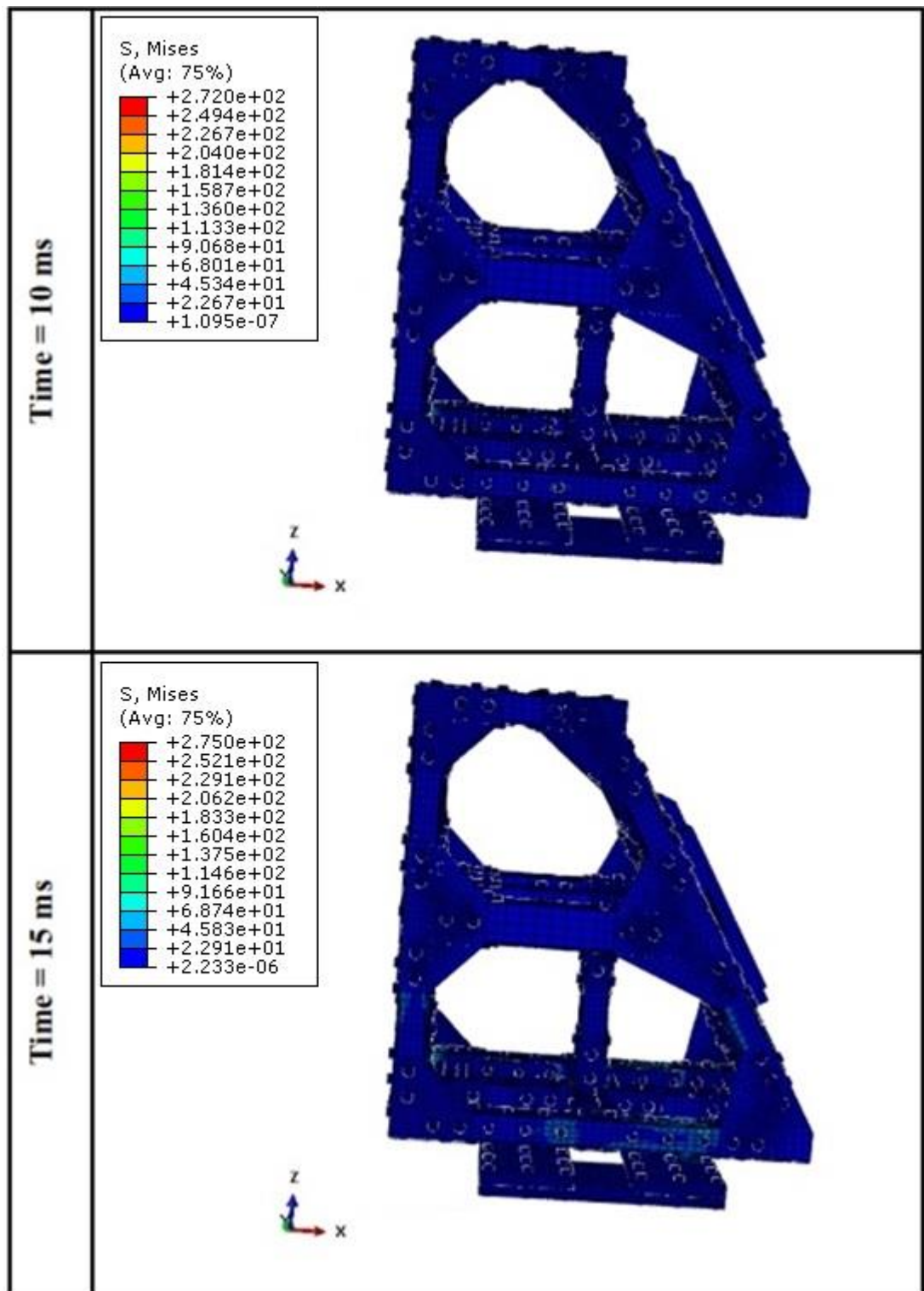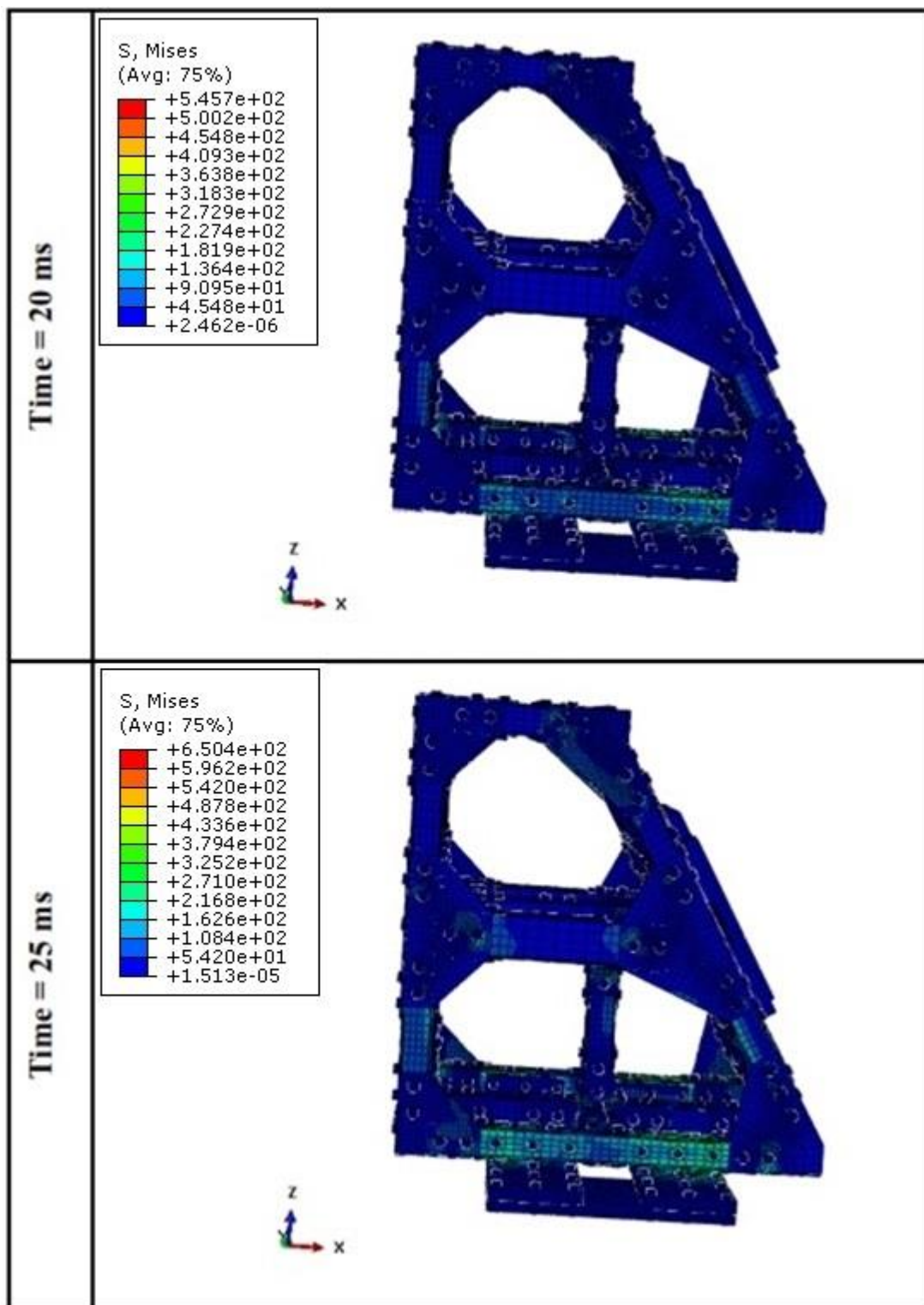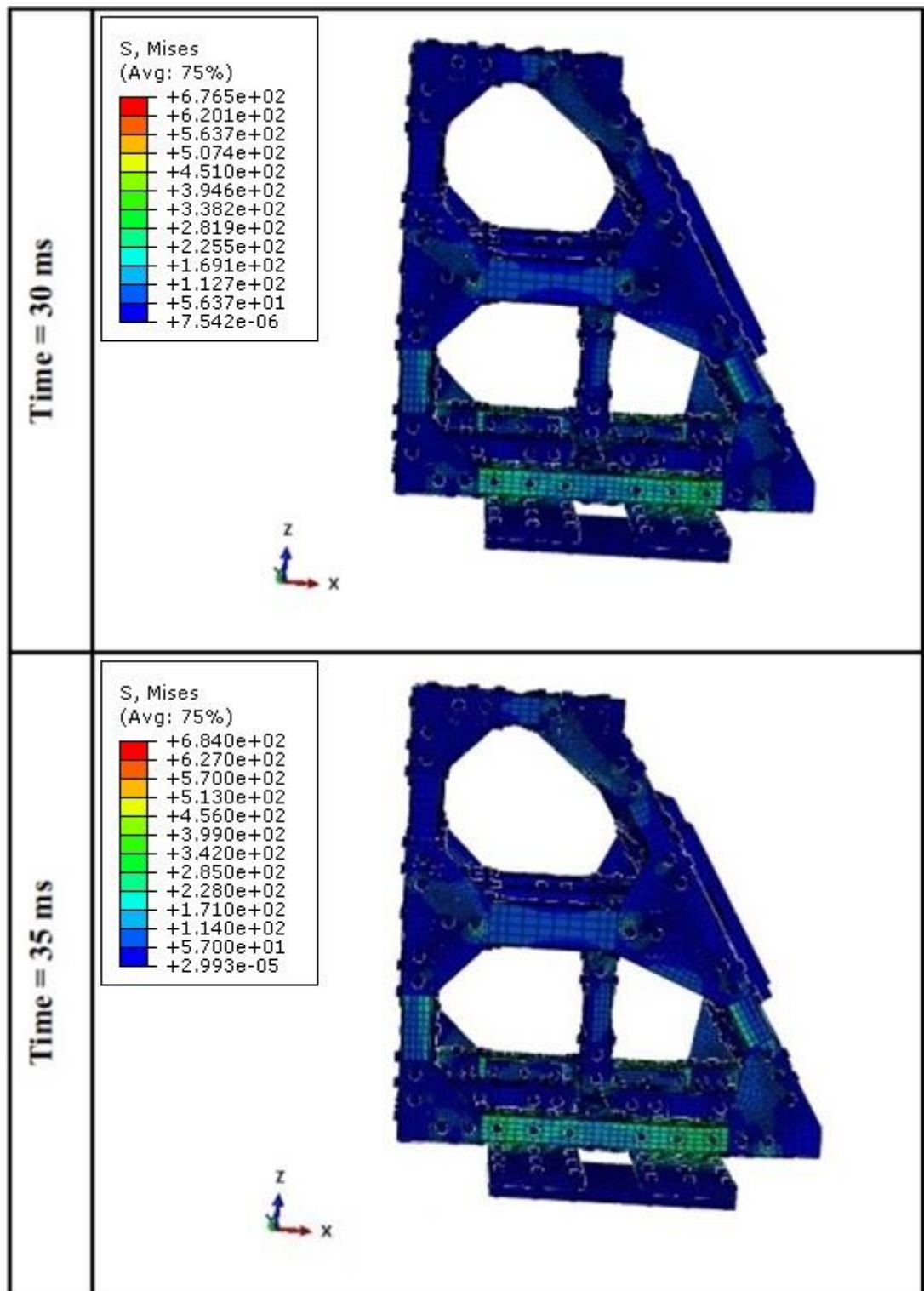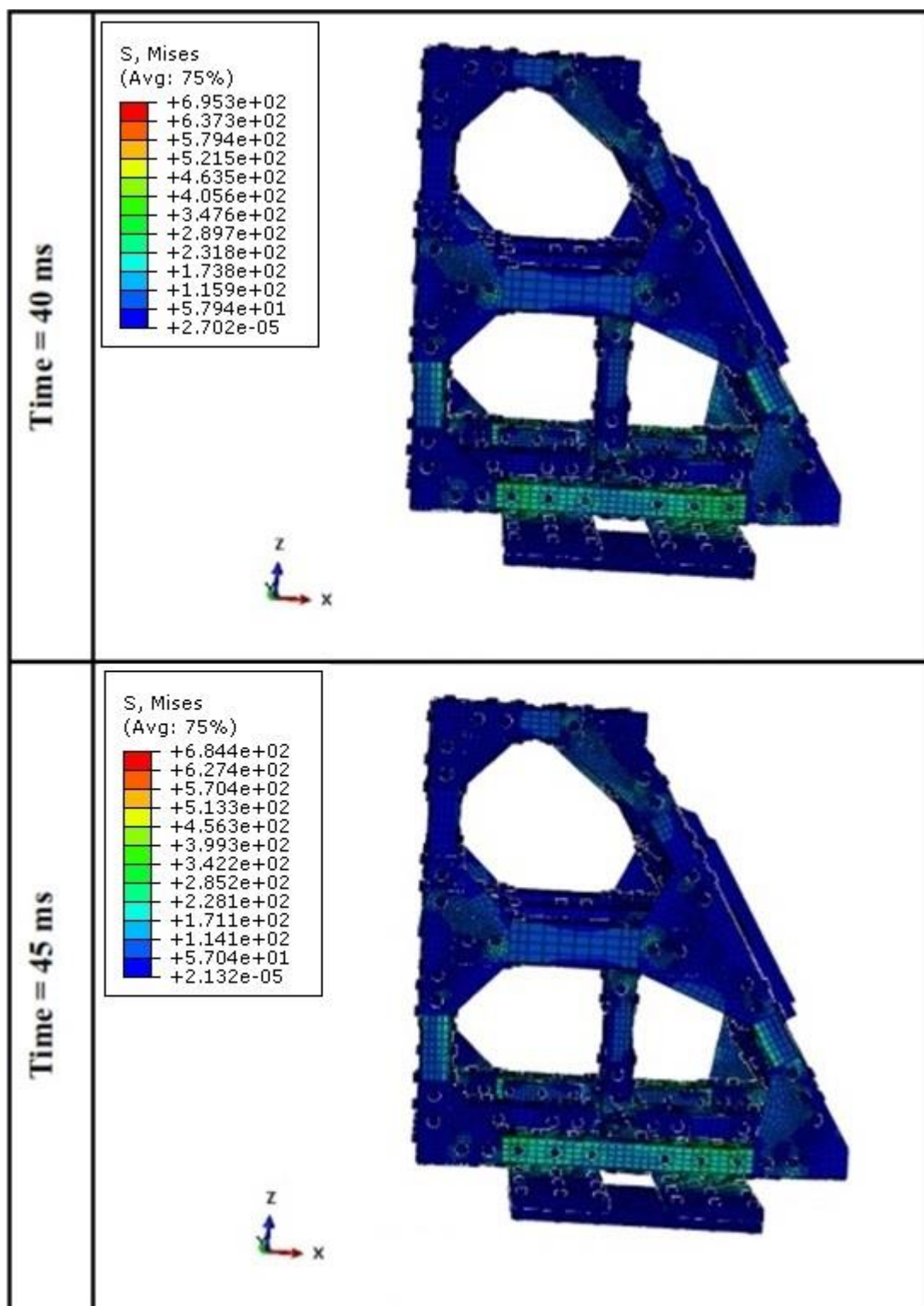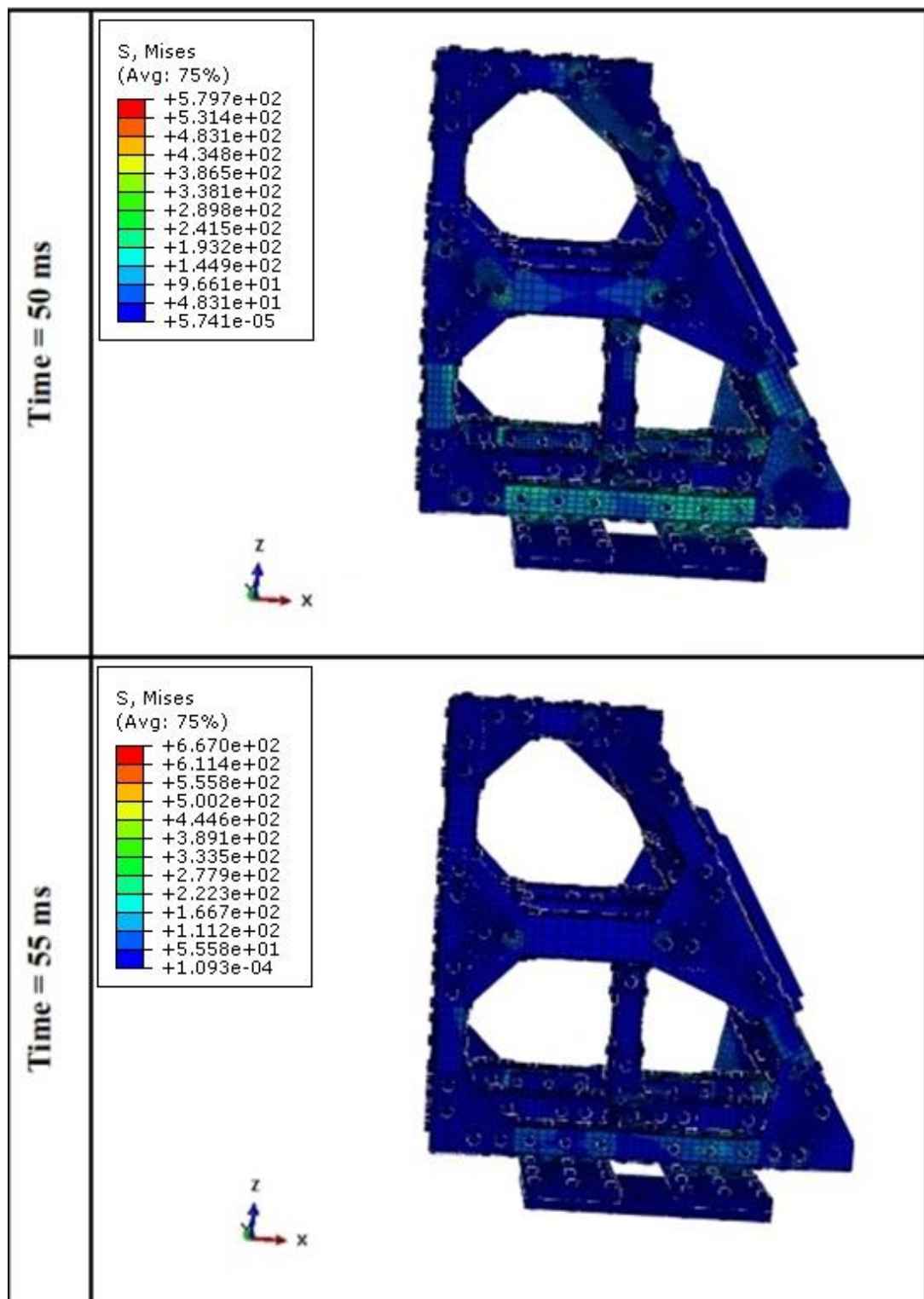
115
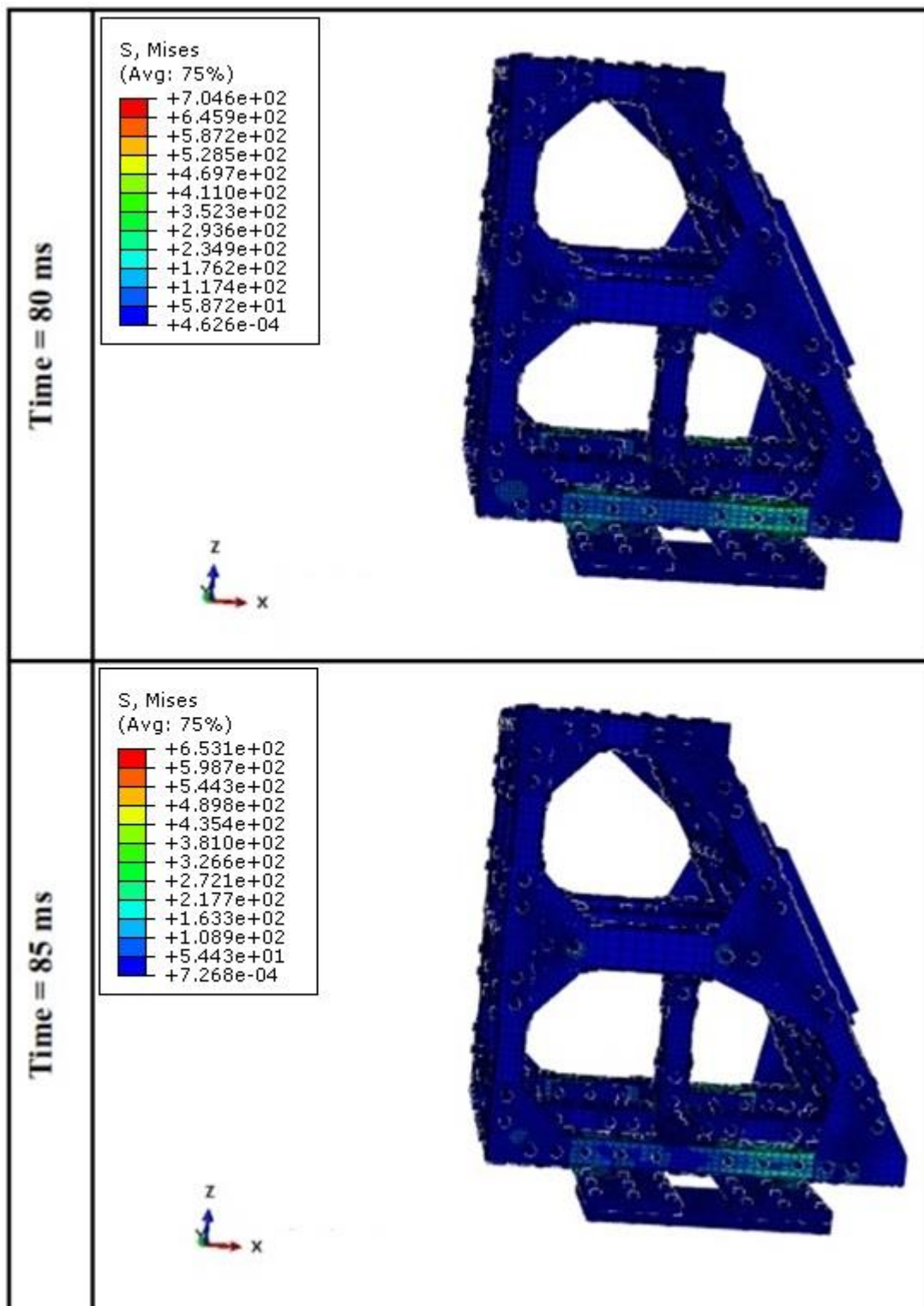
Figure 6.14. von Mises stress representation of the crash analysis of the Sled Test Fixture at 80 ms and 85 ms
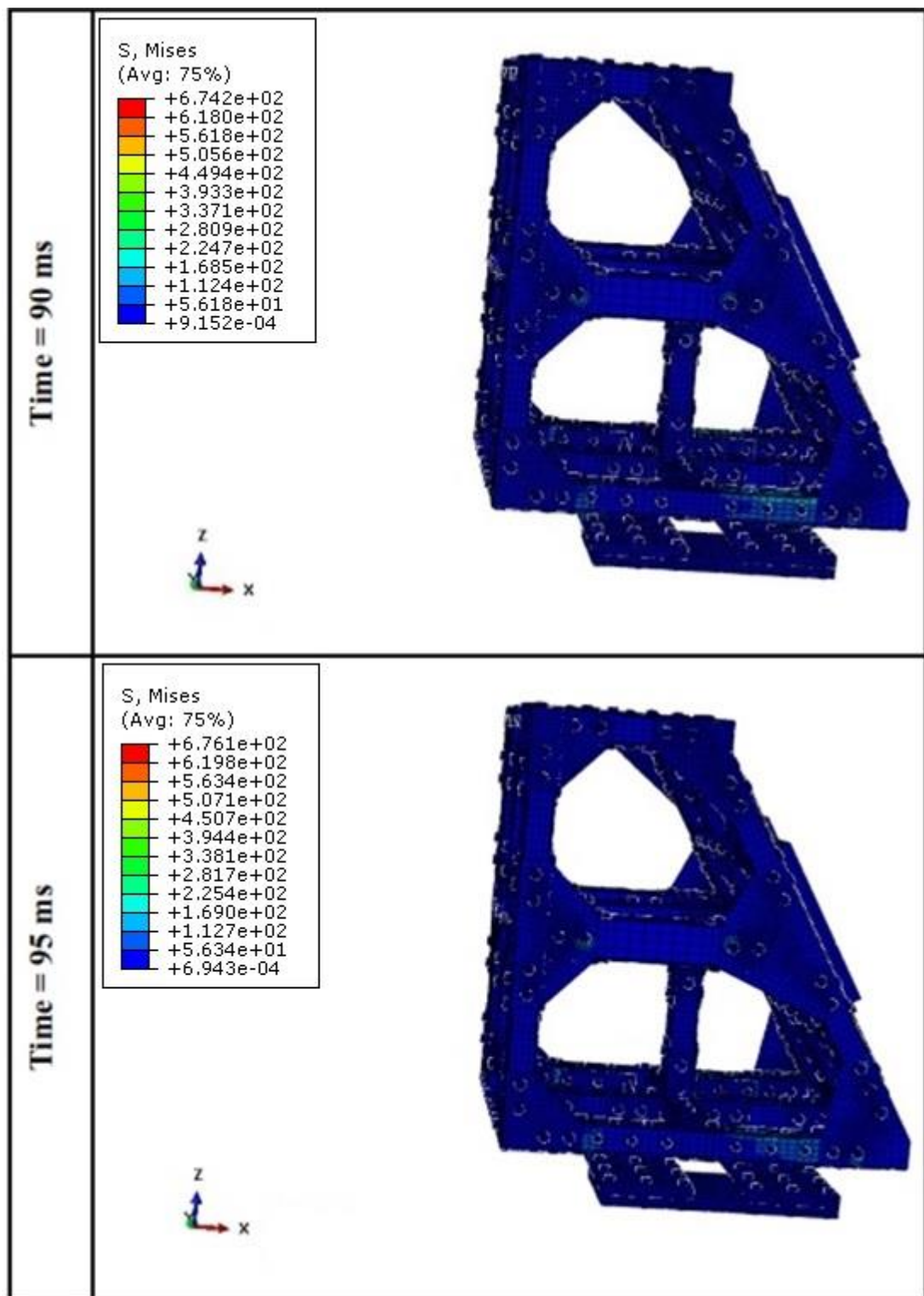
Figure 6.15. von Mises stress representation of the crash analysis of the Sled Test Fixture at 90 ms and 95 ms
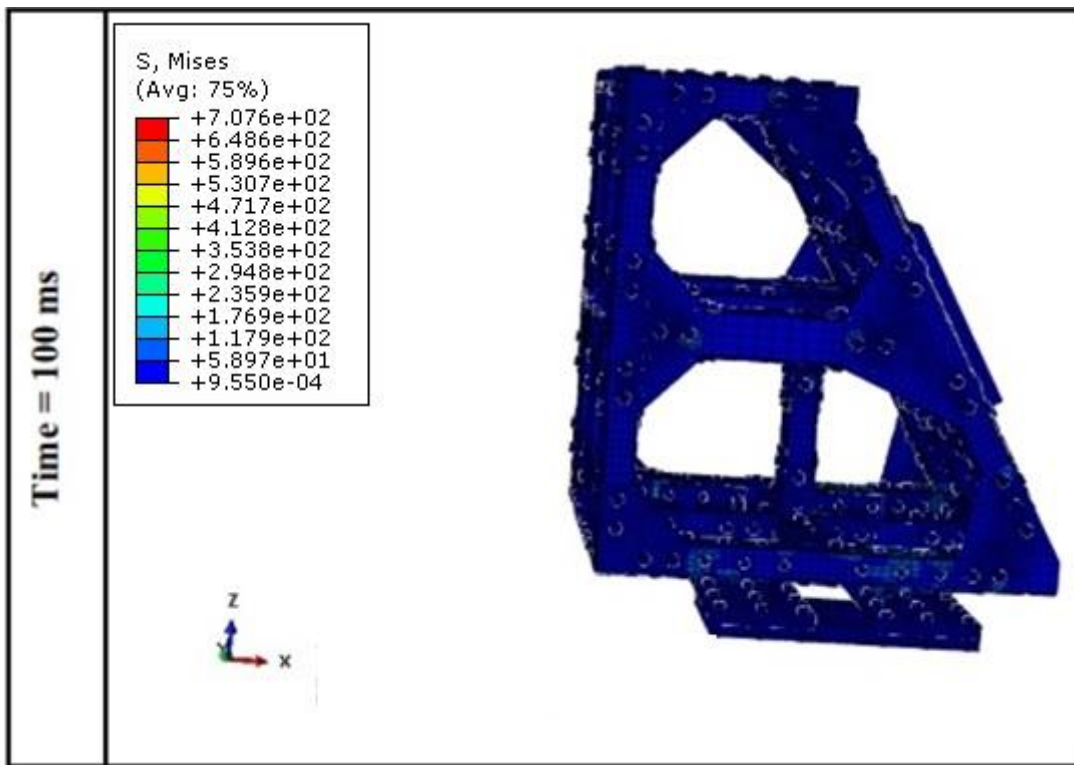
Figure 6.16. von Mises stress representation of the crash analysis of the Sled Test Fixture at 100 ms

The following results can be inferred from the results. Neither the parts nor the fasteners exceeds the ultimate tensile strength and the results satisfy the integrity of STF. The maximum stresses occur between 25 ms and 100 ms consistent with the increase of velocity. Since the center of gravity of STF is quite above the bottom and the hydraulic pistons apply loads from the bottom section, there is a moment load effect on the bottom parts of STF. Consequently, the location of stresses are mainly concentrated on the bottom part of STF as shown from Figures 6.6 – 6.16.

The acceleration of representative mass is investigated. In the sled tests, accelerometer sensors are put to the desired location to get the acceleration data. In order to make similarity, nine nodes outside of the representative mass (RM) that is shown in Figure 6.17 are selected to read the acceleration values.

118
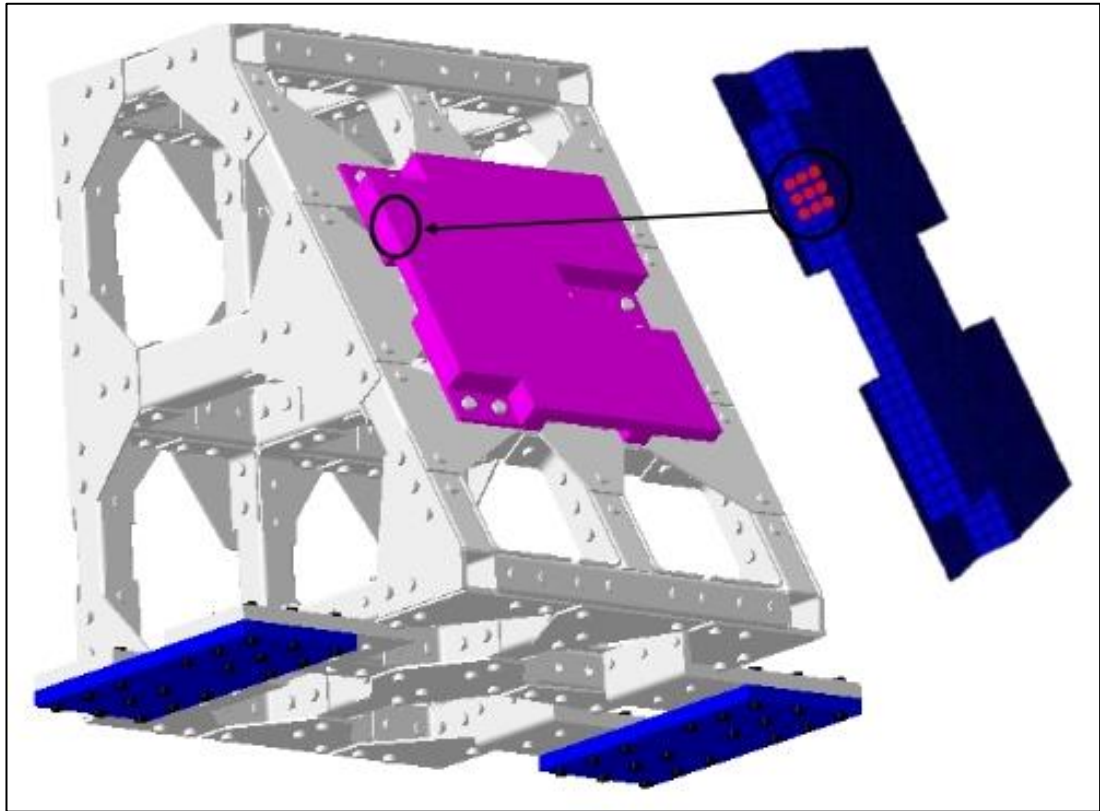
Figure 6.17. Acceleration measurement points

The acceleration values of nine nodes are collected during the analysis period of 0 ms – 100 ms. The average acceleration values of these nodes are calculated to find the average acceleration according to different time steps. The results are displayed in Figure 6.18. These results are compared with the reference values which are shown in Table 2.2 and Figure 2.3. The peak acceleration value is 37.4 G, which occurs at 30 ms. This result satisfies the criterion of "peak acceleration must occur before 31 ms and must reach at least 30 G" as shown in Section 2.1.
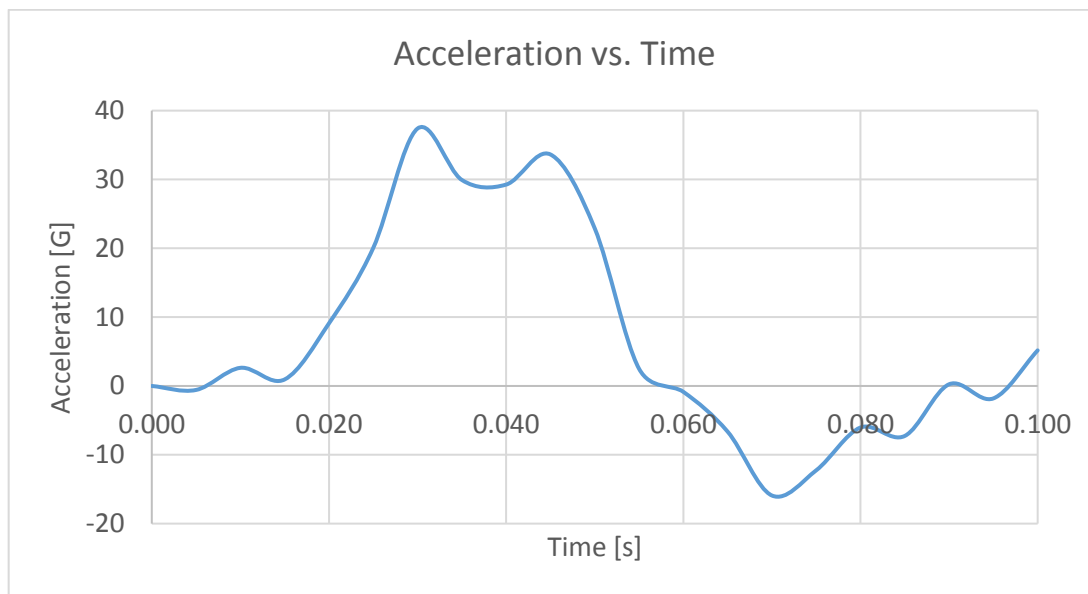
Figure 6.18. Acceleration data of the representative mass (RM)

# CHAPTER 7

# CONCLUSIONS AND FUTURE WORKS

## 7.1. Conclusions

Helicopter crash scenarios are thoroughly examined concentrating on the vertical impact criterion and the floor deformation criterion of civilian helicopter seats as they are taken from CS 29.562, which is published by European Aviation Safety Agency (EASA). These criteria form the basis for the designs and analyses of the Simplified Helicopter Seat (SHS), the Interchangeable Floor Deformation Unit (IFDU), and the Sled Test Fixture (STF).

The fundamental approaches to the analyses are outlined before the analyses to give a better intuition for the analyses regarding to SHS, IFDU, and STF. The inputs of the analyses are extremely important since they can hugely affect the results. The inputs are geometry, material properties, mesh types, assembly module, step module, interaction module, and boundary conditions. Two important techniques "mapping" and "utilization of Abaqus/Explicit to quasi-static cases" are explained.

SHS is designed instead of a real helicopter seat since the designs of passengers seats are protected in terms of intellectual property and cannot be used for research purposes. It is geometrically and functionally similar to a helicopter seat. The bolt preload analysis of SHS is performed and these results are mapped into the crash analysis of SHS. The bolt preload analysis and the crash analysis of SHS are discussed. Although SHS remains intact after the crash, the oscillations of SHS are observed since SHS lacks of energy absorbing systems unlike real civilian helicopter seats.

The design of IFDU is explained as it is implemented to observe the floor deformation criteria. It is used for the validation of civilian helicopter seats when it is subjected to floor deformation. The major feature of IFDU is the modular design in case different

121

helicopter seats are used for floor deformation analysis. The bolt preload analyses, and floor deformation analyses during crashes are examined for IFDU and SHS since they have contributions to the crashes. The mapping process is used to transfer the results of bolt preload analysis as an input to the floor deformation and pin insertion analyses. IFDU maintains its structural integrity after the floor deformation and pin insertion analyses are done. The mapping process is repeated to transfer the results of floor deformation and pin insertion analyses into the crash analyses of IFDU and SHS as an input. IFDU and SHS remain intact after the crash analysis is done.

STF is needed to perform sled tests of helicopter seats on a sled test equipment. It is used for the validation of helicopter seats when crash loads are applied. STF is designed to be mounted to the sled of METU-BILTIR Center Vehicle Safety Unit. The results of crash analyses of STF are reasonable as the structural integrity of STF resumes after it is exposed to crash loads.

## 7.2. Future Works

The followings can be performed as further works.

- A real civilian helicopter seat that has energy absorption system can be used instead of SHS.
- Military helicopter seats can be researched in terms of their regulations.
- Forward impact criterion could be investigated similar to vertical impact criterion, which is done in this study.
- Anthropomorphic Test Dummy (ATD) can utilized instead of 77 kg representative mass for the analyses to examine the crash load effects on different locations of human body.
- The analyses of this study can be validated by the implementation of sled tests since all designs of this study are manufacturable and can be assembled in real life. The results of test would be beneficial for performing improvements to the analyses of this study by making comparisons with the test results.

- The material data of A284 Steel, Grade D and 8.8 Grade Steel can be obtained and used for the analyses.
- The strain rate could be included for the material data of Al 2024-T351, 8.8 Grade Steel, and A284 Steel, Grade D.

# REFERENCES

[1] Bois P.D., Chou C.C., Fileta B.B, Khalil T.B, King A.I., Mahmood H.F., Mertz H.J., Wismans J. (2004). Vehicle Crashworthiness and Occupant Protection. American Iron and Steel Institute.

[2] Annett M.S., Horta L.G. (2011). Comparison of Test and Finite Element Analysis for Two Full-Scale Helicopter Crash Tests. American Institute of Aeronautics and Astronautics. 52nd AIAA/ASME/ASCE/AHS/ASC Structures, Structural Dynamics and Materials Conference.

[3] Huang H., Chunyang L., Zeng Q. (2015). Crash protectiveness to occupant injury and vehicle damage: An investigation on major car brands. Accident Analysis and Prevention, Volume 86, pp. 129-136.

[4] American National Standard: ANSI D16.1 (2017). Manual on Classification of Motor Vehicle Traffic Crashes, 8th edition.

[5] European New Car Assessment Programme (2018). Euro NCAP Rating Review, version 1.0.

[6] Doğan U.Ç. (2009). Effect of Strain History on Simulation of Crashworthiness of a Vehicle.

[7] Özdemir M. (2013). Analysis of Whiplash during Rear Crash and Development of an Anti-Whiplash Seat Mechanism.

[8] Göçmen U. (2009). Experimental Whiplash Analysis with Hybrid III 50 Percentile Test Dummy.

[9] Özden K. (2012). Investigation of Reducing Run Time in Vehicle Level Finite Element Analyses for Curtain Airbag Development

[10] Çöl R (2012). Developing of System to Evaluate Safety of Child Seat and Restraint System According to ECE R44

[11] Törnqvist R. (2003). Design of Crashworthy Ship Structures. DOI: 10.1007/s00726-011-1022-z

[12] Storheim M., Amdahl J. (2014). Design of offshore structures against accidental ship collisions. Marine Structures, Volume 37, pp. 135-172.

[13] Brown A., Moon W., Louie J. (2002). Structural Design for Crashworthiness in Ship Collisions. SNAME Annual Meeting T&R 2002 and SNAME Transactions, Volume 110, pp. 499-512.

[14] Hur J., Jang J. (2013). A Study on the Crashworthiness Design and Analysis for Military Helicopter. International Journal of Precision Engineering and Manufacturing, Volume 14, No 4, pp. 599-603.

[15] Fox R. G. (1989). Helicopter Crashworthiness – Part One. Flight Safety Foundation Helicopter Safety, Volume 14, No 6.

[16] Binkhorst D. (2007). Design of Helicopter Subfloor Structure to Improve Crashworthiness.

[17] Subbaramaiah R., Prusty G, Pearce G., Lim S. H., Kelly D., Thomson R. (2012). A Feasibility Study for Multi-Material Retrofittable Energy Absorbing Structure for Aged Helicopter Subfloor. 28th International Congress of the Aeronautical Sciences.

[18] Kindervater C., Deletombe E. (2000). Composite Helicopter Structural Crashworthiness: Progress in Design and Crash Simulation Approaches.

[19] Coltman J. W., Bölükbaşı A. O., Laananen D. H. (1985). Analysis of Rotorcraft Crash Dynamics for Development of Improved Crashworthiness Design Criteria.

[20] Bisagni C. (2002). Crashworthiness of Helicopter Subfloor Structures. International Journal of Impact Engineering, Volume 27, pp. 1067-1082.

[21] Xue P., Ding M. L., Qiao C. F., Yu T.X. (2014). Crashworthiness Study of a Civil Aircraft Fuselage Section. Latin American Journal of Solids and Structures.

[22] Ren Y., Xiang J., Meng S., Yan Y., Zhuang N. (2014). Crashworthiness of Civil Aircraft subject to Soft Soil and Concrete Impact Surface. Procedia Engineering, Volume 80, pp. 193-201.

[23] Mou H., Zou T., Feng Z., Ren J. (2013). Crashworthiness Simulation Research of Fuselage Section with Composite Skin. Procedia Engineering, Volume 80, pp. 59-65.

[24] Yan T., Wang J. (2014). Crashworthy Component Design of an Ultra-Light Helicopter with Energy Absorbing Composite Structure. Procedia Engineering, Volume 80, pp. 329-342.

[25] Deletombe E., Delsart D., Fabis J., Langrand B., Ortiz R. (2004). Recent Developments in Modelling and Experimentation Fields with respect to Crashworthiness and Impact on Aerospace Structures.

[26] Heimbs S. (2009). Virtual Testing of Sandwich Core Structures Using Dynamic Finite Element Simulations. Computational Materials Science, Volume 45, pp. 205-216.

[27] European Aviation Safety Agency (2012). Certification Specifications for Large Rotorcraft (CS-29), Amendment 3.

[28] Standardization Agreement (STANAG), No. 3950 (2001). Helicopter Design Criteria for Crew Crash Protection and Anthropometric Accommodation.

[29] Department of Defense of USA (1998). Crew Systems Crash Protection Handbook. Joint Service Specification Guide.

[30] Department of Defense of USA (1988). Light Fixed and Rotary-Wing Aircraft Crash Resistance.

[31] Simitçioğlu G., Doğan V. Z. (2013). Dynamic Finite Element Analysis of an Aircraft Seat.

[32] Latif M. N. H. A. (2008). Analysis and Optimization of a Crashworthy Helicopter Seat.

[33] Risby M. S., Khalid A. J., Leong K. Y., Gurunathan B. A., Sulaiman M.N., Rahman M.K. (2013). Numerical Simulation of Helicopter Cockpit Seat Subjected to Crash Impact. Journal of Applied Sciences, Engineering and Technology, Volume 5, pp. 72-78.

[34] Desjardins S. P. (2003). The Evolution of Energy Absorption Systems for Crashworthy Helicopter Seats.

[35] Lee Y., Lee J., Han K., Lee K., Lim C. (2009). A Study on the Modeling and Analysis of a Helicopter's Occupant Seat Belt for Crashworthiness. Journal of Mechanical Science and Technology, Volume 23, pp. 1027-1030.

[36] Taber M. J. (2013). Crash Attenuating Seats: Effects on Helicopter Underwater Escape Performance. Safety Science, Volume 57, pp. 179-186.

[37] Lanzi L., Airoldi A., Cacchione B., Astori P. (2012). Direct Search of Feasible Region and Application to a Crashworthy Helicopter Seat, Volume 45, pp. 875-887.

[38] Astori P., Ceresa P., Morandini M. (2003). Numerical Optimisation of a Seat Energy Absorber.

[39] Moradi R., Beheshti H.K., Lankarani H.M. (2012). Lumber Load Attenuation for Rotorcraft Occupants Using a Design Methodology for the Seat Impact Energy-Absorbing System. Central European Journal of Engineering, Volume 2, pp. 562-577.

[40] Society of Automotive Engineers (2015). AS8049 Performance Standard for Seats in Civil Rotorcraft, Transport Aircraft, and General Aviation Aircraft, Revision C.

[41] Department of Defense of the USA (1986). MIL-S-58095A (AV) Military Specification Seat System: Crash-Resistant, Non-Ejection, Aircrew, General Specification for.

[42] Department of Defense of the USA (1981). MIL-S-85510 (AS) Military Specification Seats, Helicopter Cabin, Crashworthy, General Specification for.

[43] Society of Automotive Engineers (2016). AS8049/1 Performance Standard for Side-Facing Seats in Civil Rotorcraft, Transport Aircraft, and General Aviation Aircraft, Revision A.

[44] Federal Aviation Administration (2012). Helicopter Flying Handbook. DOI: 10.1088/1751-8113/44/8/085201.

[45] Boyne W. J. (date accessed: 2019, February 2). Helicopter. Retrieved from: https://www.britannica.com/technology/helicopter

[46] Defence Blog: Online Military Magazine (date accessed: 2019, June 6). Retrieved from: https://defence-blog.com/news/u-s-army-has-no-plans-to-replace-ah-64-apache-attack-helicopter.html

[47] Defence Visual Information Distribution Service (date accessed: 2019, June 6). Retrieved from: https://www.dvidshub.net/image/4374180/uh-60-black-hawk-helicopter

[48] Private Charter Tours (date accessed: 2019, June 26). Retrieved from: https://www.thetourspecialists.com.au/tours/private-charter-tours/helicopter-tours/great-barrier-reef-helicopter.566

[49] Goosssens, P. (date accessed: 2019, February 2). Helicopter Design. Retrieved from: http://www.helistart.com/heliDesign.asp

[50] US Army Aviation Systems Command (1989). Aircraft Crash Survival Design Guide Volume I – Design Criteria and Checklist.

[51] Martin Baker:  Troop and Gunner Seats (date accessed: 2018, November 6). Retrieved from: http://martin-baker.com/products/troop-and-gunner

[52] Fischer Passenger Seat (date accessed: 2018, November 8). Retrieved from: www.aeroexpo.online/prod/b-e-aerospace-fischer-gmbh-175524.html#product-item_55713

[53] Federal Aviation Administration (2014). AC 29-2C Certification of Transport Category Rotorcraft, Change 4.

[54] METU-BILTIR Center − Vehicle Safety Unit (date accessed: 2019, June 7). Retrieved from: http://www.biltir.metu.edu.tr/tasitguven_ing.html

[55] Goldsmith W. (2001). The Theory and Physical Behaviour of Colliding Solids. Dover Publications.

[56] Dassault Systemes (2014). Abaqus 6.14 Abaqus/CAE User Guide. DOI: 10.1017/CBO9781107415324.004.

[57] Johnson G. R., Cook W.H. (1983). A Constitutive Model and Data for Metals Subjected to Large Strains, High Strain Rates and High Temperatures.

[58] Matweb (date accessed: 2019, April 7). Retrieved from: www.matweb.com

[59] Beer F. P., Johnston Jr. E.R., DeWolf J.T., Mazurek D.F. (2012). Mechanics of Materials. McGraw-Hill.

# APPENDICES

## A. The Derivation of Material Data of the Study

The yield strength for A284 Steel, Grade D is 230 MPa [58] whereas the yield strength of Steel 4340 is 792 MPa [57]. By the dividing these terms we find the correction factor ($c_1$) as 0.2904. Similarly, the true ultimate tensile strength of 8.8 Grade Steel bolt is taken as 800 MPa, whereas the true ultimate strength of Steel 4340 is 1164.93 MPa. By the dividing these terms we find the correction factor ($c_2$) as 0.6867.

Since true stress vs. true strain table is known for Steel 4340 the plasticity data of A284 Steel, Grade D and 8.8 Grade Steel could be derived as shown Table A.1.

Table A.1.The plasticity data of A284 Steel, Grade D

| True Strain | Steel 4340 | A284 Steel, Grade D ($c_1$=0.2904) | 8.8 Grade Steel ($c_2$=0.6867) |
|---|---|---|---|
| | True Stress [MPa] | True Stress [MPa] | True Stress [MPa] |
| 0.00 | 792.0 | 230.0 | 543.9 |
| 0.01 | 946.0 | 274.7 | 649.7 |
| 0.02 | 976.4 | 283.6 | 670.6 |
| 0.03 | 996.9 | 289.5 | 684.6 |
| 0.04 | 1012.9 | 294.1 | 695.6 |
| 0.05 | 1026.1 | 298.0 | 704.6 |
| 0.06 | 1037.4 | 301.3 | 712.4 |
| 0.07 | 1047.4 | 304.2 | 719.3 |
| 0.08 | 1056.5 | 306.8 | 725.5 |
| 0.09 | 1064.7 | 309.2 | 731.2 |
| 0.10 | 1072.3 | 311.4 | 736.4 |
| 0.11 | 1079.3 | 313.4 | 741.2 |
| 0.12 | 1085.9 | 315.3 | 745.7 |
| 0.13 | 1092.0 | 317.1 | 750.0 |
| 0.14 | 1097.9 | 318.8 | 753.9 |
| 0.16 | 1108.7 | 322.0 | 761.4 |
| 0.17 | 1113.7 | 323.4 | 764.8 |
| 0.18 | 1118.5 | 324.8 | 768.2 |

Table A.1. (continued)

| True Strain | Steel 4340 | A284 Steel, Grade D ($c_1$=0.2904) | 8.8 Grade Steel ($c_2$=0.6867) |
|---|---|---|---|
| | True Stress [MPa] | True Stress [MPa] | True Stress [MPa] |
| 0.19 | 1123.2 | 326.2 | 771.3 |
| 0.20 | 1127.6 | 327.5 | 774.4 |
| 0.21 | 1131.9 | 328.7 | 777.3 |
| 0.22 | 1136.0 | 329.9 | 780.2 |
| 0.23 | 1140.0 | 331.1 | 782.9 |
| 0.24 | 1143.9 | 332.2 | 785.6 |
| 0.25 | 1147.7 | 333.3 | 788.1 |
| 0.26 | 1151.3 | 334.3 | 790.7 |
| 0.27 | 1154.9 | 335.4 | 793.1 |
| 0.28 | 1158.3 | 336.4 | 795.5 |
| 0.29 | 1161.7 | 337.4 | 797.8 |
| 0.30 | 1164.9 | 338.3 | 800.0 |

## B. Success of the Utilization of Abaqus/Explicit to Floor Deformation and Pin Insertion Analyses

The floor deformation and the pin insertions are performed with Abaqus/Explicit although they are quasi-static cases as explained in Section 5.3. There is a trade-off between the run time and the accuracy of the results when Abaqus/Explicit is used for quasi-static loading cases. Due to the nature of Abaqus/Explicit, the step time to do the rotary and linear motions should be long enough not to show dynamic behavior. On the contrary, if the step time is selected too long, the total period of analysis would be too long, being an infeasible computation.

The success of Abaqus/Explicit usage to this quasi-static event should be checked. In a quasi-static analysis event, the value of the kinetic energy (KE) over the internal energy (IE) should not exceed 10% throughout the most of the process [56]. As shown in Figure B.1, the ratio of two parameters never exceeds %10 which shows that the Abaqus/Explicit utilization is quite good for this quasi-static case.
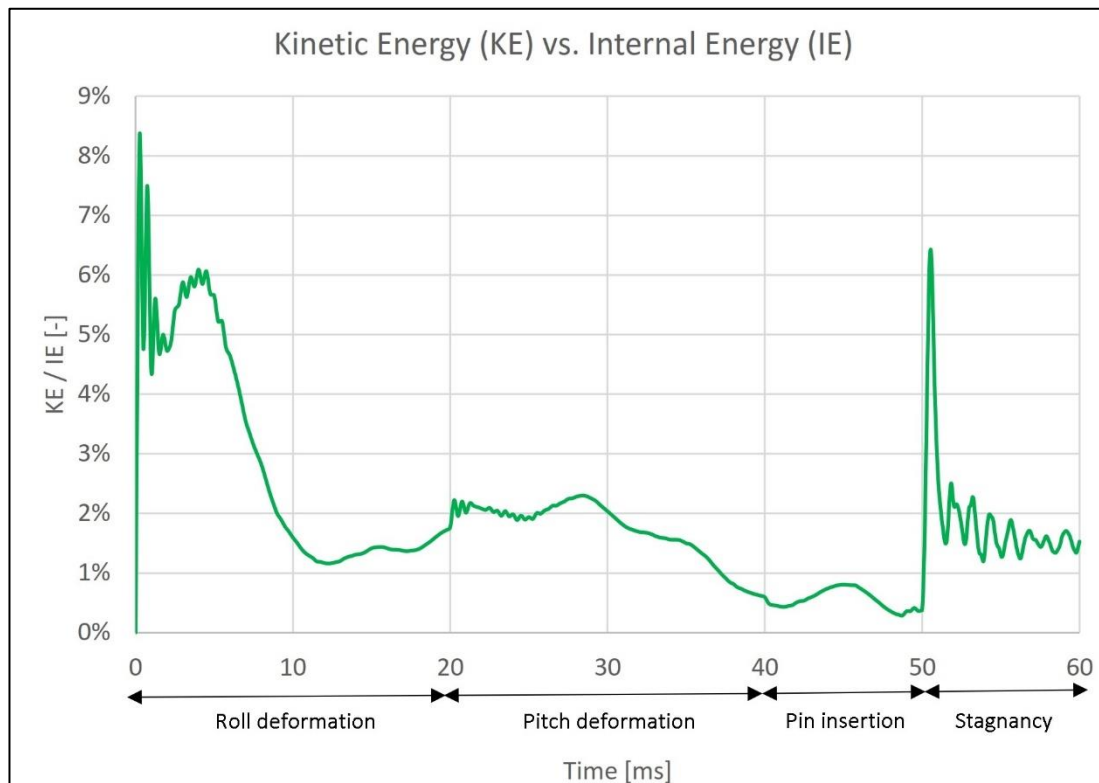
Figure B.1. Comparison of kinetic energy and internal energy for the floor
deformation and the pin insertion analyses of the Interchangeable Floor
Deformation Unit and the Simplified Helicopter Seat